AD-A182 763 AN ANALYSIS OF THE VISCOUS BURGERS EQUATION AS MODELED BY THE MACCORMACK METHOD(U) AIR FORCE ARMAMENT LAB EGLIN AFB FL J S MOUNTS ET AL. JUN 87 AFATL-TR-87-12 1/1

UNCLASSIFIED SBI-AD-E801 526 F/G 20/4 NL

FNI
8 87
DTIC

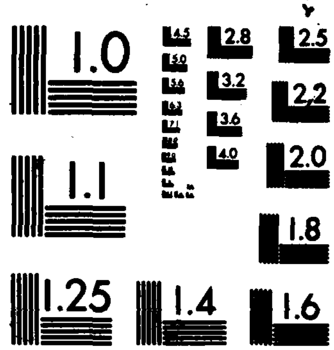
1.0
1.1
1.25
1.4
1.6
1.8
2.0
2.2
2.5
2.8
3.2
3.6
4.0

AFATL-TR-87-12 AD-A182 763

An Analysis of the Viscous Burgers Equation as Modeled by the MacCormack Method

M C Hughson, 1 Lt, USAF
J S Mounts, 1 Lt, USAF
D M Belk

FINAL REPORT FOR PERIOD OCTOBER 1985 – DECEMBER 1986

JUNE 1987

AIR FORCE ARMAMENT LABORATORY

Air Force Systems Command ▪ United States Air Force ▪ Eglin Air Force Base, Florida

NOTICE

When Government drawings, specifications, or other data are used for any purpose other than in connection with a definitely related Government procurement operation, the United States Government thereby incurs no responsibility nor any obligation whatsoever; and the fact that the Government may have formulated, furnished, or in any way supplied the said drawings, specifications, or other data, is not to be regarded by implication or otherwise as in any manner licensing the holder or any other person or corporation, or conveying any rights or permission to manufacture, use, or sell any patented invention that may in any way be related thereto.

This report has been reviewed by the Public Affairs Office (PA) and is releasable to the National Technical Information Service (NTIS). At NTIS, it will be available to the general public, including foreign nations.

This technical report has been reviewed and is approved for publication.

FOR THE COMMANDER

Donald C Daniel

DONALD C. DANIEL
Chief, Aeromechanics Division

Even though this report may contain special release rights held by the controlling office, please do not request copies from the Air Force Armament Laboratory. If you qualify as a recipient, release approval will be obtained from the originating activity by DTIC. Address your request for additional copies to:

Defense Technical Information Center
Cameron Station
Alexandria, Virginia 22304-6145

If your address has changed, if you wish to be removed from our mailing list, or if the addressee is no longer employed by your organization, please notify AFATL/FXA , Eglin AFB FL 32542-5434.

Copies of this report should not be returned unless return is required by security considerations, contractual obligations, or notice on a specific document.

6c. ADDRESS (*City, State, and ZIP Code*)		7b. ADDRESS (*City, State, and ZIP Code*)			
Air Force Armament Laboratory Eglin AFB FL 32542-5434					
8a. NAME OF FUNDING/SPONSORING ORGANIZATION Aeromechanics Division	8b. OFFICE SYMBOL (*If applicable*) AFATL/FX	9. PROCUREMENT INSTRUMENT IDENTIFICATION NUMBER			
8c. ADDRESS (*City, State, and ZIP Code*)		10. SOURCE OF FUNDING NUMBERS			
Air Force Armament Laboratory Eglin AFB FL 32542-5434		PROGRAM ELEMENT NO. 62602F	PROJECT NO. 2567	TASK NO. 03	WORK UNIT ACCESSION NO. 08

11. TITLE (*Include Security Classification*)

An Analysis of the Viscous Burgers Equation as Modeled by the MacCormack Method

12. PERSONAL AUTHOR(S)

M.C. Hughson, 1Lt, J.S. Mounts, 1Lt, and D.M. Belk

13a. TYPE OF REPORT	13b. TIME COVERED	14. DATE OF REPORT (*Year, Month, Day*)	15. PAGE COUNT
Final	FROM Oct 85 TO Dec 86	June 1987	91

16. SUPPLEMENTARY NOTATION

Availability of this report is specified on verso of front cover

17. COSATI CODES			18. SUBJECT TERMS (*Continue on reverse if necessary and identify by block number*)
FIELD	GROUP	SUB-GROUP	Finite Difference, Numerical Analysis, Burgers Equation, MacCormack Method

PREFACE

This program was conducted by Lieutenant Montgomery C. Hughson, Lieutenant Jon S. Mounts, and Dr Dave M. Belk of the Computational Fluid Dynamics Section, Aerodynamics Branch, Aeromechanics Division, Air Force Armament Laboratory, Eglin AFB, Florida. The work was performed under work unit 25670308 during the fiscal year period from 1 October 1985 to 30 November 1986.

This report presents an analysis of a computational fluid dynamics algorithm employed in current computer codes. The analysis is presented in a manner that allows this report to be used as a training manual.

TABLE OF CONTENTS

LIST OF FIGURES

LIST OF FIGURES (Concluded)

LISTING OF PROGRAMS

SECTION I

INTRODUCTION

The new generation of supercomputers (Cyber 205, Cray X-MP, Cray 2, and so on) heralds in a new era of research for aerodynamic analysis and design. The highly complex flow field about a weapon/store configuration on current and future tactical fighter aircraft can now be modeled and examined by the computer. Current aerodynamic research at the Air Force Armament Laboratory's Computational Fluid Dynamics Section is aimed at solving the fluid flow governing equations using innovative approximation techniques. These partial differential equations form a nonlinear system of equations to be solved for unknown pressures, densities, temperatures, and velocities that will, in turn, yield aerodynamic characteristics for a selected weapon/store configuration in a wide range of flight conditions.

To obtain a complete understanding of the flow field about a configuration, we must solve the Navier-Stokes equations. One of the first steps in developing the computer codes needed to solve these equations is to do an analysis of the numerical technique selected to model the equations of interest. This analysis illustrates the procedures used to evaluate a numerical technique's ability to model the original equations. The analysis yields stability criteria and limits of the numerical finite-difference technique.

This report will serve as an instructional aid for that analysis. A simple model equation with properties characteristic of the more complex equations of fluid flow will be used in this step-by-step analysis. The viscous Burgers equation is a highly useful model for this purpose as explained in the next section. The method of MacCormack will be the technique employed for the analysis.

1. BURGERS EQUATION

Within the field of computational fluid dynamics, there are a number of simple linear problems that serve as vehicles for various finite-difference methods. Unfortunately, the usual fluid mechanics problems is highly nonlinear.

A single equation that could serve as a nonlinear analog of the fluid mechanics equations would be very useful. This single equation must have terms which closely duplicate the physical properties of the fluid equations, i.e., the model equation should have a convective term, a diffusive or dissipative term, and a time-dependent term. Burgers (Reference 1) introduced a simple nonlinear equation which meets these requirements

$$\underbrace{\frac{\delta u}{\delta t}}_{\text{Unsteady Term}} + \underbrace{u\frac{\delta u}{\delta x}}_{\text{Convective Term}} = \underbrace{\mu\frac{\delta^2 u}{\delta x^2}}_{\text{Viscous Term}} \tag{1}$$

Equation 1 is a parabolic partial differential equation which can serve as a model equation for the boundary-layer equations, the parabolized Navier-Stokes equations, and the complete Navier-Stokes equations.

Burgers equation has exact analytical solutions for certain boundary and initial conditions. These exact solutions are useful when comparing finite-difference methods. The exact steady state solution, [i.e., $\lim_{t \to \infty} \Delta t\, u(x,t)$], of Equation 1 for the boundary conditions

$$u(0,t) = 1 \tag{2}$$

$$u(L,t) = 0 \tag{3}$$

is given by

$$u = \bar{u}\left\{\frac{1 - exp\left[\bar{u}\, R_{e_L}\left(\frac{x}{L} - 1\right)\right]}{1 + exp\left[\bar{u}\, R_{e_L}\left(\frac{x}{L} - 1\right)\right]}\right\} \tag{4}$$

where

$$R_{e_L} = \frac{L}{\mu} \tag{5}$$

and $\bar{u}$ is a solution of the equation

$$\frac{\bar{u} - 1}{\bar{u} + 1} = exp\left(-\bar{u}\, R_{e_L}\right) \tag{6}$$

For simplicity, the linearized Burgers equation

$$\frac{\delta u}{\delta t} + c\,\frac{\delta u}{\delta x} = \mu\,\frac{\delta^2 u}{\delta x^2} \tag{7}$$

is often used in place of Equation 2. In this analysis, we will use the nonlinear case for the computer solution and the linear case for the analysis in Section II.

2. MACCORMACK'S METHOD

The MacCormack method (Reference 2) for the complete Burgers Equation 1 is

$$\text{Predictor:} \quad \overline{u_j^{n+1}} = u_j^n - c\,\frac{\Delta t}{\Delta x}\left(F_{j+1}^n - F_j^n\right) + \mu\,\frac{\Delta t}{(\Delta x)^2}\left(u_{j+1}^n - 2u_j^n + u_{j-1}^n\right) \tag{8}$$

$$\text{Corrector:} \quad u_j^{n+1} = \frac{1}{2}\left[u_j^n + \overline{u_j^{n+1}} - \frac{\Delta t}{\Delta x}\left(\overline{F_j^{n+1}} - \overline{F_{j-1}^{n+1}}\right) + \mu\,\frac{\Delta t}{(\Delta x)^2}\left(\overline{u_{j+1}^{n+1}} - 2\overline{u_j^{n+1}} + \overline{u_{j-1}^{n+1}}\right)\right] \tag{9}$$

where

$$F = 0.5u^2$$

which is second-order accurate in both time and space. In this version of the MacCormack scheme, a forward difference is employed in the predictor step and a backward difference is used in the corrector step for the convective terms. The alternate version is vice versa and both variants are second-order accurate. However, the best resolution of discontinuities occurs when the difference in the predictor is in the direction of propagation of the discontinuity (Reference 3). Since we will be giving the discontinuities a positive direction as initial conditions, [i.e., $u(0,t) = 1$], we will use the version indicated above.

SECTION II

ANALYSIS

In this section, we will be examining the features of the linear viscous Burgers equation (Equation 7). The MacCormack method for Equation 7 is

Predictor:
$$\overline{u_j^{n+1}} = u_j^n - c\frac{\Delta t}{\Delta x}\left(u_{j+1}^n - u_j^n\right) + \mu\frac{\Delta t}{(\Delta x)^2}\left(u_{j+1}^n - 2u_j^n + u_{j-1}^n\right) \tag{10}$$

Corrector:
$$u_j^{n+1} = \frac{1}{2}\left[u_j^n + \overline{u_j^{n+1}} - c\frac{\Delta t}{\Delta x}\left(\overline{u_j^{n+1}} - \overline{u_{j-1}^{n+1}}\right) + \mu\frac{\Delta t}{(\Delta x)^2}\left(\overline{u_{j+1}^{n+1}} - 2\overline{u_{j+1}^{n+1}} + \overline{u_{j-1}^{n+1}}\right)\right] \tag{11}$$

The first step will be to combine these two equations into one. Let $\beta = c\frac{\Delta t}{\Delta x}$, $\alpha = \mu\frac{\Delta t}{(\Delta x)^2}$ to obtain

$$\begin{aligned} 2u_j^{n+1} = {} & 2u_j^n - \beta\left(u_{j+1}^n - u_{j-1}^n\right) \\ & + 2\alpha\left(u_{j+1}^n - 2u_j^n + u_{j-1}^n\right) \\ & + \beta^2\left(u_{j+1}^n - 2u_j^n + u_{j-1}^n\right) \\ & + \beta\alpha\left(2u_{j+1}^n - 2u_{j-1}^n + u_{j-2}^n - u_{j+2}^n\right) \\ & + \alpha^2\left(u_{j+2}^n - 4u_{j+1}^n + 6u_j^n - 4u_{j-1}^n + u_{j-2}^n\right) \end{aligned} \tag{12}$$

To provide a quick check of this tedious combination, note that the MacCormack method for the inviscid Burgers equation is equivalent to the Lax-Wendroff scheme (Reference 4). Therefore, if we set $\alpha = 0$, thereby removing the viscous terms, we obtain

$$2u_j^{n+1} = 2u_j^n - \beta\left(u_{j+1}^n - u_{j-1}^n\right) + \beta^2\left(u_{j+1}^n - 2u_j^n + u_{j-1}^n\right)$$

The next step in the analysis will be to check consistency.

1. CONSISTENCY

A finite-difference equation (FDE) is said to be consistent with the partial differential equation (PDE) it models if

$$\lim_{\substack{\Delta x \to 0 \\ \Delta t \to 0}} TE = 0$$

where TE is the truncation error and is found by subtracting the original partial differential equation from the finite differential equation.

The first step in evaluating the consistency of the finite differential equations obtained is to express

$$u_j^{n+1},\ u_{j+1}^{n},\ u_{j-1}^{n},\ u_{j+2}^{n},\ \text{and}\ u_{j-2}^{n}$$

in terms of u_j and its derivatives by using Taylor series expansions, i.e.,

$$u_j^{n+1} = u_j^n + \left(\frac{\delta u}{\delta t}\right)_j^n t + \left(\frac{\delta^2 u}{\delta t^2}\right)\frac{\Delta t^2}{2!} + \left(\frac{\delta^3 u}{\delta t^3}\right)\frac{\Delta t^3}{3!} + \ldots \qquad (13)$$

$$u_{j+1}^n = u_j^n + \left(\frac{\delta u}{\delta x}\right)\Delta x + \left(\frac{\delta^2 u}{\delta x^2}\right)\frac{\Delta x^2}{2!} + \left(\frac{\delta^3 u}{\delta x^3}\right)\frac{\Delta x^3}{3!} + \ldots \qquad (14)$$

$$u_{j-1}^n = u_j^n - \left(\frac{\delta u}{\delta x}\right)\Delta x + \left(\frac{\delta^2 u}{\delta x^2}\right)\frac{\Delta x^2}{2!} - \left(\frac{\delta^3 u}{\delta x^3}\right)\frac{\Delta x^3}{3!} + \ldots \qquad (15)$$

$$u_{j+2}^n = u_j^n + \left(\frac{\delta u}{\delta x}\right)2\Delta x + \left(\frac{\delta^2 u}{\delta x^2}\right)\frac{(2\Delta x)^2}{2!} + \left(\frac{\delta^3 u}{\delta x^3}\right)\frac{(2\Delta x)^3}{3!} + \ldots \qquad (16)$$

$$u_{j-2}^n = u_j^n - \left(\frac{\delta u}{\delta x}\right)2\Delta x + \left(\frac{\delta^2 u}{\delta x^2}\right)\frac{(2\Delta x)^2}{2!} - \left(\frac{\delta^3 u}{\delta x^3}\right)\frac{(2\Delta x)^3}{3!} + \ldots \qquad (17)$$

The next step is to substitute Equations 13 through 17 into the Equation 12.

$$
\begin{aligned}
&\left[\frac{\delta u}{\delta t}(\Delta t) + \left(\frac{\delta^2 u}{\delta t^2}\right)\frac{(\Delta t)^2}{2!} + \left(\frac{\delta^3 u}{\delta x^3}\right)\frac{(\Delta t)^3}{3!} + \ldots\right] = \\
&\quad -\beta\left[\frac{\delta u}{\delta x}(\Delta x) + \left(\frac{\delta^3 u}{\delta x^3}\right)\frac{(\Delta x)^3}{3!} + \left(\frac{\delta^5 u}{\delta x^5}\right)\frac{(\Delta x)^5}{5!} + \ldots\right] \\
&+ (2\alpha + \beta^2)\left[\left(\frac{\delta^2 u}{\delta x^2}\right)\frac{(\Delta x)^2}{2!} + \left(\frac{\delta^4 u}{\delta x^4}\right)\frac{(\Delta x)^4}{4!} + \left(\frac{\delta^6 u}{\delta x^6}\right)\frac{(\Delta x)^6}{6!} + \ldots\right] \\
&\quad + \beta\alpha\left[(2-2^3)\left(\frac{\delta^3 u}{\delta x^3}\right)\frac{(\Delta x)^3}{3!} + (2-2^5)\left(\frac{\delta^5 u}{\delta x^5}\right)\frac{(\Delta x)^5}{5!} + \ldots\right] \\
&\quad + \alpha^2\left[(2^4-2^2)\left(\frac{\delta^4 u}{\delta x^4}\right)\frac{(\Delta x)^4}{4!} + (2^6-2^2)\left(\frac{\delta^6 u}{\delta x^6}\right)\frac{(\Delta x)^6}{6!} + \ldots\right]
\end{aligned}
\tag{18}
$$

Finally, subtract the original PDE from the FDE. Repeating Equation 7 for reference and plugging in $\beta = \frac{c\Delta t}{\Delta x}$ and $\alpha = \mu\frac{\Delta t}{(\Delta x)^2}$ as well as dividing through by Δt yields:

$$
\begin{aligned}
&\left[\frac{\delta u}{\delta t} + \left(\frac{\delta^2 u}{\delta t^2}\right)\frac{\Delta t}{2!} + \left(\frac{\delta^3 u}{\delta x^3}\right)\frac{(\Delta t)^2}{3!} + \ldots\right] = \\
&\quad -\left[c\frac{\delta u}{\delta x} + c\left(\frac{\delta^3 u}{\delta x^3}\right)\frac{(\Delta x)^2}{3!} + c\left(\frac{\delta^5 u}{\delta x^5}\right)\frac{(\Delta x)^4}{5!} + \ldots\right] \\
&\quad +\left[\mu\frac{\delta^2 u}{\delta x^2} + 2\mu\left(\frac{\delta^4 u}{\delta x^4}\right)\frac{(\Delta x)^2}{4!} + 2\mu\left(\frac{\delta^6 u}{\delta x^6}\right)\frac{(\Delta x)^4}{6!} + \ldots\right] \\
&\quad +\left[\frac{c^2\Delta t}{2}\left(\frac{\delta^2 u}{\delta x^2}\right) + c^2\Delta t\left(\frac{\delta^4 u}{\delta x^4}\right)\frac{(\Delta x)^2}{4!} + c^2\Delta t\left(\frac{\delta^6 u}{\delta x^6}\right)\frac{(\Delta x)^4}{6!} + \ldots\right] \\
&\quad +\left[c\mu\Delta t(2-2^3)\left(\frac{\delta^3 u}{\delta x^3}\right)\frac{1}{3!} + c\mu\Delta t(2-2^5)\left(\frac{\delta^5 u}{\delta x^5}\right)\frac{(\Delta x)^2}{5!} + \ldots\right] \\
&\quad +\left[\mu^2\Delta t(2^4-2^2)\left(\frac{\delta^4 u}{\delta x^4}\right)\frac{1}{4!} + \mu^2\Delta t(2^6-2^2)\left(\frac{\delta^6 u}{\delta x^6}\right)\frac{(\Delta x)^2}{6!} + \ldots\right]
\end{aligned}
\tag{19}
$$

$$
\frac{\partial u}{\partial t} + c\frac{\partial u}{\partial x} = \mu\frac{\partial^2 u}{\partial x^2} \tag{7}
$$

Subtracting Equation 7 from Equation 19 yields the TE. It is readily apparent that Lim TE = 0 by observing that the Δx and Δt terms

$\Delta x \to 0$
$\Delta t \to 0$

appear only in the numerators of all terms. Therefore, the FDE given by the MacCormack's method for the linear viscous Burgers equation is unconditionally consistent.

2. STABILITY

The linear viscous Burgers equation will also be used for this portion of the analysis of the MacCormack FDE so that the Fourier method (or Von Neumann method) of stability analysis can be used.

In the Fourier or Von Neumann's method, the numerical stability of an FDE is analyzed by introducing a disturbance into the numerical solution at every grid point in the spatial domain at some arbitrary time level. That disturbance is then expanded into a Fourier series and each Fourier component of that series is analyzed separately. The FDE is said to be stable if all of the Fourier components do not grow in time and unstable if any one of the Fourier components grows in time (Reference 5).

If we introduce a disturbance ε (which represents roundoff errors) into the numerical solution at every grid point at an arbitrary time level n using Equation 12 we get

$$\begin{aligned} 2(u+\varepsilon)_j^{n+1} = {} & 2(u+\varepsilon)_j^n - \beta[(u+\varepsilon)_{j+1}^n - (u+\varepsilon)_{j-1}^n] \\ & +(2\alpha+\beta^2)[(u+\varepsilon)_{j+1}^n - 2(u+\varepsilon)_j^n + (u+\varepsilon)_{j-1}^n] \\ & +\beta\alpha[2(u+\varepsilon)_{j+1}^n - 2(u+\varepsilon)_{j-1}^n + (u+\varepsilon)_{j-2}^n - (u+\varepsilon)_{j+2}^n] \\ & +\alpha^2[(u+\varepsilon)_{j+2}^n + (u+\varepsilon)_{j-2}^n - 4(u+\varepsilon)_{j+1}^n - 4(u+\varepsilon)_{j-1}^n + 6(u+\varepsilon)_j^n] \end{aligned} \tag{20}$$

Subtracting Equation 12 from Equation 20 yields

$$2\left(\varepsilon_j^{n+1}-\varepsilon_j^n\right) = -\beta\left(\varepsilon_{j+1}^n-\varepsilon_{j-1}^n\right)$$
$$+\left(2\alpha+\beta^2\right)\left(\varepsilon_{j+1}^n-2\varepsilon_j^n+\varepsilon_{j-1}^n\right)$$
$$+\alpha\beta\left(2\varepsilon_{j+1}^n-2\varepsilon_{j-1}^n+\varepsilon_{j-2}^n-\varepsilon_{j+2}^n\right) \tag{21}$$
$$+\alpha^2\left[\varepsilon_{j+2}^n+\varepsilon_{j-2}^n-4\left(\varepsilon_{j+1}^n+\varepsilon_{j-1}^n\right)+6\varepsilon_j^n\right]$$

Any bounded disturbance ε on IL equally spaced grid points over a length L can be represented by a Fourier series made up of a finite number of Fourier components:

$$\varepsilon_i^n = \sum_{j=-n}^{n} A_j^n e^{Ik_j x_i} \tag{22}$$

where

$I = \sqrt{-1}$ and

$N = (IL - 1)/2$

$x_i = (i-1)\,\Delta x$

$\Delta x = L/(IL - 1)$

$k_j = \pi j/(N\Delta x)$

Substituting Equation 22 into Equation 21 yields: (Note: also changed j subscripts to i)

$$2\left(\sum_{j=-N}^{N} A_j^{n+1} e^{Ik_j x_i} - \sum_{j=-N}^{N} A_j^n e^{Ik_j x_i}\right) =$$

$$-\beta\left(\sum_{j=-N}^{N} A_j^n e^{Ik_j x_{i+1}} - \sum_{j=-N}^{N} A_j^n e^{Ik_j x_{i-1}}\right) \tag{23}$$

$$+\left(2\alpha+\beta^2\right)\left(\sum_{j=-N}^{N} A_j^n e^{Ik_j x_{i+1}} - 2\sum_{j=-N}^{N} A_j^n e^{Ik_j x_i} + \sum_{j=-N}^{N} A_j^n e^{Ik_j x_{i-1}}\right)$$

$$+\alpha\beta\left(2\sum_{j=-N}^{N} A_j^n e^{Ik_j x_{i+1}} - 2\sum_{j=-N}^{N} A_j^n e^{Ik_j x_{i-1}} + \sum_{j=-N}^{N} A_j^n e^{Ik_j x_{i-2}} - \sum_{j=-N}^{N} A_j^n e^{Ik_j x_{i+2}}\right)$$

$$+\alpha^2\left(\sum_{j=-N}^{N} A_j^n e^{Ik_j x_{i+2}} + \sum_{j=-N}^{N} A_j^n e^{Ik_j x_{i-2}} - 4\sum_{j=-N}^{N} A_j^n e^{Ik_j x_{i+1}}\right.$$

$$\left. - 4\sum_{j=-N}^{N} A_j^n e^{Ik_j x_{i-1}} + 6\sum_{j=-N}^{N} A_j^n e^{Ik_j x_i}\right)$$

Dropping the summation sign and cancelling the common exponential factor $e^{Ik_j x_i}$ yields:

(Note: $e^{Ik_j x_{i+1}} = (e^{Ik_j x_i})(e^{Ik_j \Delta x})$ and $e^{Ik_j x_{i+2}} = (e^{Ik_j x_i})(e^{Ik_j 2\Delta x})$

$$
\begin{aligned}
A_j^{n+1} = A_j^n - \tfrac{1}{2}\beta A_j^n \left(e^{Ik_j\Delta x} - e^{-Ik_j\Delta x}\right) \\
+ \alpha A_j^n \left(e^{Ik_j\Delta x} - 2 + e^{-Ik_j\Delta x}\right) \\
+\tfrac{1}{2}\beta A_j^n \left(e^{Ik_j\Delta x} - 2 + e^{-Ik_j\Delta x}\right) \\
+\tfrac{1}{2}\beta\alpha A_j^n \left(2e^{Ik_j\Delta x} - 2e^{Ik_j\Delta x} + e^{-2Ik_j\Delta x} - e^{2Ik_j\Delta x}\right) \\
+\tfrac{1}{2}\alpha^2 A_j^n \left(e^{2Ik_j\Delta x} + e^{-2Ik_j\Delta x} - 4e^{Ik_j\Delta x} - 4e^{-Ik_j\Delta x} + 6\right)
\end{aligned}
\tag{24}
$$

Dividing through by A_j^n and noting that $A_j^{n+1}/A_j^n = G_j$ (the amplification factor) yields

$$
\begin{aligned}
G_j = 1 -\tfrac{1}{2}\beta[(\cos K_j\Delta x + I\sin K_j\Delta x) - (\cos K_j\Delta x - I\sin K_j\Delta x)] \\
+(\alpha +\tfrac{1}{2}\beta)[(\cos K_j\Delta x + I\sin K_j\Delta x) - 2 + (\cos K_j\Delta x - I\sin K_j\Delta x)] \\
+\tfrac{1}{2}\beta\alpha[2(\cos K_j\Delta x + I\sin K_j\Delta x) - 2(\cos K_j\Delta x - I\sin K_j\Delta x) \\
+(\cos 2K_j\Delta x - I\sin 2K_j\Delta x) - (\cos 2K_j\Delta x + I\sin 2K_j\Delta x)] \\
+\tfrac{1}{2}\alpha^2[(\cos 2K_j\Delta x + I\sin 2K_j\Delta x) + (\cos 2K_j\Delta x - I\sin 2K_j\Delta x) \\
- 4(\cos K_j\Delta x + I\sin K_j\Delta x) - 4(\cos K_j\Delta x - I\sin K_j\Delta x) + 6]
\end{aligned}
\tag{25}
$$

or, let $\gamma = kj\Delta x$,

$$G_j = 1 - \tfrac{1}{2}\beta(2I\sin\gamma)$$

$$+(\alpha + \tfrac{1}{2}\beta^2)[2(\cos\gamma - 1)] \tag{26}$$

$$+\tfrac{1}{2}\beta\alpha(4I\sin\gamma - 2I\sin 2\gamma)$$

$$+\tfrac{1}{2}\alpha^2(2\cos 2\gamma - 8\cos\gamma + 6)$$

Using the following trigonometric identities

$\cos 2\gamma = 2\cos^2\gamma - 1$ and $\sin 2\gamma = 2\sin\gamma\cos\gamma$

we obtain

$$G_j = [1 + (2\alpha + \beta^2)(\cos\gamma - 1) + 2\alpha^2(\cos\gamma - 1)^2] \tag{27}$$

$$+ I\{-\beta\sin\gamma[2\alpha(\cos\gamma - 1) + 1]\}$$

Now, if $|G_j| \leq 1$, the disturbance ε will not grow. Therefore, if

$|\text{Equation 27}| \leq 1$

or (square both sides)

$|\text{Equation 27}|^2 \leq 1^2$

Let $A = \cos\gamma - 1$, then

$$[1 + (2\alpha + \beta^2)A + 2\alpha^2 A^2]^2 \tag{28}$$

$$+[-\beta\sin\gamma(2\alpha A + 1)]^2 \leq 1$$

Since it is not easy to obtain simple stability criteria with the three variables in Equation 28, use of a simple computer program can determine these criteria. This is program 1 in the Program Section. The first step will be to set $\alpha = 0$ and determine the limits on β. Remember that

$$\alpha = \mu\frac{\Delta t}{(\Delta x)^2} \qquad \beta = c\frac{\Delta t}{\Delta x}$$

Therefore, when $\alpha = 0$, the equation reduces to the inviscid Burgers equation. The MacCormack method applied to the inviscid Burgers equation is the same as the Lax-Wendroff method mentioned previously and, hence, the stability criteria are the same, i.e., $\beta \leq 1$. The results are depicted graphically in Figure 1. Note that when $\beta = 1.1$, the resulting plot fell outside the unit circle.

When $\beta = 0$, the equation becomes the one-dimensional heat equation. The closest explicit FDE that represents this case is the simple explicit finite differential equation

$$\frac{u_j^{n+1} - u_j^n}{\Delta t} = \mu \frac{u_{j+1}^n - 2u_j^n + u_{j-1}^n}{(\Delta x)^2} \tag{29}$$

The amplification factor for this scheme is

$$G = 1 + 2\alpha(\cos\gamma - 1) \tag{30}$$

while for FDE (Equation 27)

$$G = 1 + 2\alpha(\cos\gamma - 1) + 2\alpha^2(\cos\gamma - 1)^2 \tag{31}$$

The additional term does not affect the stability criteria since both are stable when $\alpha \leq \frac{1}{2}$. Figures 2 through 4 show graphically α at .25, .5, and .6. Notice that at $\alpha = .6$, instability occurs.

The final phase of the stability analysis is to try to determine a relationship between α and β when they take on values within their respective stability ranges (i.e., $\beta \leq 1$ and $\alpha \leq \frac{1}{2}$). To accomplish this task, set α at a fixed value and vary β until the stability limit is reached. Set $\alpha = .25$ and .5 and then show how values greater than .5 are unstable no matter what value β takes on.

First, let $\alpha = .25$ and run β at 0, .25, .75, .8, and 1 in Figures 5(a) and (b). The β limit is isolated at .86 in Figures 6-9. Next, examine $\alpha =$ .5 at $\beta = .5$, .75, .9, 1, and 2 in Figures 10(a) and (b). The β limit is isolated at .96 in Figures 11 and 12. Finally, let $\alpha = .75$ and run β at .15 and .25 in Figure 13. Since $\alpha > .5$ in this case, there is no value of β that yields stability.

The final results are tabulated below. These values will be used as limits in the rest of the analysis.

α	β
0.00	1.00 - Boundary Limit
0.25	0.86
0.50	0.92
0.50	0.00 - Boundary Limit

An exponential curve fit for the values of α and β between their limits (i.e., $\alpha = .25$ and $.5$ while $\beta = .86$ and $.92$) resulted in the following relationship for stability

$$\beta \leq 0.7704e^{0.44\alpha} \tag{32}$$

To check this, plug in $\alpha = .3$ and $.4$ which yields $\beta = 0.8791$ and 0.9187, respectively. For a safety margin, round down to two significant figures. Figures 14 and 15 are plots of $\alpha = .3$ for $\beta = .88$ and $.87$. Notice in Figure 15 that the rounding down provided an appropriate margin of safety needed. Figures 16 and 17 are plots of $\alpha = .4$ for $\beta = .92$ and $.91$. From these four plots, one can see that Equation 32 can be used confidently for the relationship between α and β within their respective stability ranges not to include the boundaries.

3. CONVERGENCE

For this section of the analysis, we will use the following discussion from Anderson (Reference 3):

"Generally, we find that a consistent, stable scheme is convergent. Convergence here means that the solution to the finite differential equation approaches the true solution to the partial differential equations having the same initial and boundary conditions as the mesh is refined. A proof of this is available for initial value (marching) problems governed by linear PDEs. The theorem, due to Lax, is stated here without proof (Reference 6):"

"Lax's Equivalence Theorem. Given a properly posed initial value problem and a finite-difference approximation to it that satisfies the consistency condition, stability is the necessary and sufficient condition for convergence."

Since we have shown consistency and, if we stay within the limits of stability, then convergence is assured.

4. CONSERVATIVE PROPERTY

Consider the PDE with the following boundary conditions:

$$\frac{\partial u}{\partial t} + c\,\frac{\partial u}{\partial x} = \mu\,\frac{\partial^2 u}{\partial x^2} \tag{7}$$

or

$$\frac{\delta u}{\delta t} + \frac{\delta}{\delta x}\left(cu - \mu\,\frac{\delta u}{\delta x}\right) = 0 \tag{33}$$

and remember c and μ are constants. The BCs are

$$u(0,t) = U_1$$

$$u(L,t) = 0$$

Equation 33 describes the following conservation principle over any control volume with boundaries at x_1 and x_2.

$$\int_{x_1}^{x_2} \frac{\delta u}{\delta t}\,dx = \left(cu - \mu\frac{\delta u}{\delta x}\right)_{x_1} - \left(cu - \mu\frac{\delta u}{\delta x}\right)_{x_2} \tag{34}$$

Discretize the domain as shown below

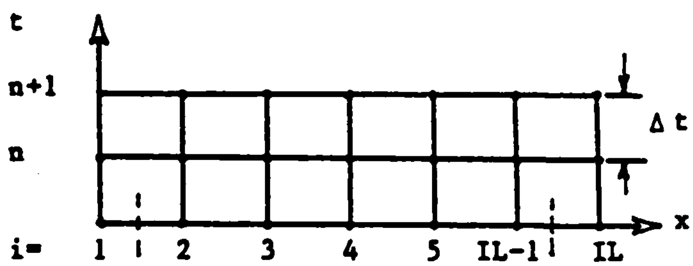

i = 1 1/2 and at i = IL - 1/2 are the boundary for the control volume enclosing all interior points

Remember that MacCormack's method for the FDE is a two-step technique repeated here

Predictor:
$$u_j^{\overline{n+1}} = u_j^n - c\frac{\Delta t}{\Delta x}\left(u_{j+1}^n - u_j^n\right) + \mu\frac{\Delta t}{(\Delta x)^2}\left(u_{j+1}^n - 2u_j^n + u_{j-1}^n\right) \tag{10}$$

Corrector:
$$u_j^{n+1} = \frac{1}{2}\left[u_j^n + u_j^{\overline{n+1}} - c\frac{\Delta t}{\Delta x}\left(u_j^{\overline{n+1}} - u_{j-1}^{\overline{n+1}}\right) + \mu\frac{\Delta t}{(\Delta x)^2}\left(u_{j+1}^{\overline{n+1}} - 2u_{j+1}^{\overline{n+1}} + u_{j-1}^{\overline{n+1}}\right)\right] \tag{11}$$

Considering the corrector step only (without plugging in the predictor step's algorithm)

$$\frac{2u_j^{n+1} - u_j^n - u_j^{\overline{n+1}}}{\Delta t} = c\,\frac{u_{j-1}^{\overline{n+1}} - u_j^{\overline{n+1}}}{\Delta x} + \mu\,\frac{u_{j+1}^{\overline{n+1}} - 2u_j^{\overline{n+1}} - u_{j-1}^{\overline{n+1}}}{(\Delta x)^2} \tag{35}$$

or

$$\frac{2u_j^{n+1} - u_j^n - u_j^{\overline{n+1}}}{\Delta t} = \left[\frac{c\,u_{j-1}}{\Delta x} - \frac{\mu}{(\Delta x)^2}\left(u_j - u_{j-1}\right)\right]^{\overline{n+1}} - \left[\frac{c\,u_j}{\Delta x} - \frac{\mu}{(\Delta x)^2}\right]\left(u_{j+1} - u_j\right)\Big]^{\overline{n+1}} \tag{36}$$

for j = 2, 3, ...IL-1

Now, sum the FDEs given by Equation 36 over the control volume enclosing the interior grid points.

$$\sum_{j=2}^{I1-1}\left(\frac{2u_j^{n+1}-u_j^n-u_j^{\overline{n+1}}}{\Delta t}\right)\Delta x = \left[cu_1-\frac{\mu}{(\Delta x)}(u_2-u_1)\right]^{\overline{n+1}}-\left[cu_2-\frac{\mu}{(\Delta x)}(u_3-u_2)\right]^{\overline{n+1}}$$

$$+\left[cu_2-\frac{\mu}{(\Delta x)}(u_3-u_2)\right]^{\overline{n+1}}- \qquad (37)$$

$$\circ$$

$$\circ$$

$$\circ$$

$$-\left[cu_{I1-1}-\frac{\mu}{(\Delta x)}(u_{I1}-u_{I1-1})\right]^{\overline{n+1}}$$

$$=\left[cu_1-\frac{\mu}{(\Delta x)^2}(u_2-u_1)\right]^{\overline{n+1}}-\left[cu_{I1-1}-\frac{\mu}{(\Delta x)^2}(u_{I1}-u_{I1-1})\right]^{\overline{n+1}}$$

Now, remember the Predictor step

$$u_j^{\overline{n+1}} = u_j^n - c\frac{\Delta t}{\Delta x}(u_{j+1}^n-u_j^n) \qquad (10)$$

$$+\mu\frac{\Delta t}{(\Delta x)^2}(u_{j+1}^n-2u_j^n+u_{j+1}^n)$$

Therefore, LHS of Equation 37 becomes

$$2\sum_{j=2}^{I1-1}\frac{u_j^{n+1}-u_j^n}{\Delta t}$$

with the RHS of the Predictor step taken to the RHS of this equation. Dividing through by 2 yields:

$$(38)$$

$$\frac{u_j^{n+1}-u_j^n}{\Delta t} = \frac{1}{2}\left\{\left[\frac{cu_j}{x}-\frac{\mu}{(\Delta x)^2}(u_j-u_{j-1})\right]^n-\left[\frac{cu_{j+1}}{x}-\frac{\mu}{(\Delta x)^2}(u_{j+1}-u_j)\right]^n\right.$$

$$\left.+\left[\frac{cu_{j-1}}{x}-\frac{\mu}{(\Delta x)^2}(u_j-u_{j-1})\right]^{\overline{n+1}}-\left[\frac{cu_j}{x}-\frac{\mu}{(\Delta x)^2}(u_{j+1}-u_j)\right]^{\overline{n+1}}\right\}$$

Now, $\displaystyle\sum_{j=2}^{I1-1}(\mathrm{LHS})\Delta x = \sum_{j=2}^{I1-1}(\mathrm{RHS})\Delta x$

Therefore,

$$= \left[c\,\frac{u_2^n + \overline{u_1^{n+1}}}{2} - \frac{\mu}{2\Delta x}\left(u_2^n + \overline{u_2^{n+1}} - u_1^n - \overline{u_1^{n+1}} \right) \right] \qquad (39)$$

$$- \left[c\,\frac{u_{IL}^n + \overline{u_{IL-1}^{n+1}}}{2} - \frac{\mu}{2\Delta x}\left(u_{IL}^n + \overline{u_{IL}^{n+1}} - u_{IL-1}^n - \overline{u_{IL-1}^{n+1}} \right) \right]$$

$$= A - B$$

Note that A and B "sort of" represent the fluxes at $i = 1\ 1/2$ and at $i = IL - 1/2$ (which correspond to the control surfaces of the control volume). It appears that the convective terms of A and B are questionable whereas the dissipative terms are legitimate. In the dissipative terms

$$\frac{\mu}{2\Delta x}\left(u_2^n + \overline{u_2^{n+1}} - u_1^n - \overline{u_1^{n+1}} \right) \qquad \text{for example,}$$

we obtain an averaging of the predicted and corrected values. This is as expected from a close examination of this two-step method. In the convective terms, however, note the forward differencing in the predictor step and backward differencing in the corrector step. For this reason, within the convective terms, u_1 and u_{IL-1} are from the predictor step while u_2 and u_{IL} are from the corrector step. It is difficult to say which terms, convective or dissipative, are better models for the conservation principle in this FDE. The averaging within the dissipative terms may smooth things out too much or it may be just the smoothing needed. The mixing of steps in the convective terms may leave information behind or add data too soon (similar to sinks and sources). In conclusion, MacCormack's FDE possesses the conservation principle. As with all else in numerical analysis, as Δx and Δt approach their ideal values within stability limits, this conservation property of the FDE gets stronger and stronger.

5. TRANSPORTIVE PROPERTY AND TRANSPORTIVE ERROR

For fluid flow, heat transfer, and combustion problems, a disturbance at any location in the flow field can spread to other locations by these mechanisms:

a) Convection or advection (due to fluid motion)

b) Diffusion (due to random molecular motion)

c) Pressure waves

For subsonic flows, diffusion and pressure waves can spread a disturbance in every direction. Convection, however, can only transport the disturbance in one direction; the direction of the fluid velocity.

Since the linear viscous Burgers equation has characteristics similar to the viscous incompressible flow equations, we expect convection and diffusion transportive properties. The MacCormack method FDE will possess the transportive property if it has these properties.

Consider Equation 7, the linear viscous Burgers equation

$$\frac{\delta u}{\delta t} + c\,\frac{\delta u}{\delta x} = \mu\,\frac{\delta^2 u}{\delta x^2} \tag{7}$$

We have seen that the FDE given by the two-step MacCormack method is

$$\begin{aligned} 2u_j^{n+1} = {} & 2u_j^n - \beta(u_{j+1}^n - u_{j-1}^n) \\ & + 2\alpha(u_{j+1}^n - 2u_j^n + u_{j-1}^n) \\ & + \beta^2(u_{j+1}^n - 2u_j^n + u_{j-1}^n) \\ & + \beta\alpha(2u_{j+1}^n - 2u_{j-1}^n + u_{j-2}^n - u_{j+2}^n) \\ & + \alpha^2(u_{j+2}^n - 4u_{j+1}^n + 6u_j^n - 4u_{j-1}^n + u_{j-2}^n) \end{aligned} \tag{12}$$

where $\alpha = \mu\,\frac{\Delta t}{(\Delta x)^2}$ and $\beta = c\,\frac{\Delta t}{\Delta x}$

Suppose that at time level n, u is zero everywhere. Now, consider a disturbance $\gamma > 0$ at grid point j and time level n and examine how this disturbance spreads to the neighboring grid points.

at j

$$2(u_j^{n+1} - \gamma) = (2\alpha + \beta^2)(-2\gamma) + \alpha^2(6\gamma) \tag{40}$$

$$u_j^{n+1} = \gamma(1 + 3\alpha^2 - 2\alpha - \beta^2)$$

at j+1

$$2(u_{j+1}^{n+1}) = \beta(\gamma) + (2\alpha + \beta^2)(\gamma) + \beta\alpha(-2\gamma) + \alpha^2(-4\gamma) \tag{41}$$

$$u_{j+1}^{n+1} = \gamma\left(\tfrac{1}{2}\beta + \tfrac{1}{2}\beta^2 + \alpha - \beta\alpha - 2\alpha^2\right)$$

at j+2

$$2(u_{j+2}^{n+1}) = \beta\alpha(\gamma) + \alpha^2(\gamma) \tag{42}$$

$$u_{j+2}^{n+1} = \tfrac{1}{2}\gamma(\alpha^2 + \beta\alpha)$$

at j-1

$$u_{j-1}^{n+1} = \gamma\left(-\tfrac{1}{2}\beta + \tfrac{1}{2}\beta^2 + \alpha + \beta\alpha - 2\alpha^2\right) \tag{43}$$

at j-2

$$u_{j-2}^{n+1} = \tfrac{1}{2}\gamma(\alpha^2 - \beta\alpha) \tag{44}$$

Recall that, for numerical stability, we found these two criteria

$$\alpha = 0, \ \beta \leq 1,$$

$$\beta = 0, \ \alpha \leq 1/2$$

For $\alpha = 0$ at time level n+1, we get

$$u_j = \gamma(1 - \beta^2) \tag{45}$$

$$u_{j+1} = \tfrac{1}{2}\gamma(\beta^2 + \beta) \tag{46}$$

$$u_{j+2} = 0 \tag{47}$$

$$u_{j-1} = \tfrac{1}{2}\gamma(\beta^2 - \beta) \tag{48}$$

$$u_{j-2} = 0 \tag{49}$$

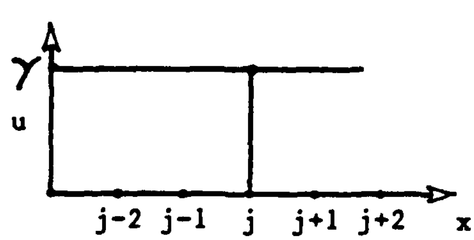

$$\beta = 0, \ u_j = \gamma$$

$$u_{j+1} = u_{j+2} = u_{j-1} = u_{j-2} = 0$$

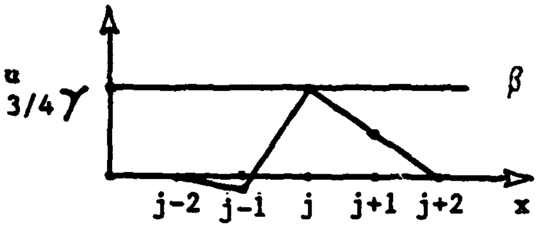

$\beta = \frac{1}{2}$, $u_j = \frac{3}{4}\gamma$, $u_{j+1} = \frac{3}{8}\gamma$, $u_{j-1} = -\frac{1}{8}\gamma$

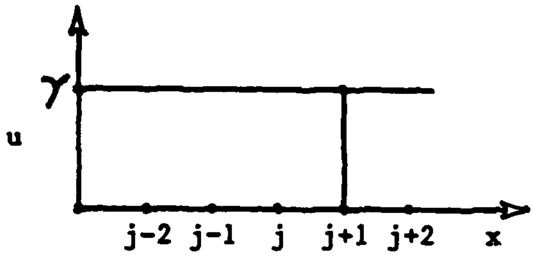

$\beta = 1$, $u_j = u_{j-1} = u_{j-2} = u_{j+2} = 0$

$u_{j+1} = 1$

This is a very interesting result because $\beta = c\,\frac{\Delta t}{\Delta x}$ is the convection term and here we have perfect convection at $\beta = 1$.

For $\beta = 0$ at time level n+1, we get

$$u_j = \gamma\,(3\alpha^2 - 2\alpha + 1) \qquad (50)$$

$$u_{j+1} = \gamma\,(\alpha - 2\alpha^2) \qquad (51)$$

$$u_{j+2} = \gamma\,(\tfrac{1}{2}\alpha^2) \qquad (52)$$

$$u_{j-1} = \gamma\,(\alpha - 2\alpha^2) \qquad (53)$$

$$u_{j-2} = \gamma\,(\tfrac{1}{2}\alpha^2) \qquad (54)$$

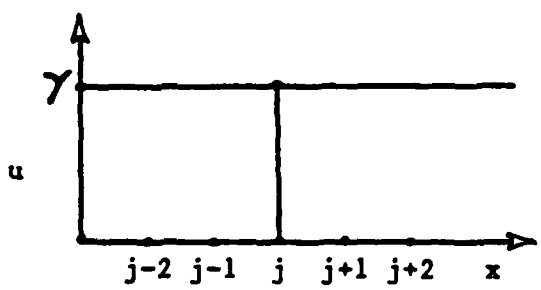

$\alpha = 0$, $u_j = \gamma$

$u_{j+1} = u_{j-1} = u_{j+2} = u_{j-2} = 0$

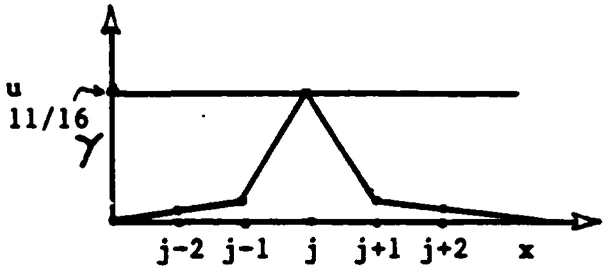

$\alpha = \frac{1}{4}$, $u_j = \frac{11}{16}\gamma$

$u_{j+1} = u_{j-1} = \frac{1}{8}\gamma$, $u_{j+2} = u_{j-2} = \frac{1}{32}\gamma$

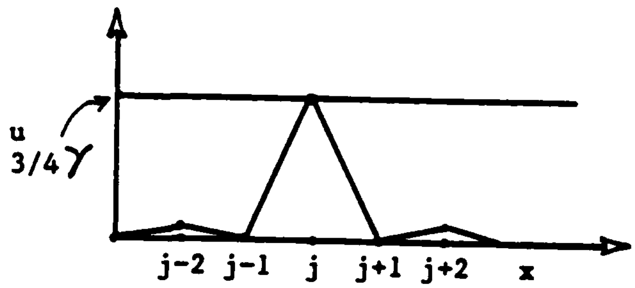

$\alpha = \frac{1}{2}$, $u_j = \frac{3}{4}\gamma$, $u_{j+1} = u_{j-1} = 0$

$u_{j+2} = u_{j-2} = \frac{1}{8}\gamma$

To truly represent the physics in the process, the u_{j+2} and u_{j-2} terms must be less than our equal to the u_{j+1} and u_{j-1} terms. Therefore,

$$
\begin{aligned}
&\tfrac{1}{2}\alpha^2 \leq \alpha - 2\alpha^2 \\
&\tfrac{5}{2}\alpha \leq 1 \qquad\qquad (55) \\
&\alpha \leq \tfrac{2}{5} \quad \text{or} \quad \mu\frac{\Delta t}{(\Delta x)^2} \leq \tfrac{2}{5}
\end{aligned}
$$

The results for $\beta = 0$ and these figures tell us

1. For all $\alpha \in [0,1/2]$, the disturbance spreads in every direction (+ and - x-axis). This is consistent with the transport characteristics given by Equation 2.

2. For a disturbance of the form $\delta(x-x_j)$ where $\delta(x-x_j)$ is the delta function, $\mu \frac{\Delta t}{(\Delta x)^2}$ should be less than 2/5 in order to obtain physically reasonable results for the first time step.

An investigation of the transportive property for the α and β terms varying within their respective stability ranges is difficult analytically and a numerical result is presented. Please note that the program used to

generate these figures models the original nonlinear viscous equation rather than the linear equation. We give the domain a disturbance at u(15) of 1 at time level 0. At time step 1 (Figure 18), we see the convective property in that u(17) is 0.1875, and we see the diffusion property in u(14), u(16) and in u(17). At time step 30 (Figure 19), we see a history of the disturbances passing through the discretized domain. Since the value u takes on between u(15) and u(29) is greater than its counterparts' value between u(2) and u(14) at this time step, coupled with the smoothing out of the disturbance, we can say that the FDE has the same transportive properties as the PDE. (Note: u(1) = u(30) = 0 are fixed boundary conditions within the code.) One thing to point out, though, is that we have been looking at $\beta = .5$ in Figures 18 and 19. If we set $\beta = .4$, the limiting value for a true representation of physics, we get the results shown in Figures 20 and 21. Notice how these plots display the transportive properties in a more realistic manner. For this reason, $\beta \leq .4$ is recommended.

6. DISSIPATION ERROR

Diffusion spreads a disturbance in every direction by random molecular motion. As diffusion spreads a disturbance in every direction, the disturbance is smoothed out over an increasingly larger region of space, thus reducing spatial gradients and lowering the magnitude of the disturbance. This effect is called dissipation.

Diffusion is mathematically described by even-order derivatives, i.e., $c_n \dfrac{\partial^{2n} u}{\partial x_i^{2n}}$, $c_n \dfrac{\partial^{2n} u}{\partial x_i^n \partial x_j^n}$, n=1,2,... Specific examples include $\mu\Delta^2 V$ in the momentum equation which represents the diffusion of momentum and $k\nabla^2 T$ in the thermal energy equation which represents the diffusion of thermal energy. If all of the coefficients of the even-order spatial derivatives in a PDE are zero, then that PDE does not have any dissipative characteristics.

In order for an FDE to have the same dissipative characteristics as the PDE that it is to represent, the coefficients of the even-order spatial derivatives in the modified equation (for the FDE) must be identical to the corresponding coefficients in the PDE. The modified equation is the

PDE which is actually solved when a finite-difference method is applied to a PDE. If the corresponding coefficients are different, then the solutions of the FDE will contain dissipation errors.

The dissipation errors in the solutions of FDEs are usually examined by the Von Neumann's method. The dissipation error for each Fourier component of a disturbance after n time steps is given by

$$[|G_{PDE}|^{(n)} - |G|^{(n)}]A^{0} \tag{56}$$

where

G_{PDE} = amplification factor of the PDE

G = amplification factor of the FDE

A^{0} = initial amplitude of the Fourier component

$|\Phi|$ = modulus of Φ

Dissipation error is given by Equation 56 because the modulus of the amplification factor depends solely on the even-order spatial derivatives when the highest time-derivative is first order.

Once again, consider the linear viscous Burgers Equation

$$\frac{\delta u}{\delta t} + c\,\frac{\delta u}{\delta x} = \mu\,\frac{\delta^{2} u}{\delta x^{2}} \quad c \text{ and } \mu \text{ are real constants} \tag{7}$$

This equation obviously has dissipative characteristics since the coefficient of the even-order spatial derivative is not zero. To find the amplification factor of Equation 2, substitute a Fourier component

$$u_j = e^{\alpha j t} e^{I k j x} \tag{57}$$

where

k_j = wave number

I = $\sqrt{-1}$

α = unknown complex number (a+bI)[Equation 7 will be used to determine α, i.e., only disturbances that are also solutions of Equation 7 are considered]

of the disturbance $u = \sum_j u_j$

into Equation 7 and obtain

$$\alpha_j e^{\alpha_j t} e^{I k_j x} + c I k_j e^{\alpha_j t} e^{I k_j x} = \mu (I k_j)^2 e^{\alpha_j t} e^{I k_j x}$$

Since $I^2 = -1$ and eliminating $uj = e^{\alpha j t} e^{Ikjx}$, we get

$$\alpha_j = -\mu k_j^2 - c I k_j \text{ , i.e. , } a = -\mu k_j^2 \text{ and } b = -c k_j \tag{58}$$

By using Equation 58, the amplification factor for Equation 7 is

$$G_{PDE} = e^{-\mu k_j^2 \Delta t} e^{I \Phi_{PDE}} \tag{59}$$

Since

$$G_{PDE} = |G_{PDE}| e^{I\Phi_{PDE}}$$

then

$$|G_{PDE}| = e^{-\mu k_j^2 \Delta t}$$

and, therefore,

$$|G_{PDE}| \leq 1$$

We see the disturbance is dissipated as expected. Let us now evaluate the dissipation error for our FDE repeated below

$$\begin{aligned} 2u_j^{n+1} = {} & 2u_j^n - \beta(u_{j+1}^n - u_{j-1}^n) \\ & + 2\alpha(u_{j+1}^n - 2u_j^n + u_{j-1}^n) \\ & + \beta^2(u_{j+1}^n - 2u_j^n + u_{j-1}^n) \\ & + \beta\alpha(2u_{j+1}^n - 2u_{j-1}^n + u_{j-2}^n - u_{j+2}^n) \\ & + \alpha^2(u_{j+2}^n - 4u_{j+1}^n + 6u_j^n - 4u_{j-1}^n + u_{j-2}^n) \end{aligned} \tag{12}$$

The modified equation for Equation 12 is

$$\frac{\partial u}{\partial t} + c\,\frac{\partial u}{\partial x} - \mu\frac{\partial^2 u}{\partial x^2} = -\frac{c}{6}\,(\Delta x^2 - c^2\Delta t^2)\,\frac{\partial^3 u}{\partial x^3}$$

$$-\frac{c^2\Delta t}{8}\,(\Delta x^2 - c^2\Delta t^2) + \frac{\mu}{2}\,(c^2\Delta t^2 - \frac{\Delta x^2}{6})\;\frac{\partial^4 u}{\partial x^2}\;\ldots$$

Since all the coefficients of the even-order spatial derivatives in the modified equation do not match all the corresponding coefficients in Equation 7, there is a dissipation error in the solution. The modified equation is said to have fourth-order dissipation because the second-order dissipative term coefficient matches the dissipative term coefficient of the PDE.

The amplification factor for Equation 7 is given be the Von Neumann's method (from the stability analysis done earlier) as

$$G_j = [1 + (2\alpha + \beta^2)(\cos\gamma - 1) + 2\alpha^2(\cos\gamma - 1)^2] \quad (27)$$

$$+ I\{-\beta\sin\gamma[2\alpha(\cos\gamma - 1) + 1]\}$$

where

$$\alpha = \mu\,\frac{\Delta t}{(\Delta x)^2}$$

$$\beta = c\,\frac{\Delta t}{\Delta x}$$

$$\gamma = k_j\Delta x$$

If $A = (\cos\gamma - 1)$, then the modulus of the amplification factor is

$$|G| = \{[1 + (2\alpha + \beta^2)A + 2\alpha^2A^2]^2$$

$$+ [-\beta\sin\gamma\,(2\alpha A + 1)]^2\}^{\frac{1}{2}}$$

The dissipation error for each Fourier component of the solution of Equation 7 after n time steps is (assuming initial amplitude of unity)

$$|G_{PDE}|^{(n)} - |G|^{(n)}$$

Recall that $|G_{PDE}| = e^{-\mu k_j^2 \Delta t}$ and $\gamma = k_j \Delta x$. Thus, the following can be written

$$|G_{PDE}| = e^{-\gamma^2 \mu \frac{\Delta t}{(\Delta x)^2}}$$

$$|G_{PDE}| = e^{-\gamma^2 \alpha}$$

Programs 2 and 3 in the program section generate this curve and the curve for $|G|$ in the figures to be discussed next.

When $\alpha = 0$, the result is

$$|G_{PDE}| = 1$$

and so the dissipation error is

$$1 - |G|^{(n)}$$

Note that when $\alpha = 0$, the Lax-Wendroff scheme is obtained. Figure 22 is the plot for the dissipation error in this case which agrees with previous work on the Lax-Wendroff scheme (Reference 4). The dissipation error is small when β (also known as the Courant number) is small, not just when γ is small. This indicates that when β is small (and $\alpha = 0$), the dissipation for every Fourier component is small.

For α at other values within its stability limits, the following must be considered

$$(|G_{PDE}|^{(n)} - |G|^{(n)})$$

where $|G_{PDE}|$ is defined above. First, set $\alpha = .25$ and run β at .25, .5, .75, and .86 - values within the stability limits for this α. Also run β at .9 for curiosity's sake. In Figure 23, the dissipation error grows as γ increases at the same rate for all values of β examined. For larger values of β, the error grows faster. Next, set $\alpha = .5$ and run β at .25, .5, .75, .96, and 1 in Figure 24. The results are roughly the same as at $\alpha = .25$ in Figure 23.

For many problems, the solution depends primarily on the first few terms of the Fourier series which correspond to Fourier components with low wave numbers (i.e., long wavelengths). In these cases, it would be acceptable to

have a large amount of dissipation error in Fourier components with large wave numbers (i.e., short wavelengths) since these terms are very small and do not contribute significantly to the solution.

Furthermore, since Fourier components with the largest wave numbers are the least stable, it is often desirable to have more dissipation at the larger wave numbers to assure stability.

FDEs with

$$|G| \leq 1$$

for every Fourier component are said to be dissipative FDEs. Note that $|G| \leq 1$ also indicates numerical stability. The total error in the solutions of FDEs is made up, in general, of two parts: discretization error and stability error. Stability error is small for stable FDEs since, by definition, disturbances and errors cannot grow for stable FDEs. Thus, discretization error accounts for most of the total error. The discretization error can be broken up into two parts: the dissipation error and the dispersion error. Recall that

$$u^{n+1} = Gu^n$$

so that if G and u are correct, then u will be correct and

$$G = |G| \, e^{I\Phi}$$

The error in $|G|$ gives rise to dissipation error and the error in Φ (the phase angle) gives rise to dispersion error. Dispersion error will be discussed in the next section.

Since $|G|$ is related to even-order spatial derivatives and Φ is related to odd-order spatial derivatives, dissipation error dominates over dispersion error if the lowest-order term in the truncation error is an even-order spatial derivative. The reverse is true if the lowest-order term in the truncation error is an odd-order spatial derivative. For the MacCormack method FDE examined, note from the modified equation that the lowest-order spatial derivative is of odd-order. Therefore, dispersion error dominates.

In fluid flow, heat transfer, and combustion problems, dissipation error arises from differencing the convection terms (first-order spatial derivatives). Dissipation error should be minimized so that numerical dissipation does not swamp physical dissipation. From the coefficient for the fourth-order spatial derivative in the modified equation for the MacCormack FDE, a functional relationship can be derived between α and β that will eliminate this error term as follows

$$\frac{c^2 \Delta t}{8}\left(\Delta x^2 - c^2 \Delta t^2\right) = \frac{\mu}{2}\left(\frac{\Delta x^2}{6} - c^2 \Delta t^2\right)$$

$$\alpha = \frac{1}{4}\frac{(\beta^2 - \beta^4)}{(\frac{1}{6} - \beta^2)}$$

A plot of this relationship is shown in Figure 25.

7. PHASE AND DISPERSION ERROR

A medium is said to be dispersive if the phase velocities of waves propagating in that medium depend on the wavelengths of the waves. In a dispersive medium, waves with different wavelengths will separate more and more from each other in space. The phase velocity of a sinusoidal wave

$$e^{at}\, e^{ik_j x} = e^{at}\, e^{i(k_j x + bt)} = e^{at}\, e^{ik_j(x + \frac{b}{k_j}t)} \text{ is } -\frac{b}{k_j}.$$

Dispersion is mathematically described by odd-order spatial derivatives, i.e., $c_n \dfrac{\partial^{2n+1} u}{\partial x_1^{2n+1}}$, n=1,2,... if the highest-order time derivative is first-order. In order for an FDE to have the same dispersive characteristics as the PDE that it is to represent, the coefficients of the odd-order spatial derivatives in the modified equation (for that FDE) must be identical to the corresponding coefficients in the PDE. If the corresponding coefficients are different, then the solutions of the FDEs would contain dispersive errors.

Dispersion error, like dissipation error, is also examined by the Von Neumann's method. The dispersion error for each Fourier component of a disturbance after n time steps is given by

$$\eta\,(\Phi_{pde} - \Phi) \tag{60}$$

where

Φ_{PDE} = phase angle of the amplification factor of the PDE

Φ = phase angle of the amplification factor of the FDE

The relative phase shift error for a given Fourier component after a one time step is defined as

$$\frac{\Phi}{\Phi_{pde}} \tag{61}$$

If the relative phase shift error > 1 for a given Fourier component, then the numerical solution for that Fourier component gives a wave speed > the wave speed given by the exact solution. This is called a leading phase error. If the relative phase shift error < 1, then the numerical solution gives a wave speed < the wave speed of the exact solution. This is called lagging phase error.

Dispersion error is given by Equations 60 and 61 because the phase angle of the amplification factor depends solely on the odd-order spatial derivatives when the highest time derivative is first-order.

Once again, consider the linear viscous Burgers equation

$$\frac{\delta u}{\delta t} + c\,\frac{\delta u}{\delta x} = \mu\,\frac{\delta^2 u}{\delta x^2} \tag{7}$$

where c and μ are real constants. The amplification factor for Equation 2 was derived in the previous section where the phase angle Φ_{PDE} is =

$$-ck_j\Delta t = -\beta\gamma,\ \beta = c\frac{\Delta t}{\Delta x},\ \gamma = k_j\Delta x$$

The phase velocity is $-\frac{b}{k_j} = -(-\frac{ck_j}{k_j}) = c$ and is the same for every Fourier component. Thus, Equation 7 does not possess any dispersive characteristics.

Evaluation of the dispersion error of the MacCormack method applied to Equation 7 yields:

Predictor:
$$u_j^{\overline{n+1}} = u_j^n - c\frac{\Delta t}{\Delta x}(u_{j+1}^n - u_j^n) \tag{10}$$
$$+ \mu\frac{\Delta t}{(\Delta x)^2}(u_{j+1}^n - 2u_j^n + u_{j-1}^n)$$

Corrector:
$$u_j^{n+1} = \frac{1}{2}\left[u_j^n + u_j^{\overline{n+1}} - c\frac{\Delta t}{\Delta x}(u_j^{\overline{n+1}} - u_{j-1}^{\overline{n+1}}) \right. \tag{11}$$
$$\left. + \mu\frac{\Delta t}{(\Delta x)^2}(u_{j+1}^{\overline{n+1}} - 2u_{j+1}^{\overline{n+1}} + u_{j-1}^{\overline{n+1}})\right]$$

The modified equation for the FDE is
$$\frac{\delta u}{\delta t} + C\frac{\delta u}{\delta x} - \mu\frac{\delta^2 u}{\delta x^2} = -\frac{C}{6}(\Delta x^2 - C^2\Delta t^2)\frac{\delta^3 u}{\delta x^3}$$
$$-\left[\frac{c^2\Delta t}{8}(\Delta x^2 - c^2\Delta t) + \frac{\mu}{2}\left(c^2\Delta t^2 - \frac{\Delta x^2}{6}\right)\right]\frac{\delta^4 u}{\delta x^2} - \ldots$$

Since the coefficients of the odd-order spatial derivatives in the modified equation do not match the corresponding coefficients in Equation 7, the solutions of the FDE contain dispersion error of third-order. The order of dispersion is equal to the order of the lowest order odd-order spatial derivative with nonzero coefficients excluding the first-order spatial derivative. In general, the higher the order of dispersion, the lower the dispersion error.

The phase angle of the amplification factor for Equation 7 is

$$\Phi_{FDE} = \tan^{-1}\frac{\mathrm{Im}(G)}{\mathrm{Re}(G)} \tag{62}$$

$$\Phi_{FDE} = \frac{-\beta\sin\gamma(2\alpha A + 1)}{1 + (2\alpha + \beta^2)A + 2\alpha^2 A^2}$$

where $\alpha = \mu\frac{\Delta t}{(\Delta x)^2}$; $\beta = c\frac{\Delta t}{\Delta x}$, $A = \cos\gamma - 1, \gamma = k_j\Delta x$

If $\alpha = 0$

$$\Phi_{FDE} = \frac{-\beta \sin\gamma}{1 + \beta^2 A}$$

$$\Phi_{FDE} = \frac{-\beta \sin\gamma}{1 - \beta^2(1-\cos\gamma)} \tag{63}$$

The dispersion error for each Fourier component of the solutions of the FDE after n time steps is

$$n(\Phi_{PDE} - \Phi) = n\left[-\beta\gamma - \tan^{-1} \frac{-\beta \sin\gamma\,(2\alpha A + 1)}{1 + (2\alpha + \beta^2)A + 2\alpha^2 A^2}\right] \tag{64}$$

The relative phase shift error for each Fourier component after one time step is

$$\frac{\Phi}{\Phi_{PDE}} = \frac{\tan^{-1} \dfrac{-\beta \sin\gamma\,(2\alpha A + 1)}{1 + (2\alpha + \beta^2)A + 2\alpha^2 A^2}}{-\beta\gamma} \tag{65}$$

For $\alpha = 0$, or the Lax-Wendroff scheme for the linear inviscid Burgers equation, a plot for $\beta = .25, .5, .75$, and 1 is in Figure 26. The solution here has predominantly lagging phase error except for large wave numbers with $\beta \epsilon$ $(\sqrt{.5}, 1.)$. For $\beta = 1$, the relative phase shift error increases as γ increases. From Figure 22, notice that when $\alpha = 0$, the FDE is not very dissipative for any β when γ is low (Figure 22). As a result, dispersion error is very important when $\alpha = 0$. For $\alpha = .25$, a plot of $\beta = .25, .5, .75, .86$, and .9 is in Figure 27. Observe that the solution here has lagging phase error for all wave numbers when $\beta \epsilon$ (0,.5) which increases as γ increases. For $\beta \epsilon$ (.5,.9), small lagging phase error is observed for γ up to 60°. When $\gamma > 60$, the leading phase shift error takes over which increases as γ increases. At approximately $\gamma > 110^{\circ}$, the leading error decreases as γ increases. For $\alpha = .5$, a plot of $\beta = .25, .5, .75, .96$, and 1 is in Figure 28. For $\beta \epsilon$ (0,.5), lagging phase error occurs. For $\beta \epsilon$ (.5, 1), leading phase error occurs which increases dramatically as γ increases. The same conclusions that were drawn from Figure 22 for the $\alpha = 0$ case can be drawn from Figures 23 and 24 for these two cases since the general trend seems to be the same. The program that generated the data for this figure is in the Program Listing Section (Program 4).

SECTION III

COMPUTER SOLUTION

For this section of the analysis, the nonlinear viscous Burgers equation will be solved

$$\frac{\delta u}{\delta t} + u\frac{\delta u}{\delta x} = \mu\frac{\delta^2 u}{\delta x^2} \tag{1}$$

Equation 1 will be solved numerically by rewriting it in conservative law form

$$\frac{\delta u}{\delta t} + \frac{\delta}{\delta x}\left(\frac{1}{2}u^2\right) = \mu\frac{\delta^2 u}{\delta x^2} \tag{66}$$

The conservative law form of PDEs occurs when the coefficients of the derivative terms are either constant, or, if variable, their derivatives appear nowhere in the equation. This form of the PDE circumvents some numerical problems where discontinuities, such as shock waves, show up.

The MacCormack method for this PDE is

Predictor:
$$\overline{u_j^{n+1}} = u_j^n - \frac{\Delta t}{\Delta x}\left[\left(\frac{1}{2}u^2\right)_{j+1}^n - \left(\frac{1}{2}u^2\right)_j^n\right] \tag{67}$$

$$+\mu\frac{\Delta t}{(\Delta x)^2}\left(u_{j+1}^n - 2u_j^n + u_{j-1}^n\right)$$

Corrector:
$$u_j^{n+1} = \frac{1}{2}\left\{u_j^n + \overline{u_j^{n+1}} - \frac{\Delta t}{\Delta x}\left[\left(\frac{1}{2}u^2\right)_j^{\overline{n+1}} - \left(\frac{1}{2}u^2\right)_{j-1}^{\overline{n+1}}\right]\right. \tag{68}$$

$$\left.+\mu\frac{\Delta t}{(\Delta x)^2}\left(\overline{u_{j+1}^{n+1}} - 2\overline{u_j^{n+1}} + \overline{u_{j-1}^{n+1}}\right)\right\}$$

A listing of the exact algorithm used to implement MacCormack's method is in Program 5. Within the program were options for boundary condition values which remain fixed during program execution. One could also change the starting solution as was demonstrated in the Transportive Property section when a point disturbance was introduced in the middle of the discretized domain.

For all the runs discussed, Δt and $\Delta x = .1$. This made $\frac{\Delta t}{\Delta x} = 1$ and simplified the analysis of other parameters. The MR parameter in the output figures represent the mesh Reynolds number in a sense. It actually is $\frac{\Delta x}{\mu}$ since the velocity type term is variable here rather than a constant c. This MR parameter also tells about $\beta = \mu\frac{\Delta t}{(\Delta x)^2}$ which is just $\frac{1}{MR}$ (since $\frac{\Delta t}{\Delta x}$ = 1). The domain is discretized into 30 sections and the time parameter can run as long as one wishes. The parameter μ is the only variable that will be used here besides time. Also, u(1) = 1 and u(30) = 0 for all cases. The stability limits and other results from Section II can be extrapolated if a small safety margin is used (to account for the crossing into the nonlinear domain from the linear realm).

Begin with $\mu = .1$ which yields MR = 1 and hence $\beta = 1$. The β limit derived earlier for the linear case was $\beta \leq .5$ so instability is expected in this case. Figures 29 and 30 show the first two time steps at these values, and the solution goes unstable very fast. When $\mu = .4$, MR = .25, and hence $\beta = 4$, the instability grows even faster as can be seen in Figure 31. As the value of MR approaches 2, i.e., β approaches .5, the effects of dispersion error lessens and a more stable solution evolves. Figures 32 through 37 show the histories of the solution as β takes on values of .67, .57, .556, .54, .53, and .5. Notice in Figure 37 also that the solution is very smooth and resembles the exact solution with dissipative characteristics extremely well.

The analysis for the transportive property showed that for the linear FDE, a value of $\beta \leq .4$ models the physics of the diffusion process in a more realistic sense. When β is run at values of .4, .38, .36, and .33 in Figures 39 through 42, it can be seen that as the value of β decreases the amount of time it takes for the dispersion error to grow decreases. From this small test, it would seem that keeping β between .4 and .5 would yield the most robust solutions.

SECTION IV

CONCLUSIONS

This report has illustrated the procedures used to evaluate a numerical technique's ability to model a partial differential equation. The MacCormack numerical technique, as applied to the linear viscous Burgers equation, was used for the analysis. The finite difference equation from the MacCormack method was examined for consistency, stability, convergence, dissipation, phase and dispersion. A computer solution using the MacCormack method was compared to the analytical results. Valuable stability limits and parameters for maintaining accurate physics modeling determined in the analytic study were demonstrated with the computer solutions.

The procedures documented herein are applicable to a wide range of problems that require an analytical evaluation of a numerical technique before actual computer implementation. This analytical evaluation is necessary if computer results are to be used with confidence.

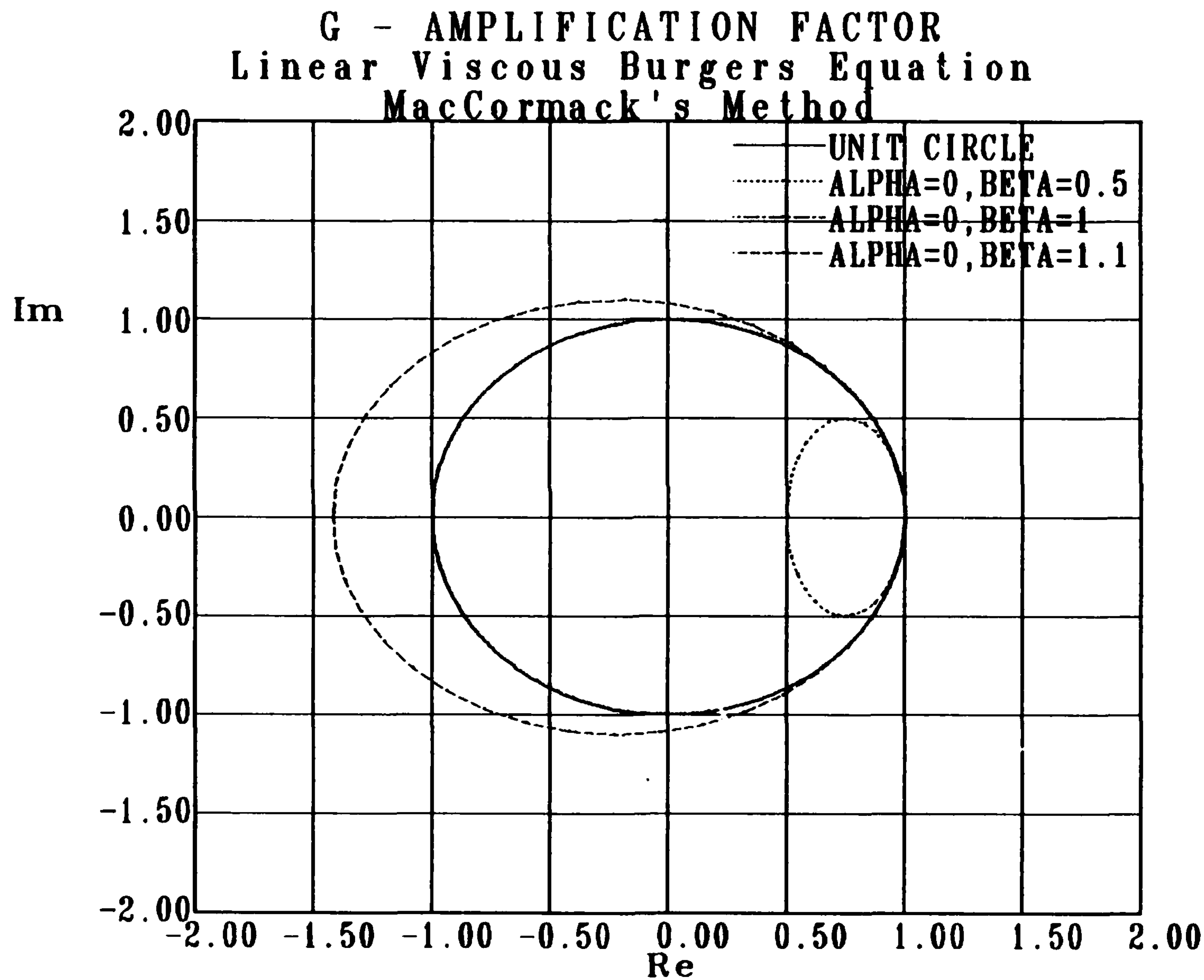

Figure 1. Stability at $\alpha = 0$ (a.k.a. Lax-Wendroff method)

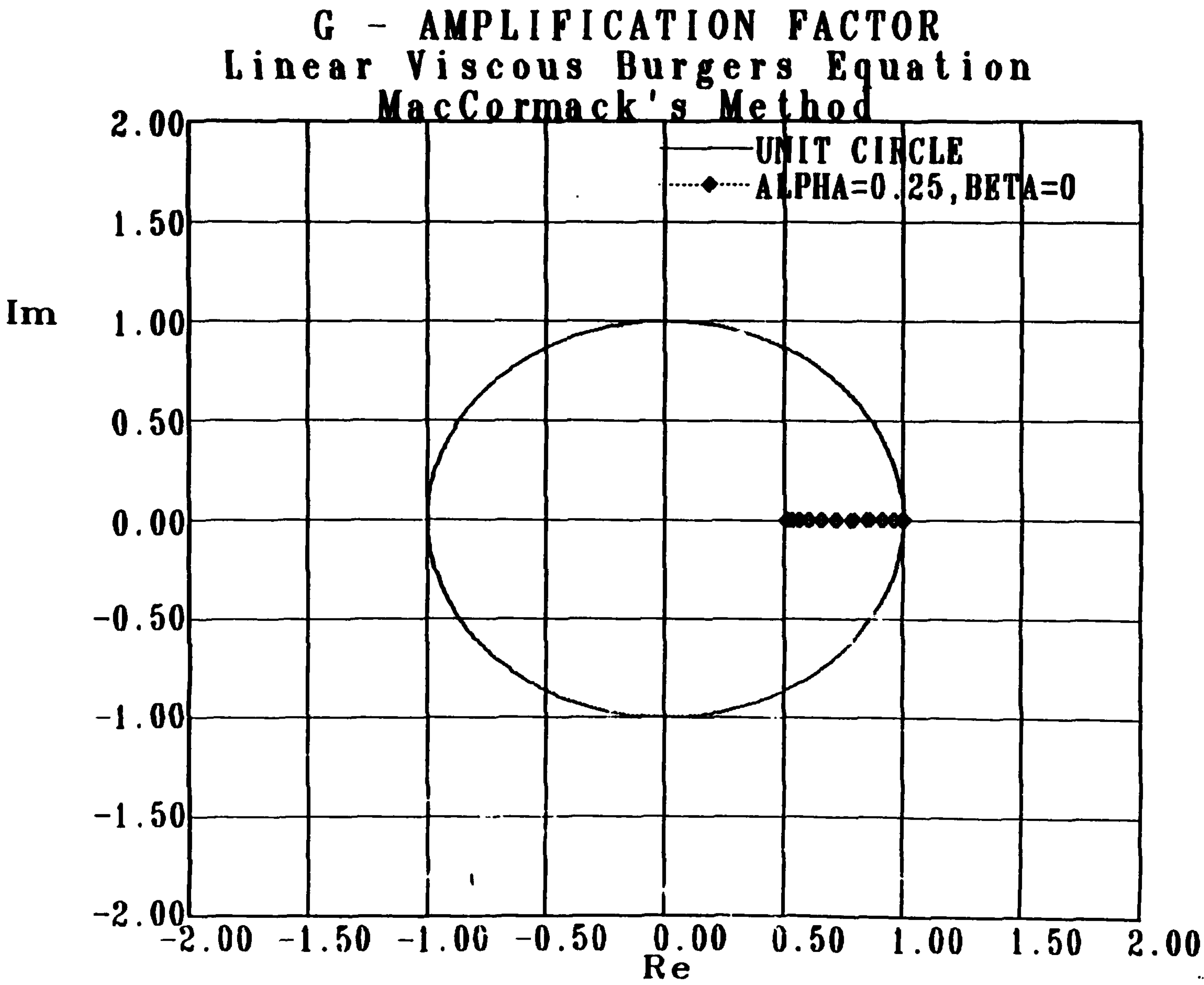

Figure 2. Stability for heat equation at $\alpha = .25$.

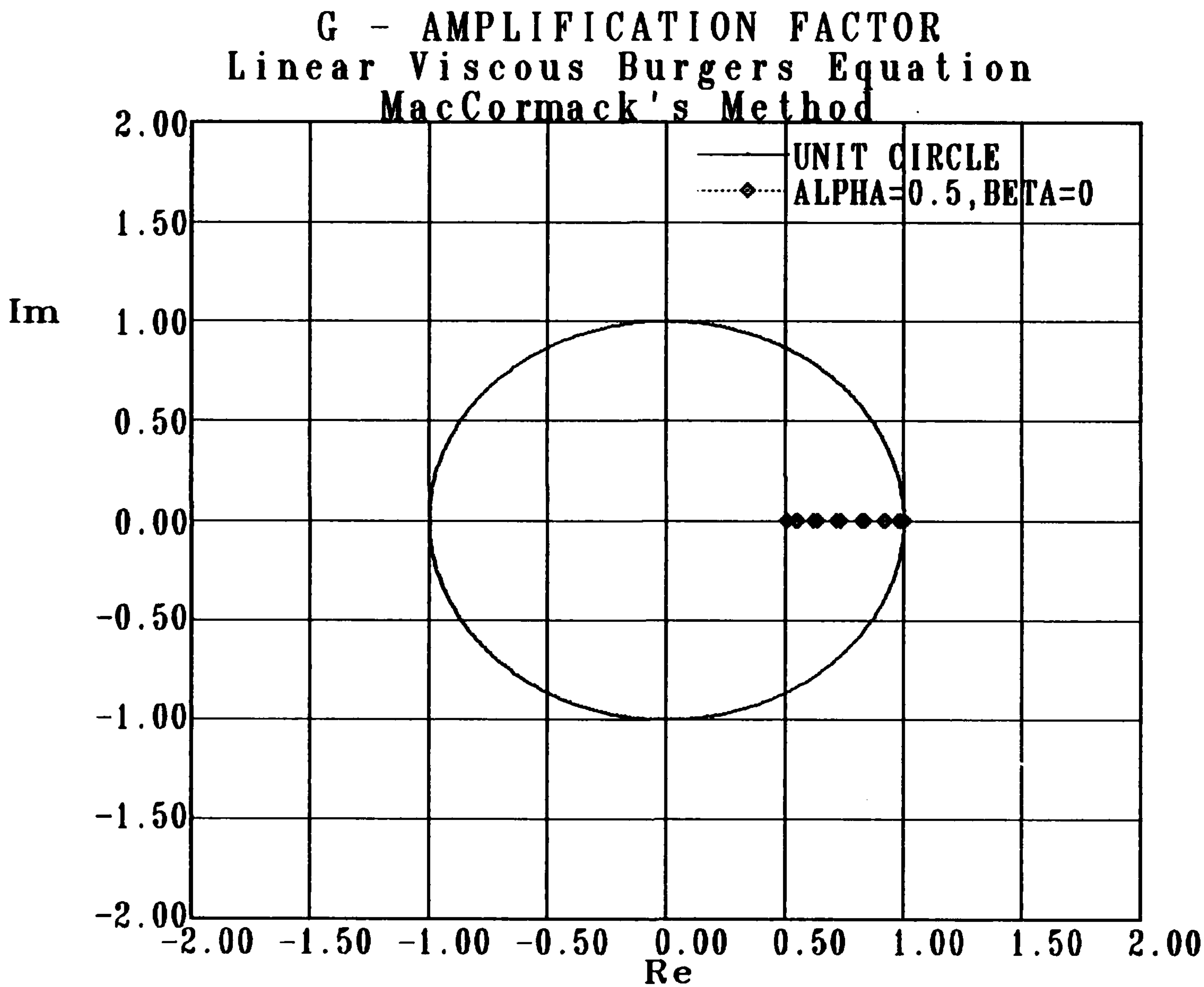

Figure 3. Stability for heat equation at $\alpha = .5$.

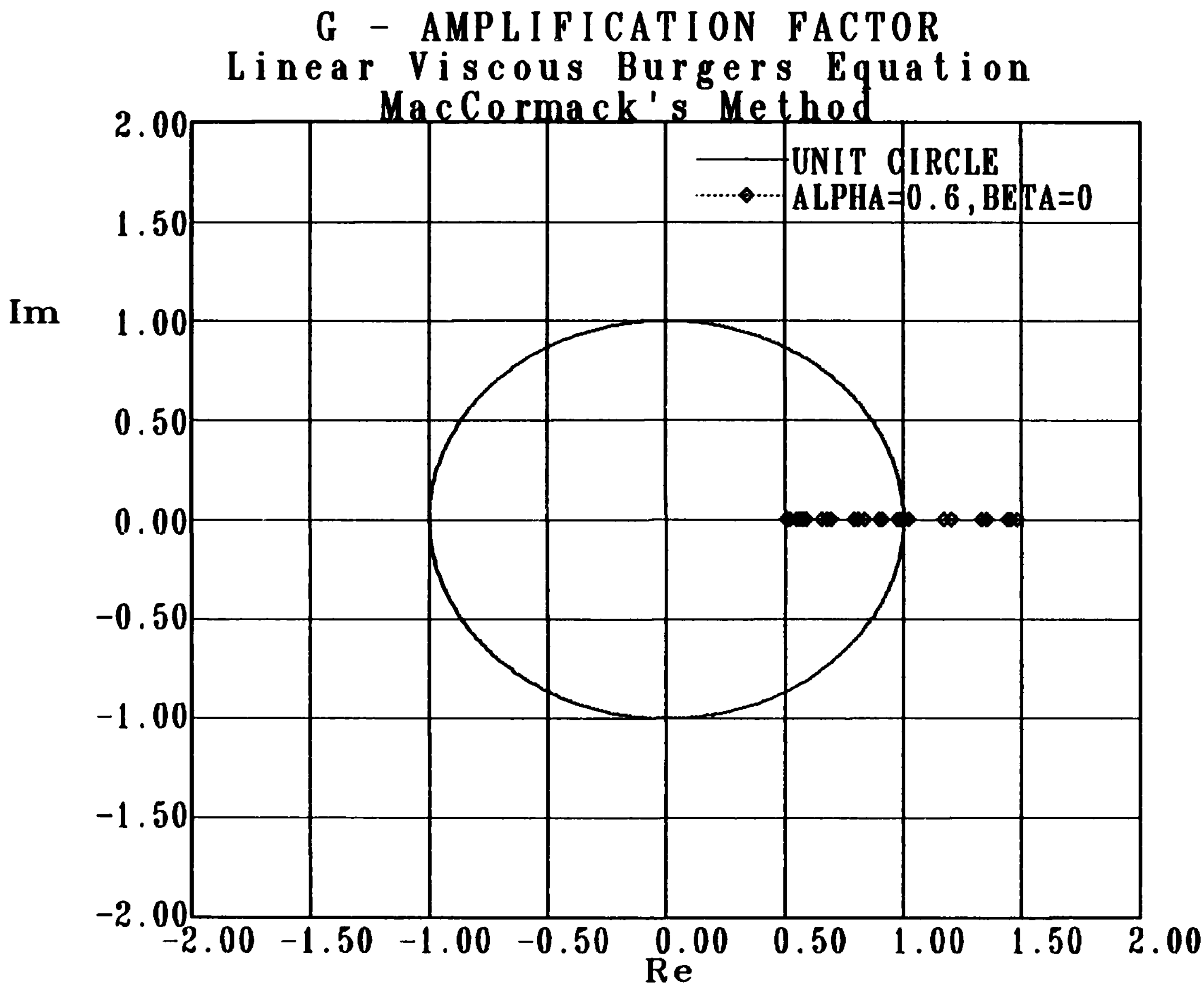

Figure 4. Instability of heat equation at $\alpha > .5$ (i.e., $\alpha = .6$).

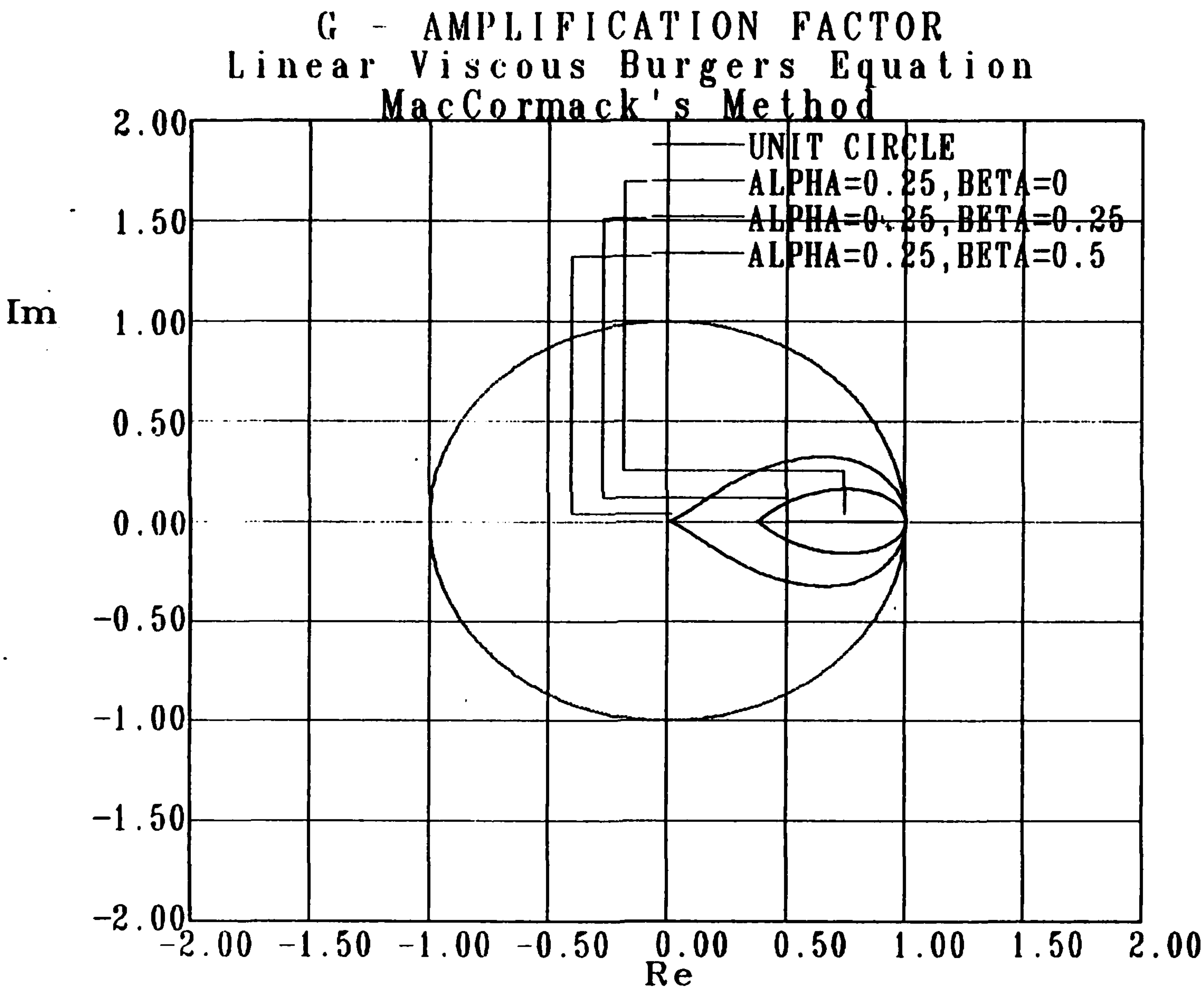

Figure 5(a). Stability of $\alpha = .25$ for $\beta = 0, .25, .5$.

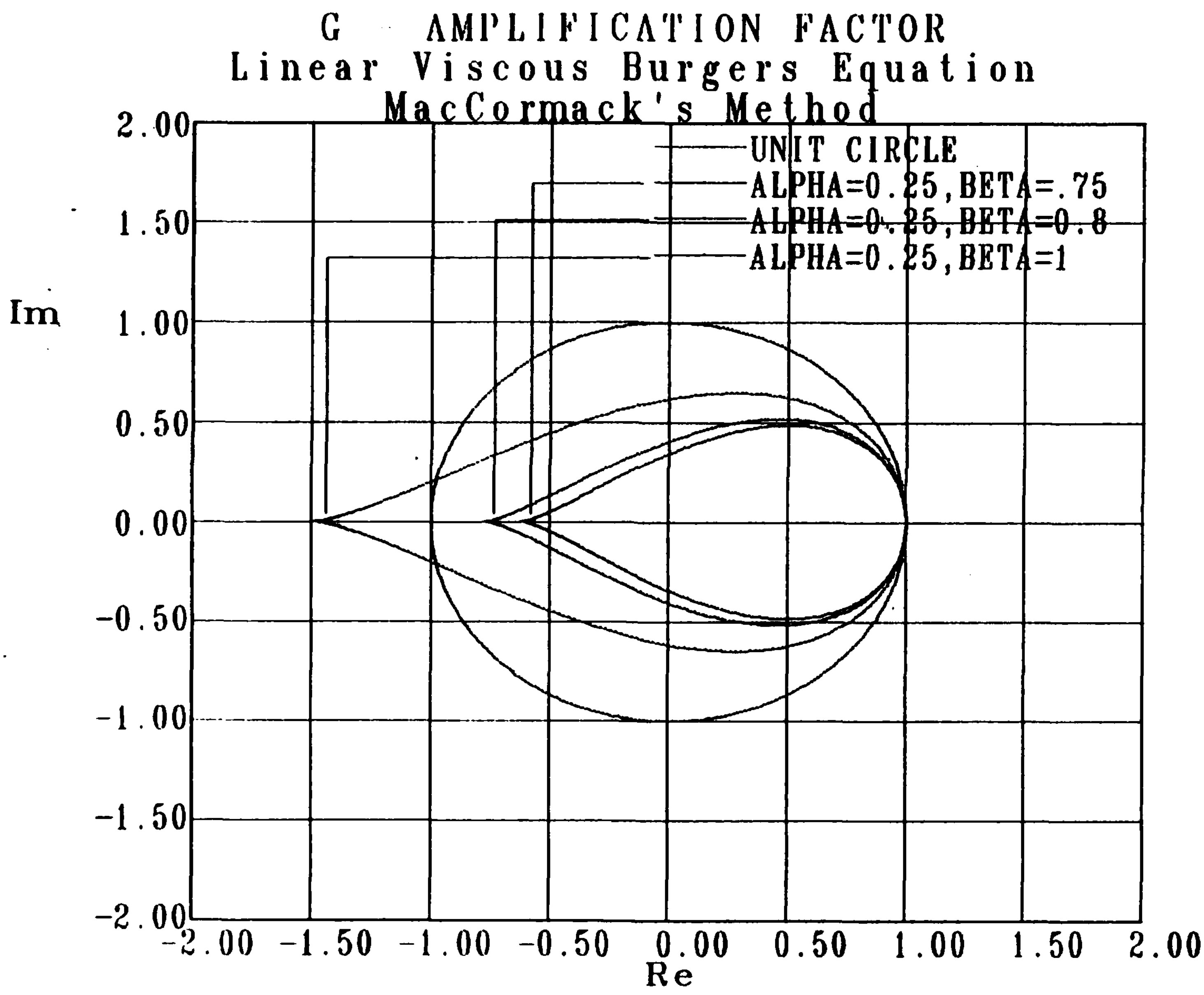

Figure 5(b). Stability of $\alpha = .25$ for $\beta = .75$, .8, and 1.

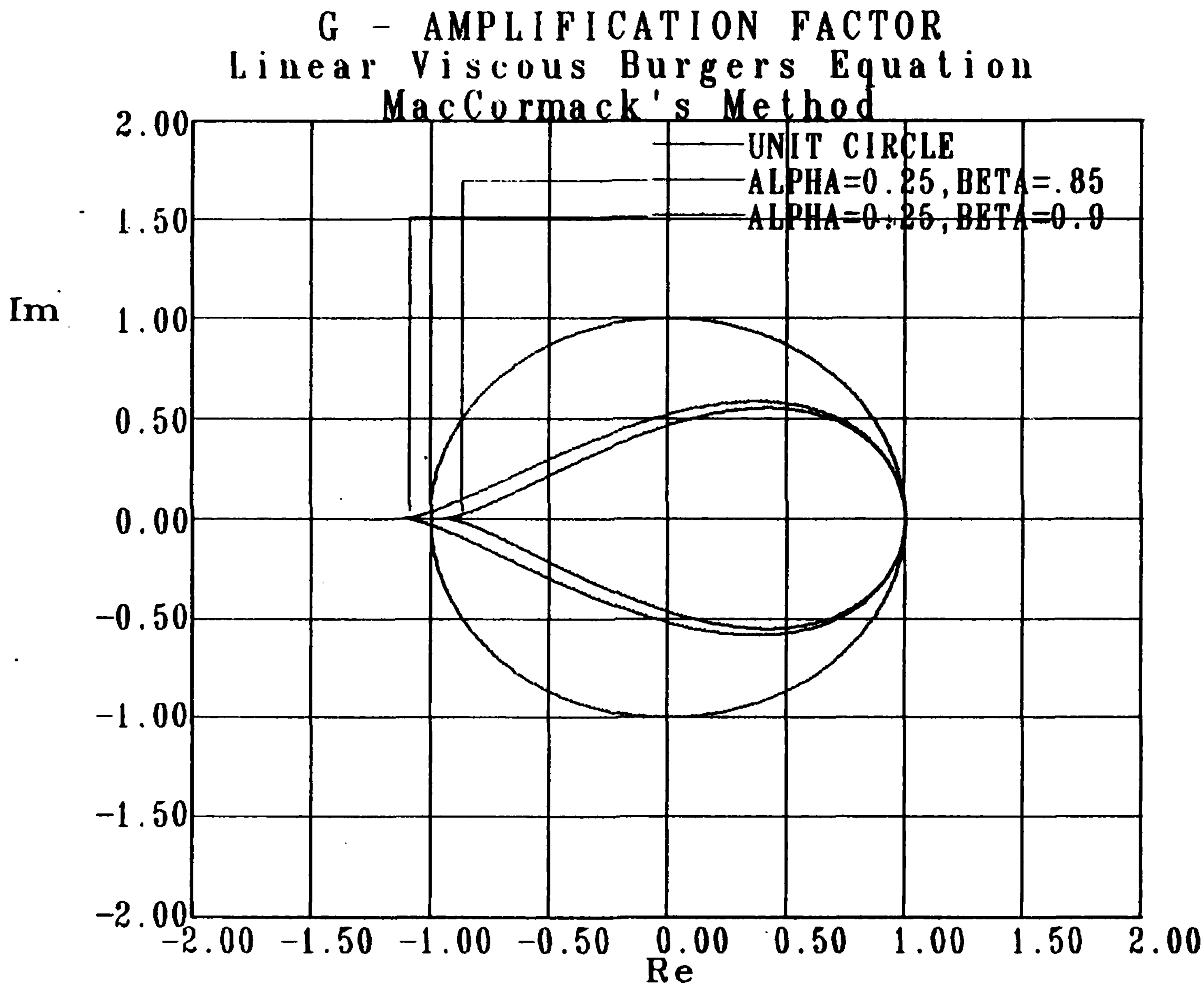

Figure 6. Stability of $\alpha = .25$ at $\beta = .85$ and $.9$.

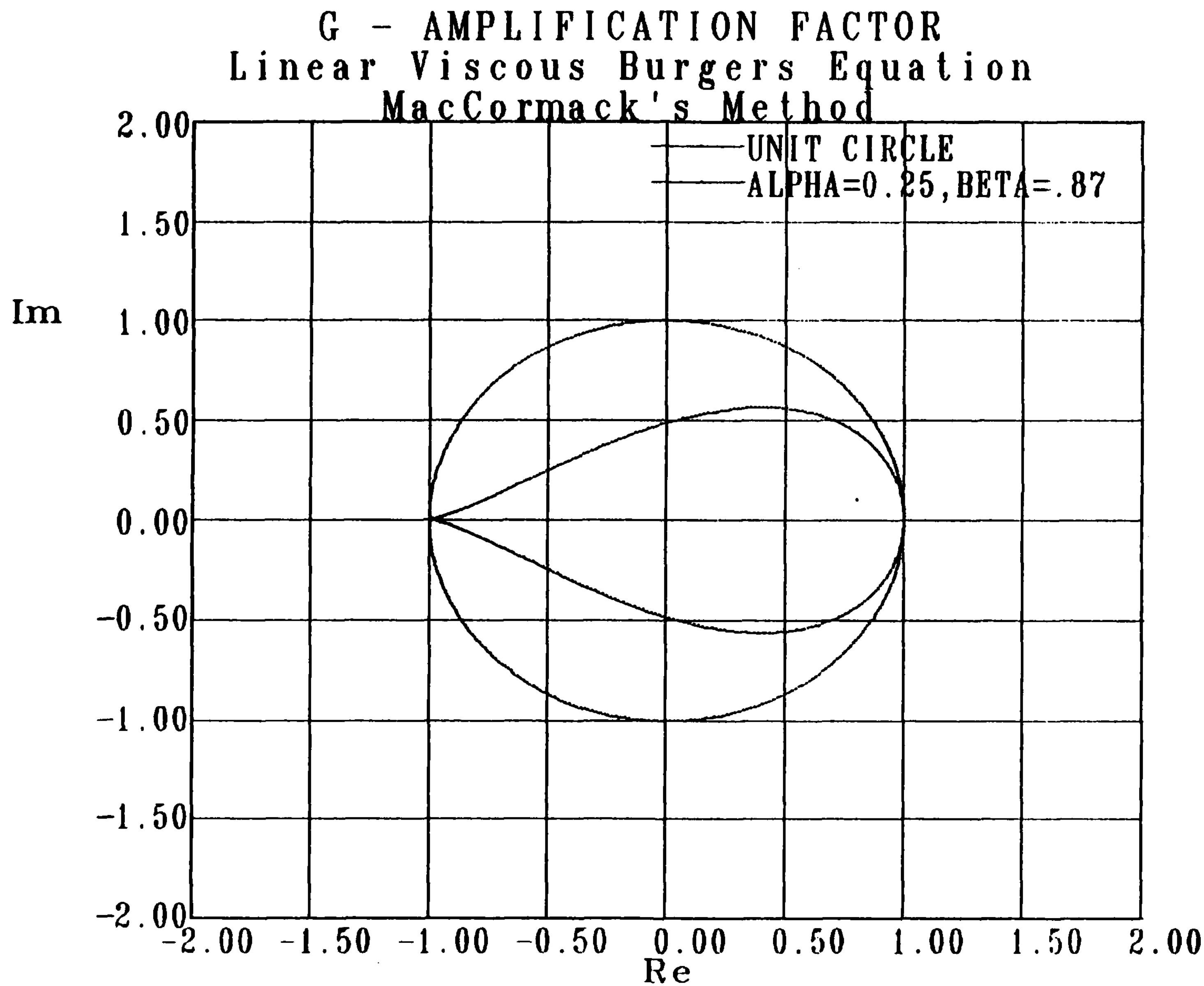

Figure 7. Stability at $\alpha = .25$ and $\beta = .87$.

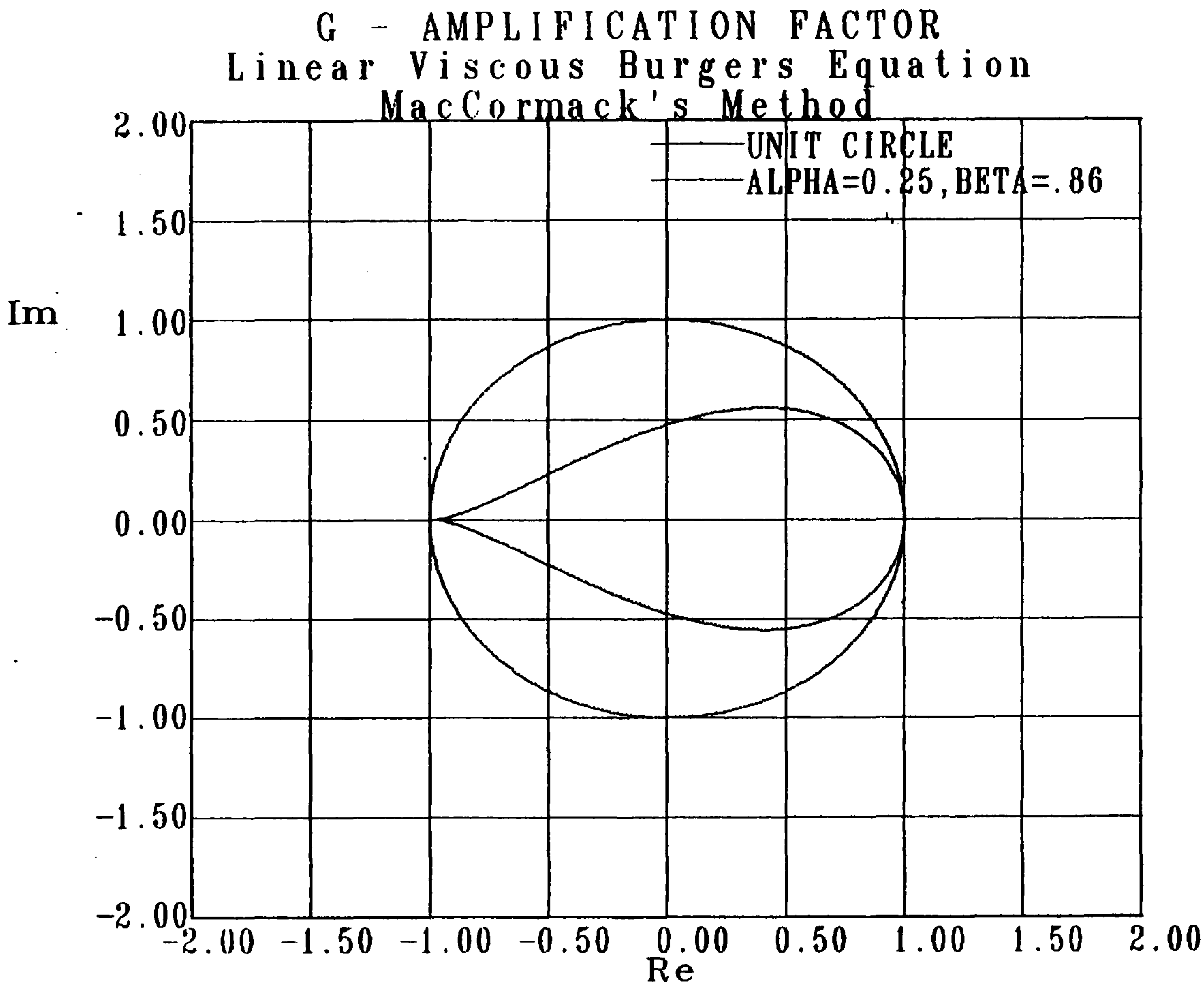

Figure 8. Stability at $\alpha = .25$ and $\beta = .86$.

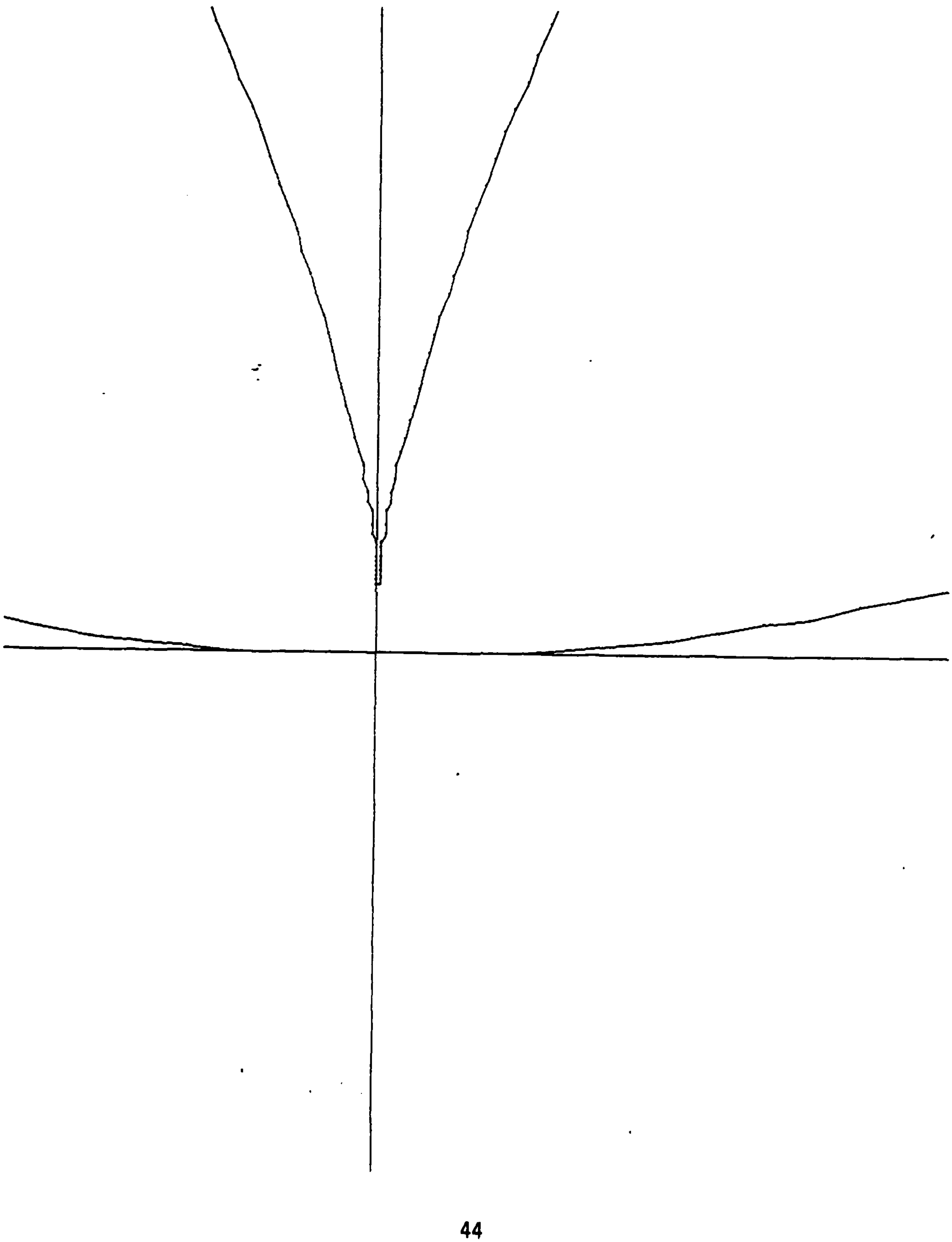

Figure 9. Stability at $\alpha = .25$ and $\beta = .86$.

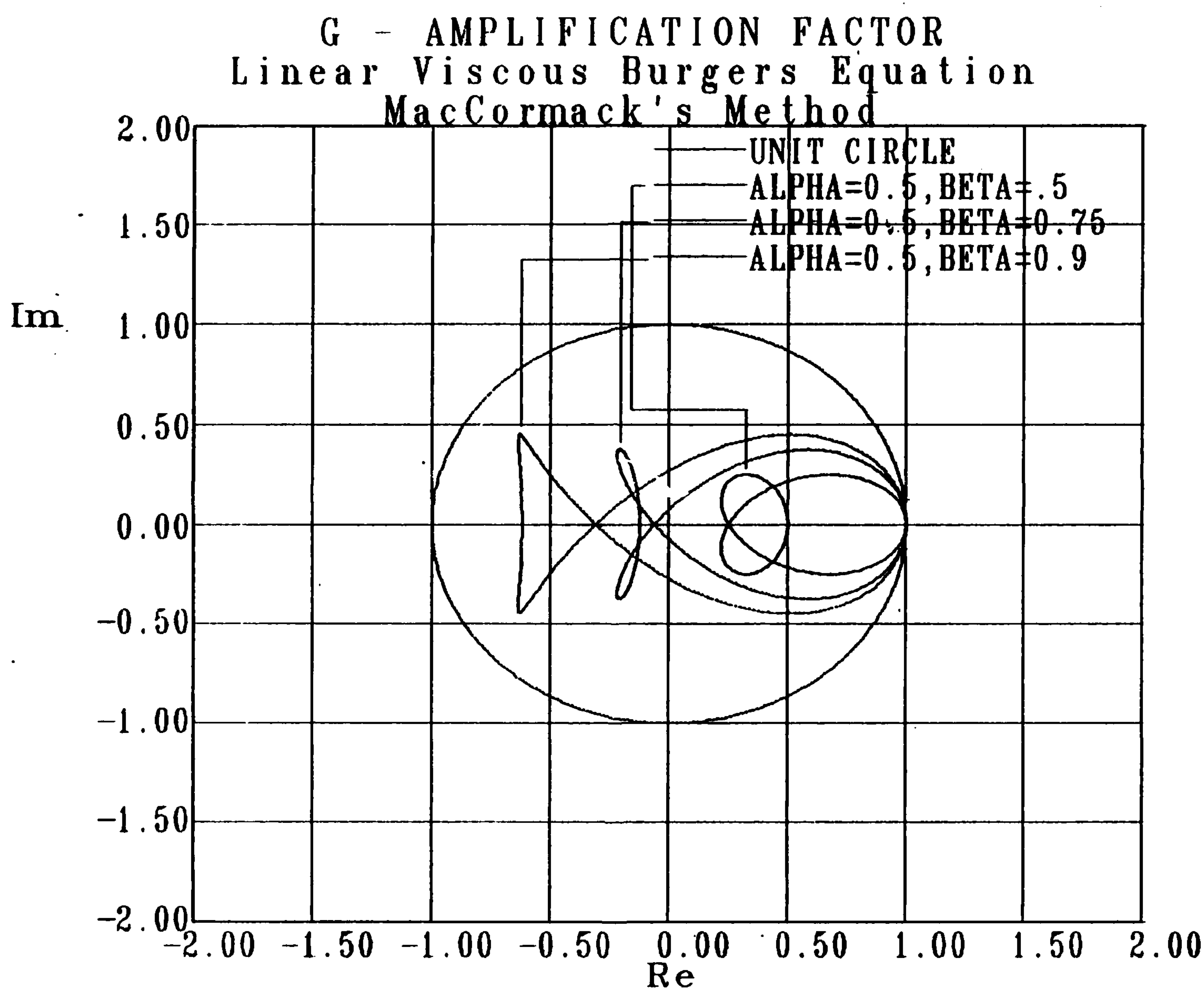

Figure 10(a). Stability at $\alpha = .5$ and $\beta = .5, .75$, and .9.

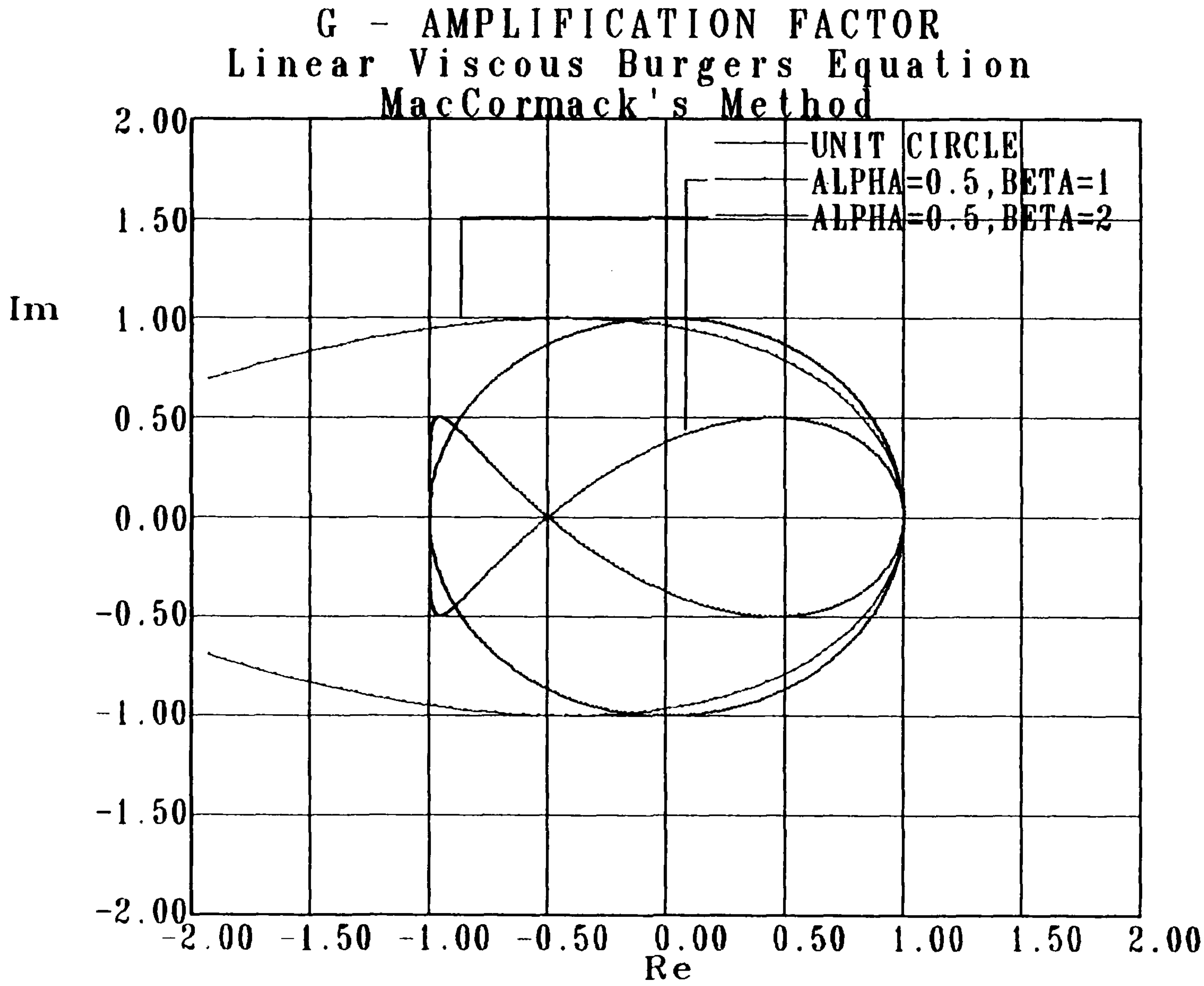

Figure 10(b). Stability of $\alpha = .5$ and $\beta = 1$, and 2.

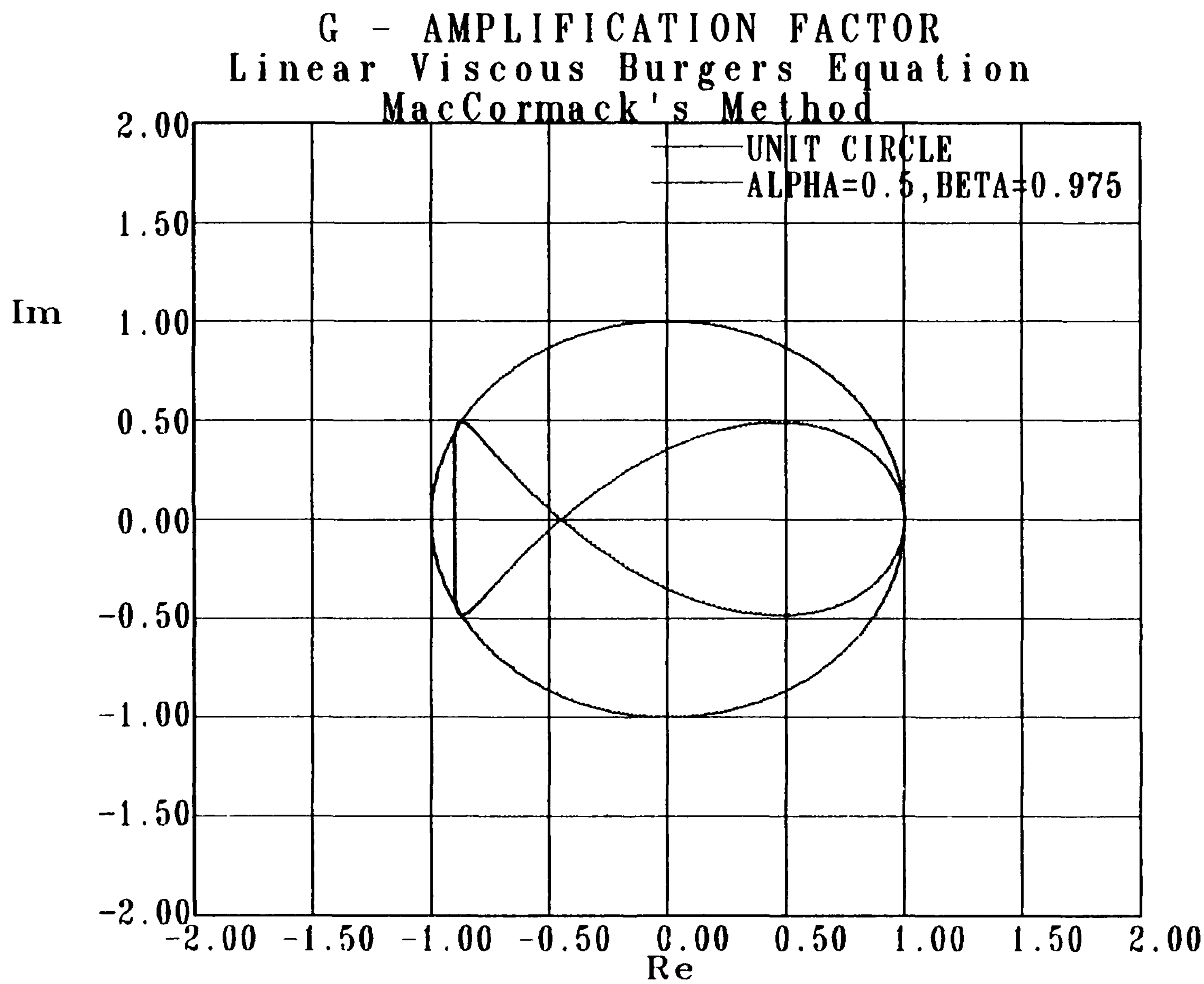

Figure 11. Stability at α = .5 and β = .975.

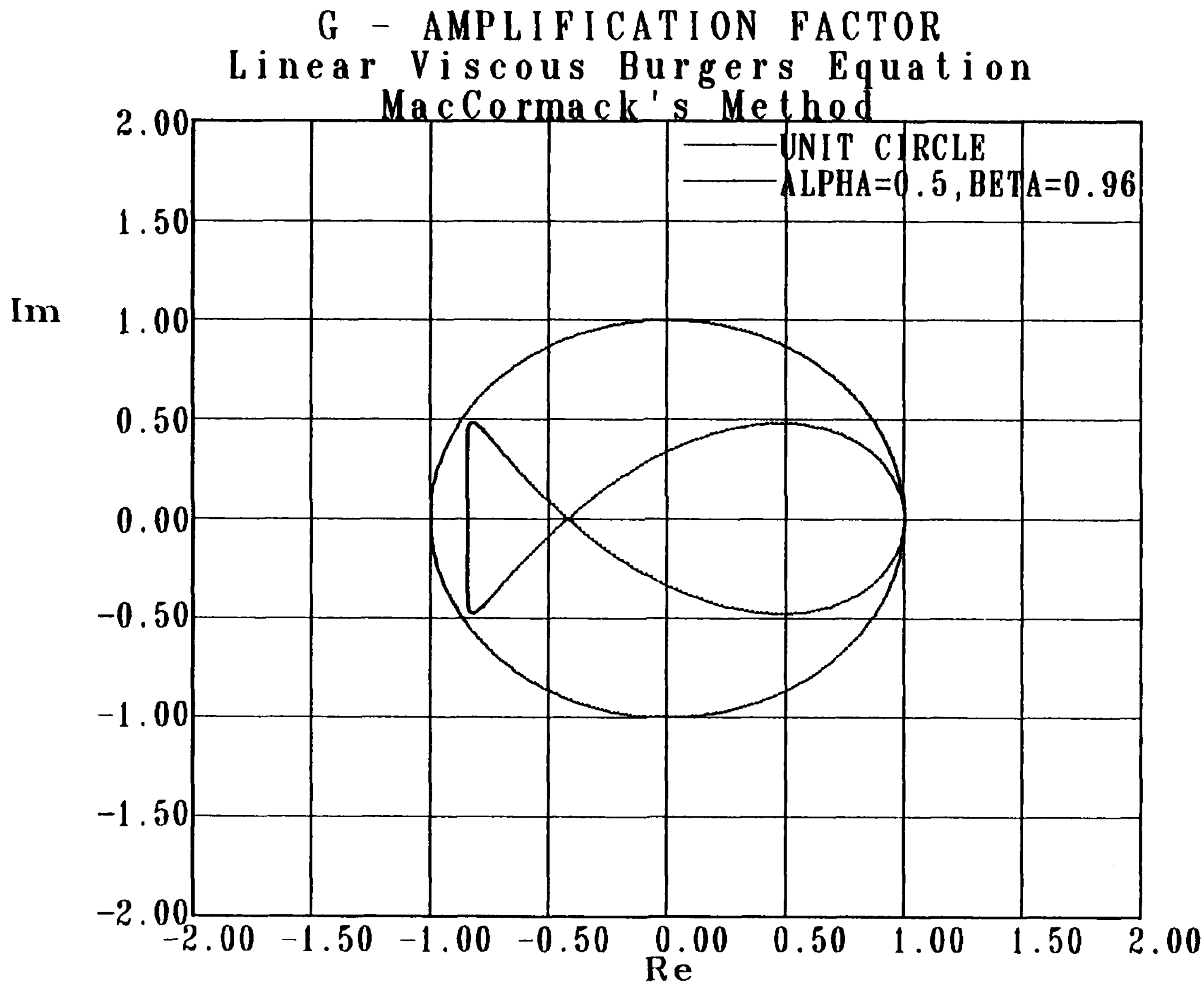

Figure 12. Stability at $\alpha = .5$ and $\beta = .96$.

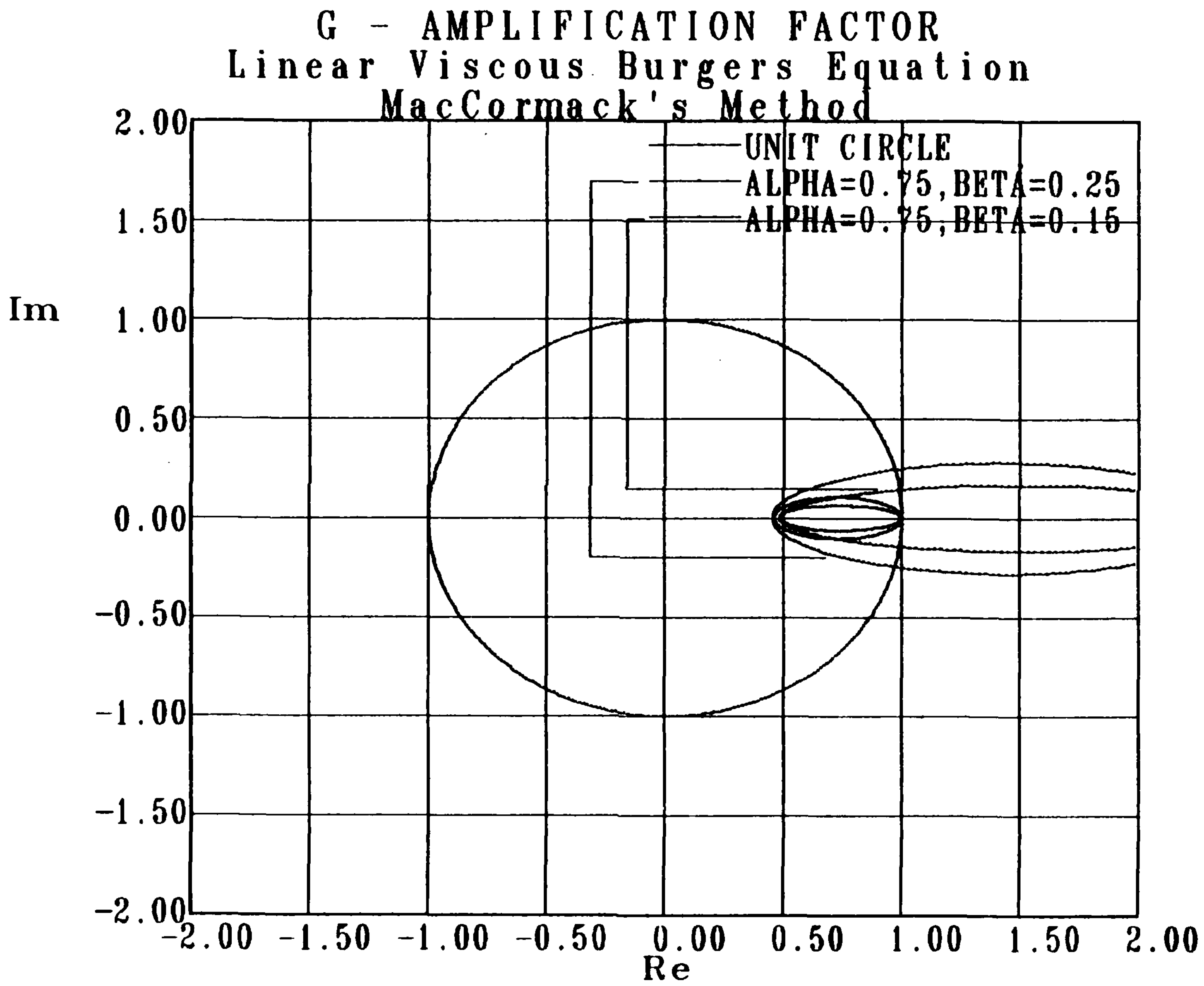

Figure 13. Instability at α = .75 and β = .25 and .15.

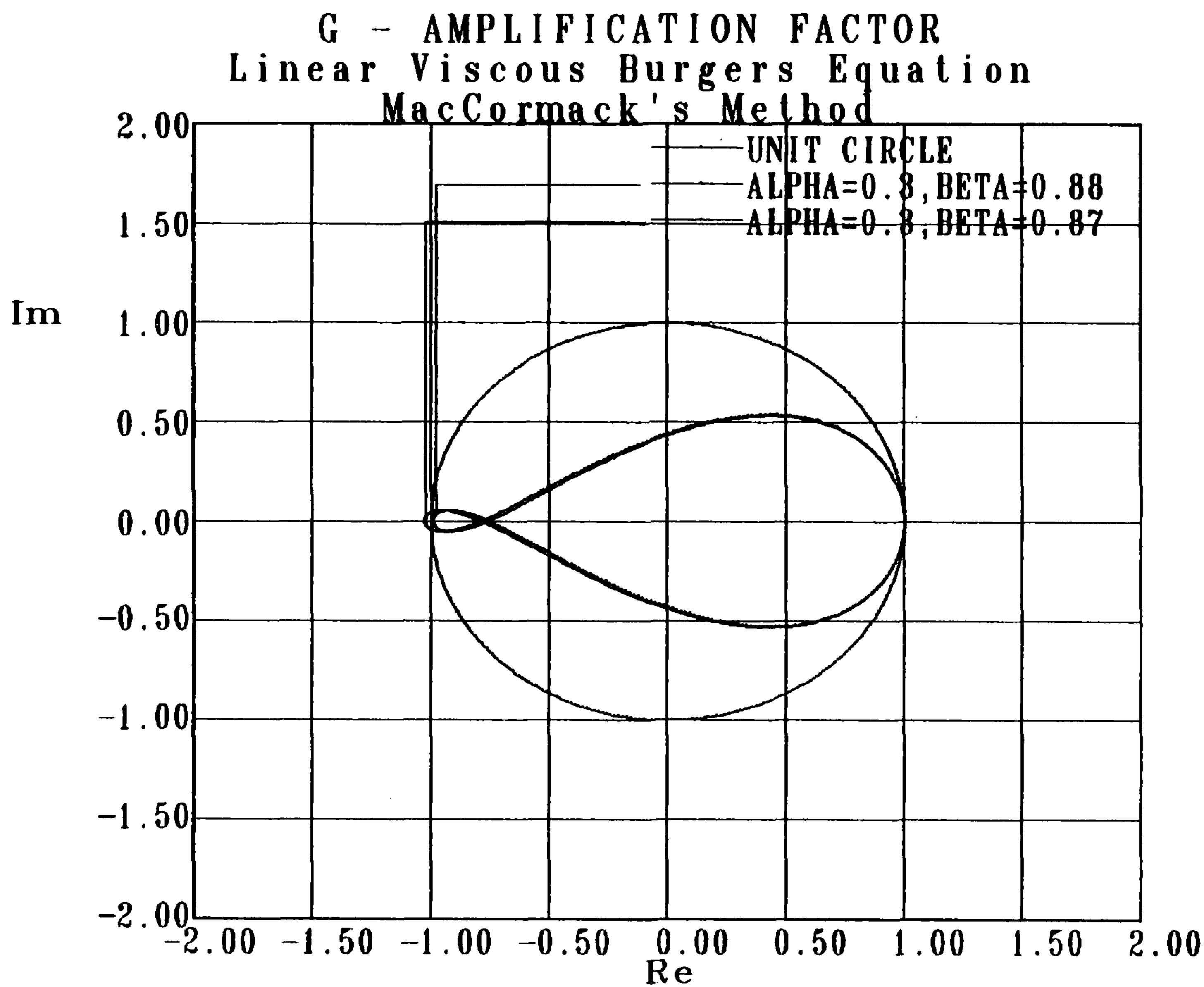

Figure 14. Stability at $\alpha = .3$ and $\beta = .88$ and .87.

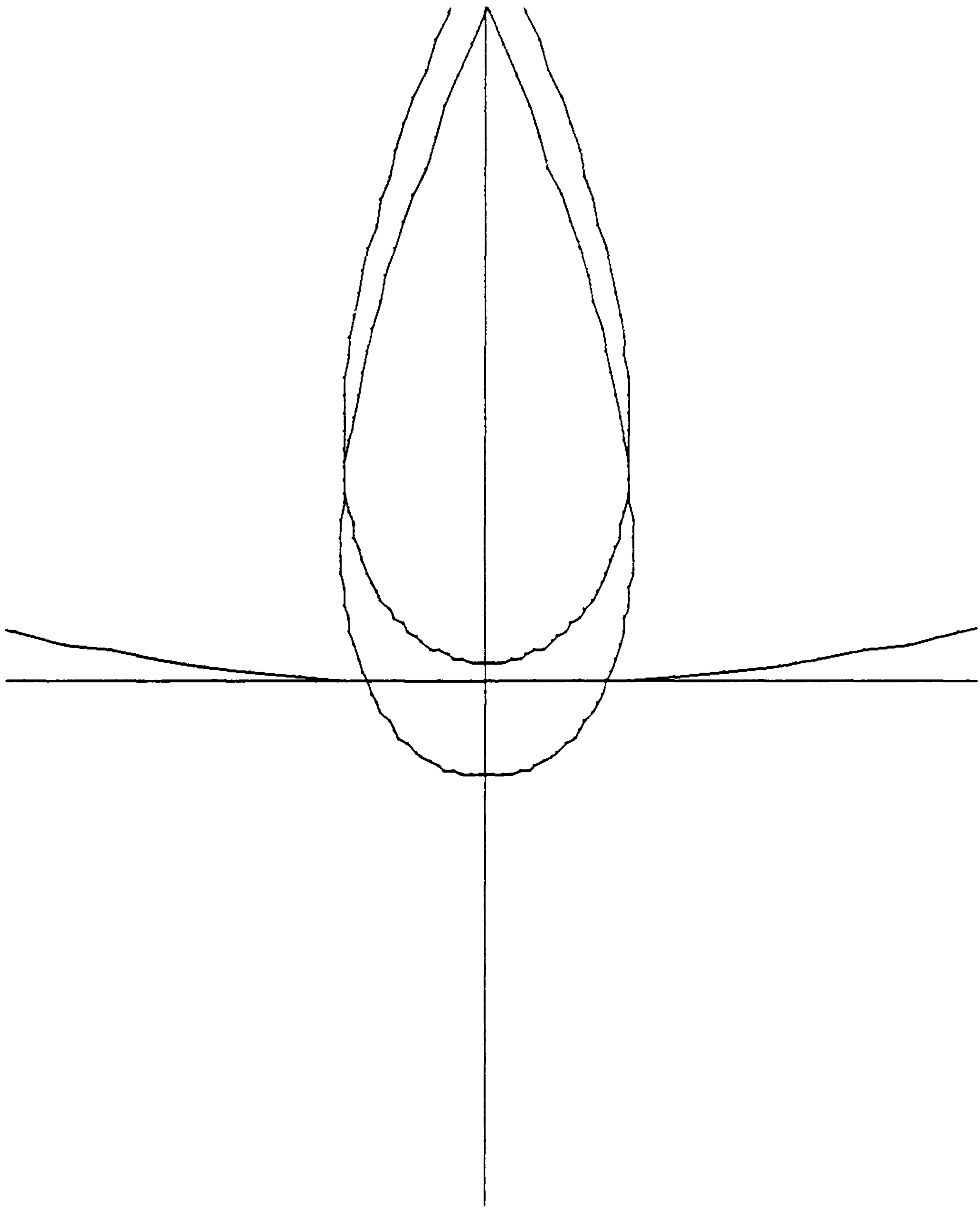

Figure 15. Closeup for Figure 14 for α = .3 and β = .88 and .87.

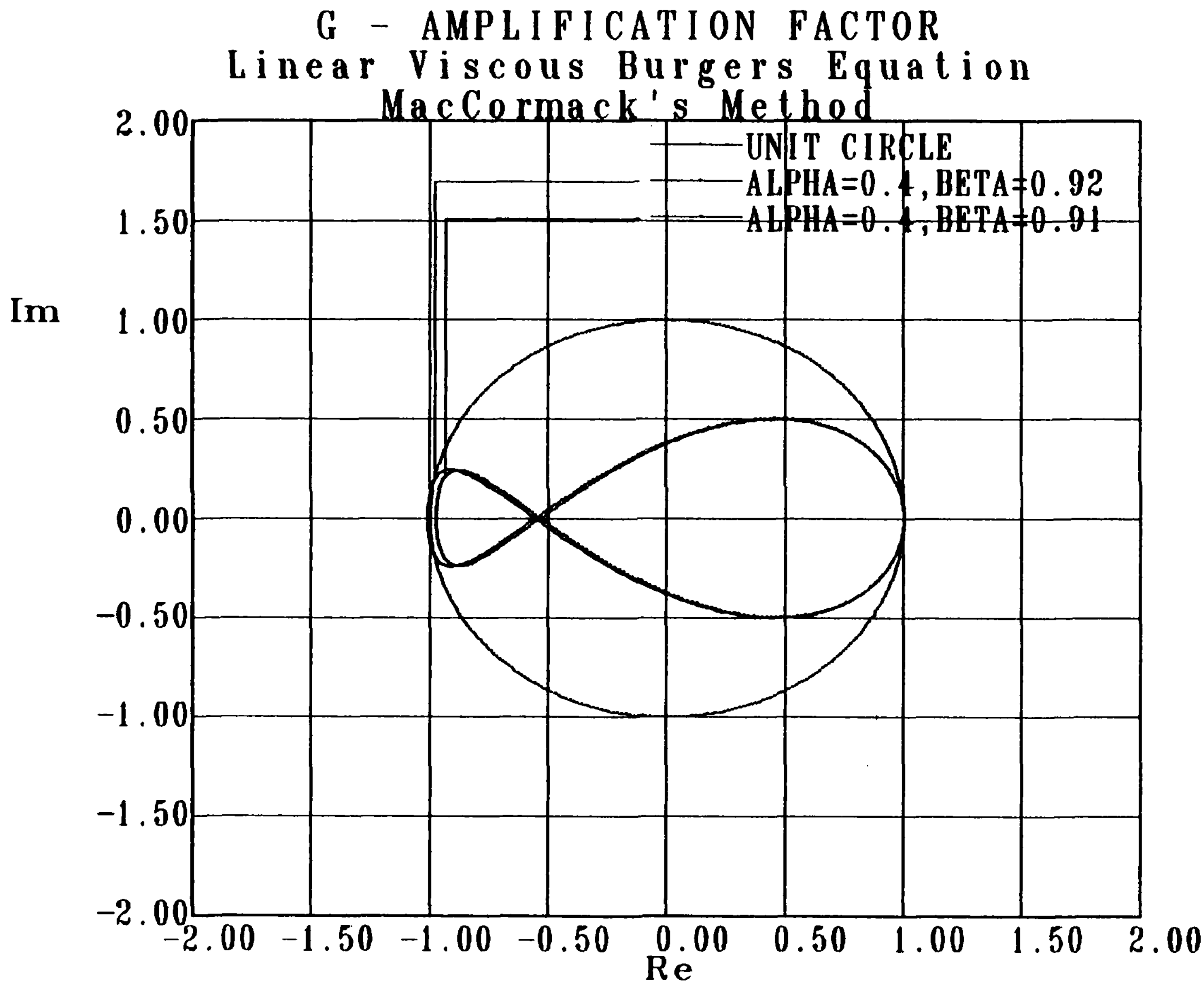

Figure 16. Stability at $\alpha = .4$ and $\beta = .92$ and $.91$.

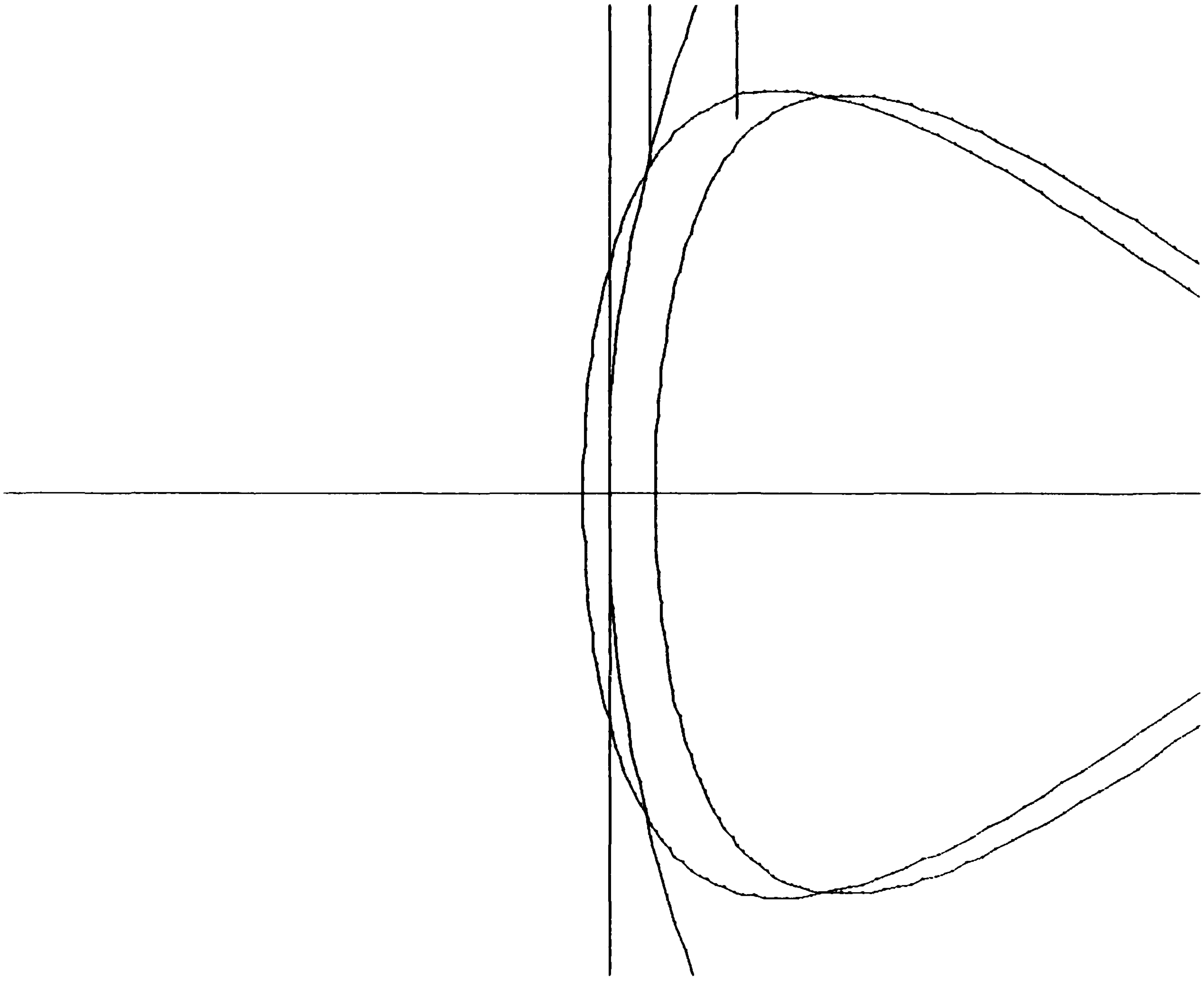

Figure 17. Closeup of Figure 16 for $\alpha = .4$ and $\beta = .92$ and .91.

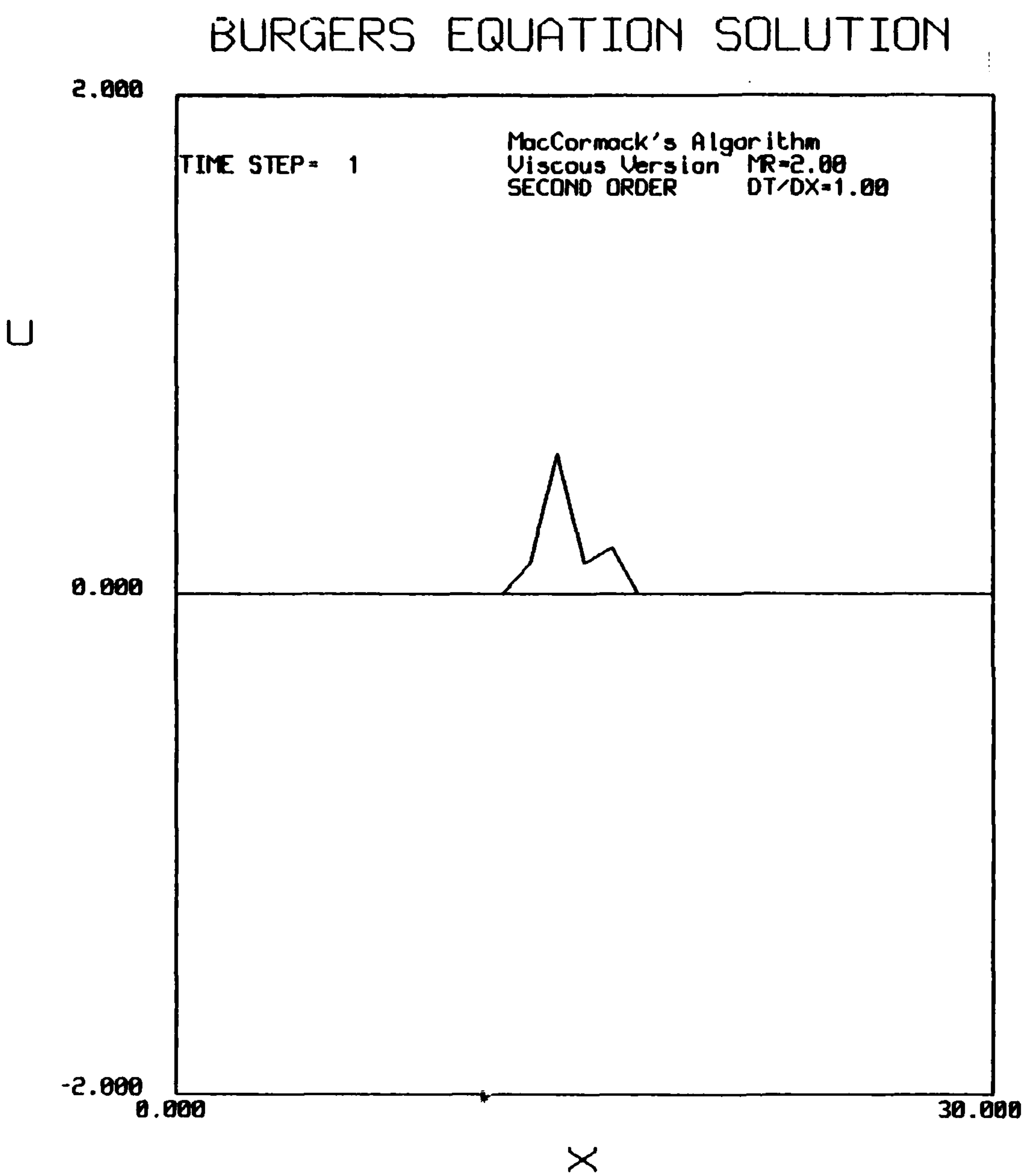

TIME STEP: 1

U(1)=	0.0000000
U(2)=	0.0000000
U(3)=	0.0000000
U(4)=	0.0000000
U(5)=	0.0000000
U(6)=	0.0000000
U(7)=	0.0000000
U(8)=	0.0000000
U(9)=	0.0000000
U(10)=	0.0000000
U(11)=	0.0000000
U(12)=	0.0000000
U(13)=	0.0000000
U(14)=	0.1250000
U(15)=	0.5625000
U(16)=	0.1250000
U(17)=	0.1875000
U(18)=	0.0000000
U(19)=	0.0000000
U(20)=	0.0000000
U(21)=	0.0000000
U(22)=	0.0000000
U(23)=	0.0000000
U(24)=	0.0000000
U(25)=	0.0000000
U(26)=	0.0000000
U(27)=	0.0000000
U(28)=	0.0000000
U(29)=	0.0000000
U(30)=	0.0000000

Figure 18. Transportive property for $\mu\frac{\Delta t}{(\Delta x)^2} = .5$ (i.e., $\beta = .5$). MR $= \frac{\Delta x}{\mu}$ and $\Delta x = 1$.

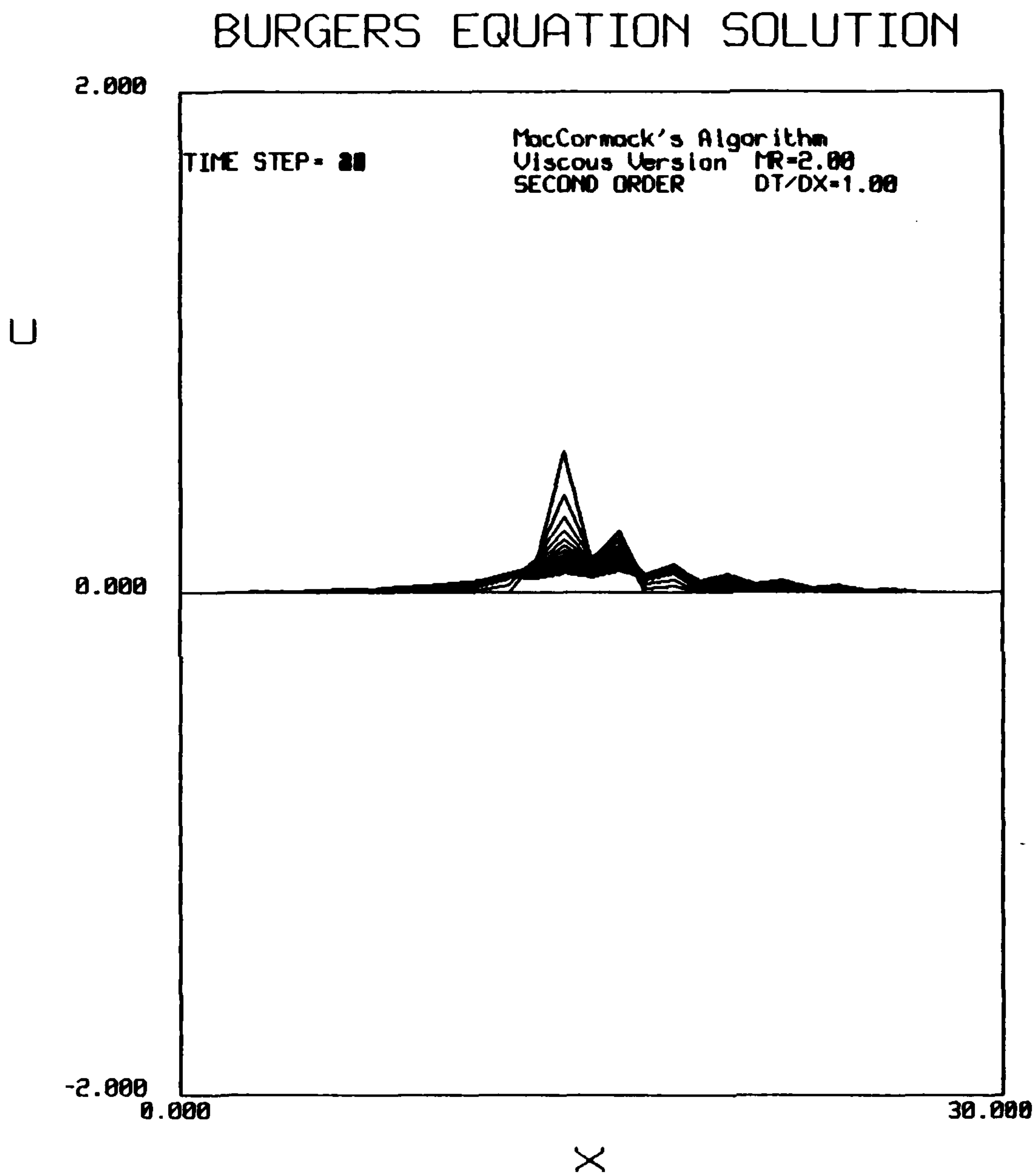

TIME STEP: 30

U(1)=	0.0000000
U(2)=	0.1452142E-02
U(3)=	0.3279515E-02
U(4)=	0.5052492E-02
U(5)=	0.8181246E-02
U(6)=	0.1061998E-01
U(7)=	0.1610387E-01
U(8)=	0.1897772E-01
U(9)=	0.2783907E-01
U(10)=	0.3007637E-01
U(11)=	0.4308008E-01
U(12)=	0.4260902E-01
U(13)=	0.6004106E-01
U(14)=	0.5390451E-01
U(15)=	0.7539532E-01
U(16)=	0.6040123E-01
U(17)=	0.8474383E-01
U(18)=	0.5907381E-01
U(19)=	0.8399857E-01
U(20)=	0.4959094E-01
U(21)=	0.7189851E-01
U(22)=	0.3532169E-01
U(23)=	0.5211863E-01
U(24)=	0.2128886E-01
U(25)=	0.3160601E-01
U(26)=	0.1081652E-01
U(27)=	0.1555475E-01
U(28)=	0.4260208E-02
U(29)=	0.4506469E-02
U(30)=	0.0000000

Figure 19. Transportive property history for $\beta = .5$.

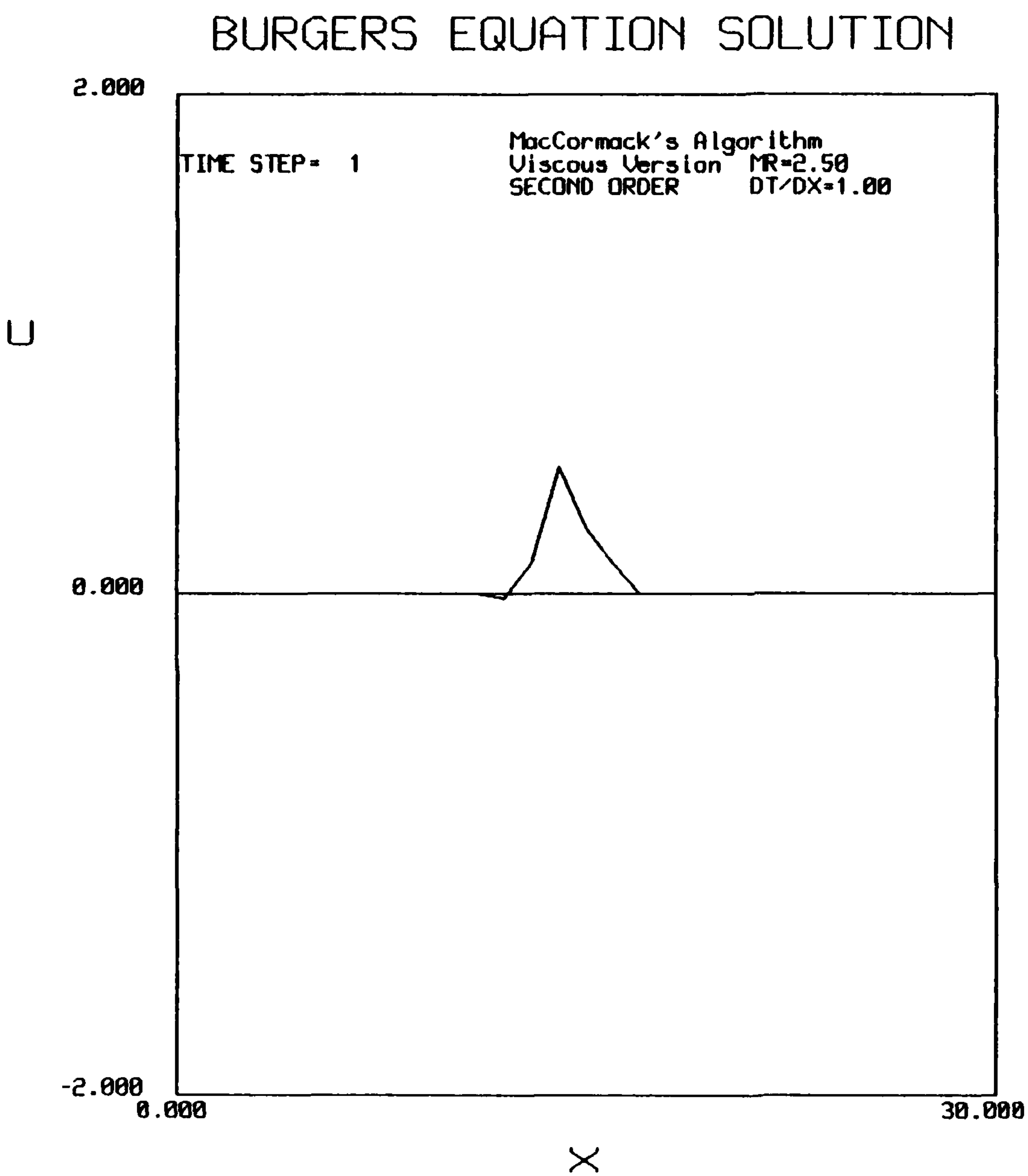

TIME STEP: 1

U(1)=	0.0000000
U(2)=	0.0000000
U(3)=	0.0000000
U(4)=	0.0000000
U(5)=	0.0000000
U(6)=	0.0000000
U(7)=	0.0000000
U(8)=	0.0000000
U(9)=	0.0000000
U(10)=	0.0000000
U(11)=	0.0000000
U(12)=	0.0000000
U(13)=	-0.2000000E-01
U(14)=	0.1275000
U(15)=	0.5100000
U(16)=	0.2625000
U(17)=	0.1200000
U(18)=	0.0000000
U(19)=	0.0000000
U(20)=	0.0000000
U(21)=	0.0000000
U(22)=	0.0000000
U(23)=	0.0000000
U(24)=	0.0000000
U(25)=	0.0000000
U(26)=	0.0000000
U(27)=	0.0000000
U(28)=	0.0000000
U(29)=	0.0000000
U(30)=	0.0000000

Figure 20. Transportive property at $\mu\frac{\Delta t}{(\Delta x)^2}$ = .4.

BURGERS EQUATION SOLUTION

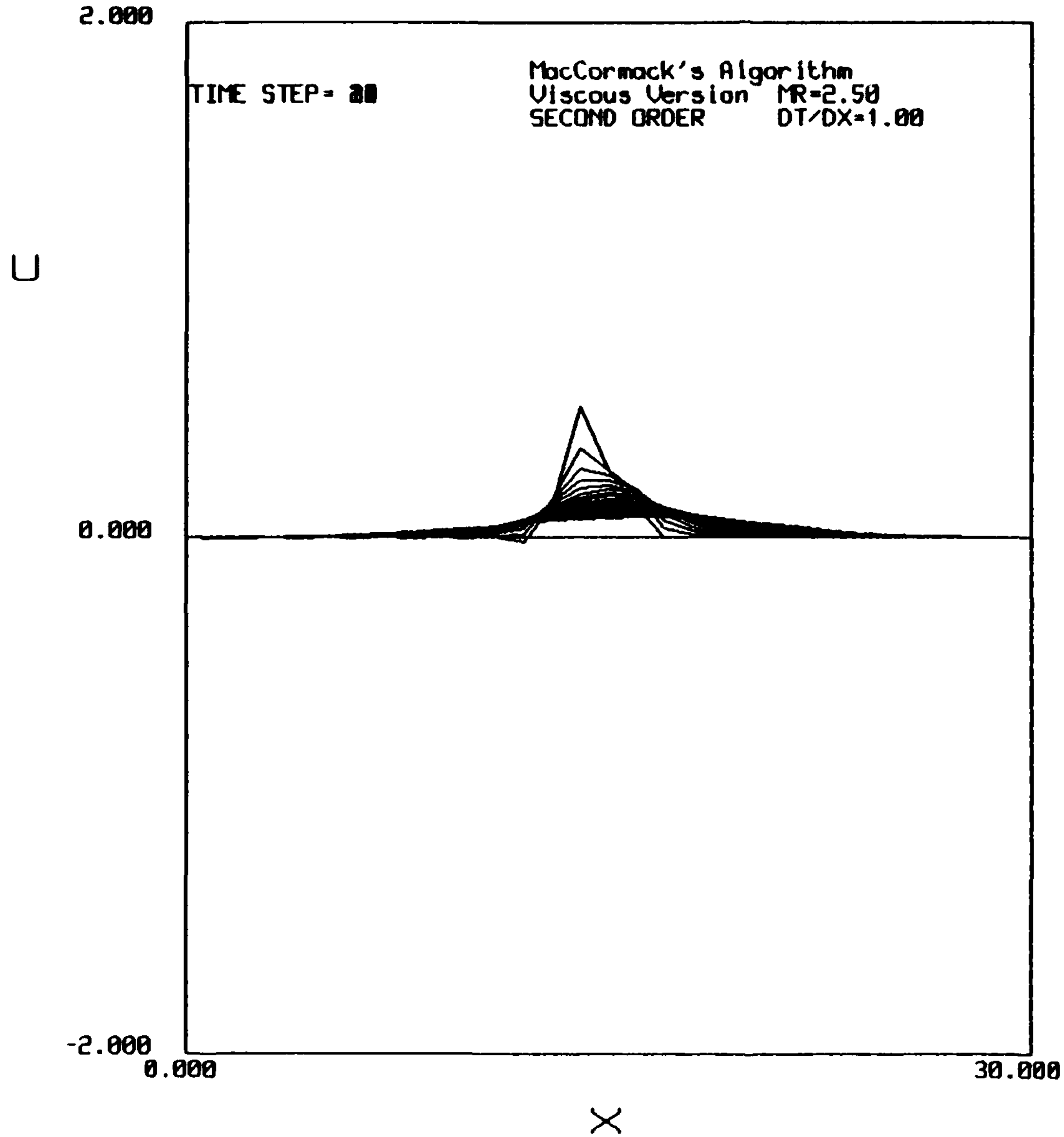

TIME STEP: 30

```
U( 1)=  0.0000000
U( 2)=  0.8095566E-03
U( 3)=  0.1801763E-02
U( 4)=  0.3166157E-02
U( 5)=  0.5100113E-02
U( 6)=  0.7803082E-02
U( 7)=  0.1146031E-01
U( 8)=  0.1621885E-01
U( 9)=  0.2215793E-01
U(10)=  0.2925978E-01
U(11)=  0.3738309E-01
U(12)=  0.4624447E-01
U(13)=  0.5540704E-01
U(14)=  0.6428181E-01
U(15)=  0.7214540E-01
U(16)=  0.7818812E-01
U(17)=  0.8160497E-01
U(18)=  0.8173924E-01
U(19)=  0.7826383E-01
U(20)=  0.7134599E-01
U(21)=  0.6171231E-01
U(22)=  0.5053566E-01
U(23)=  0.3915303E-01
U(24)=  0.2872218E-01
U(25)=  0.1997950E-01
U(26)=  0.1317970E-01
U(27)=  0.8190669E-02
U(28)=  0.4646140E-02
U(29)=  0.2079873E-02
U(30)=  0.0000000
```

Figure 21. Transportive property history at β = .4.

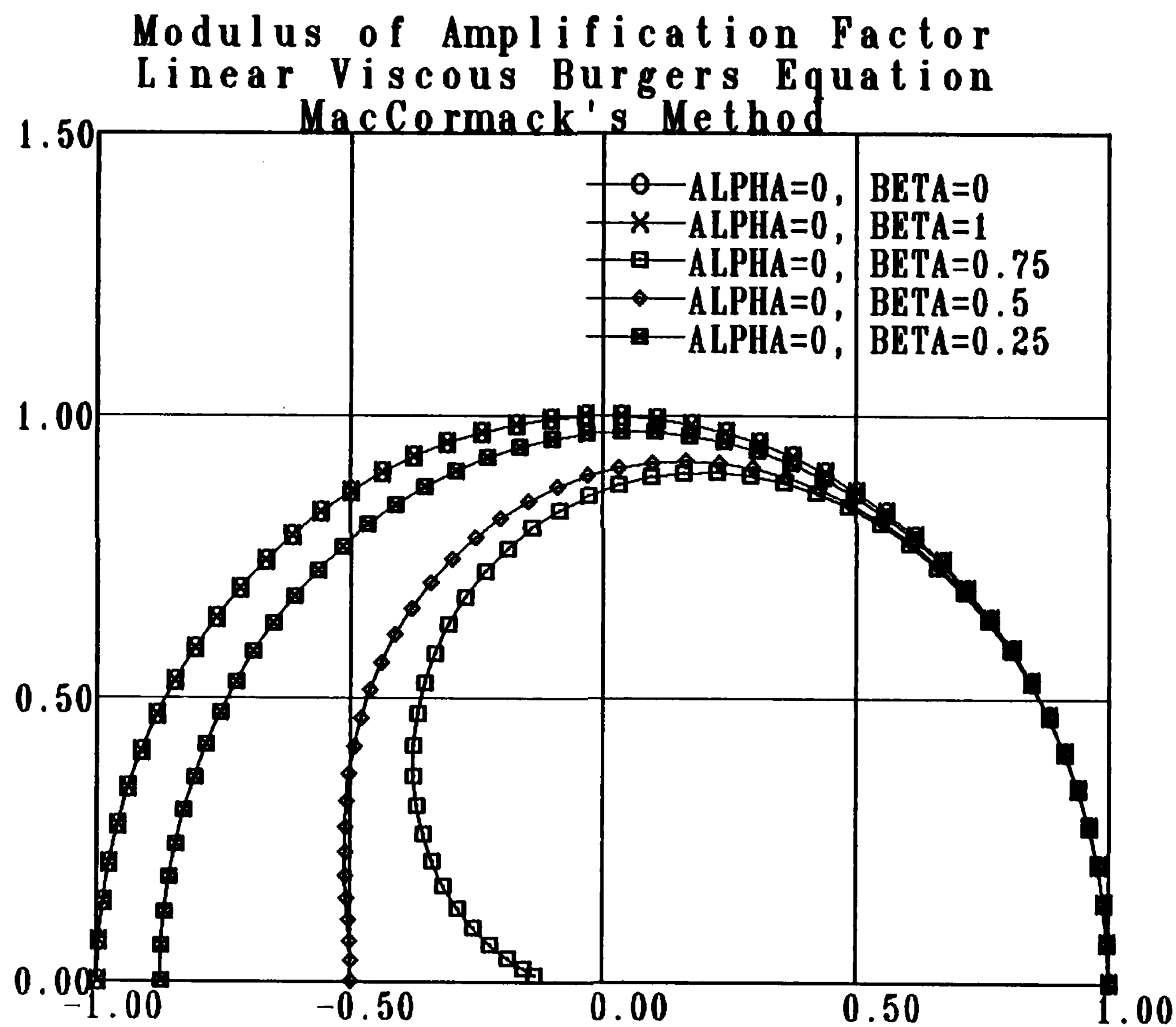

Figure 22. Modulus of amplification factor at $\alpha = 0$ and $\beta = 1$, .75, .5, and .25. Note that the $\alpha = 0, \beta = 1$ curve wrote over the $\alpha = 0$ curve.

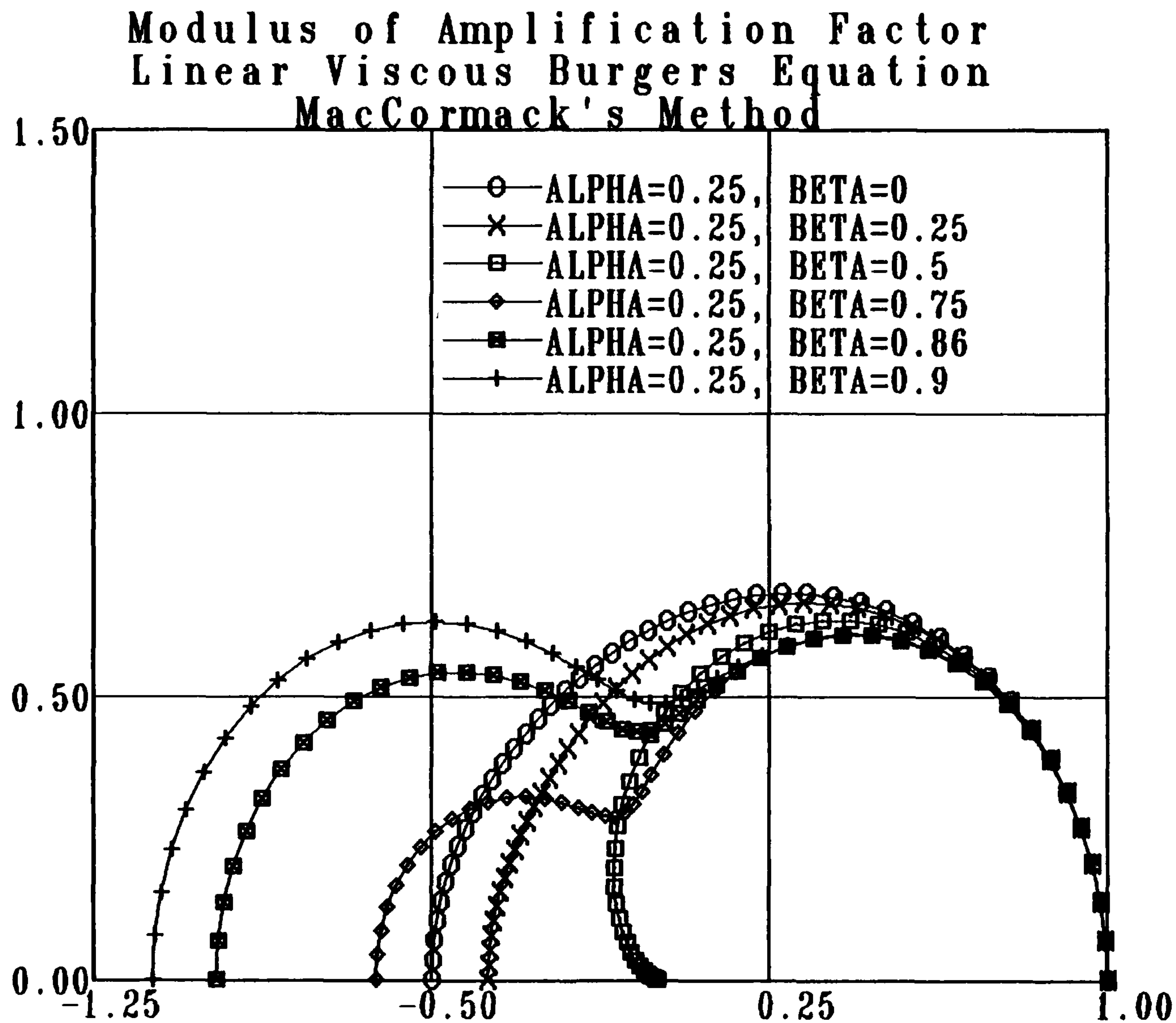

Figure 23. Modulus of amplification for α = .25 and β = .25, .5, .75, .86, and .9.

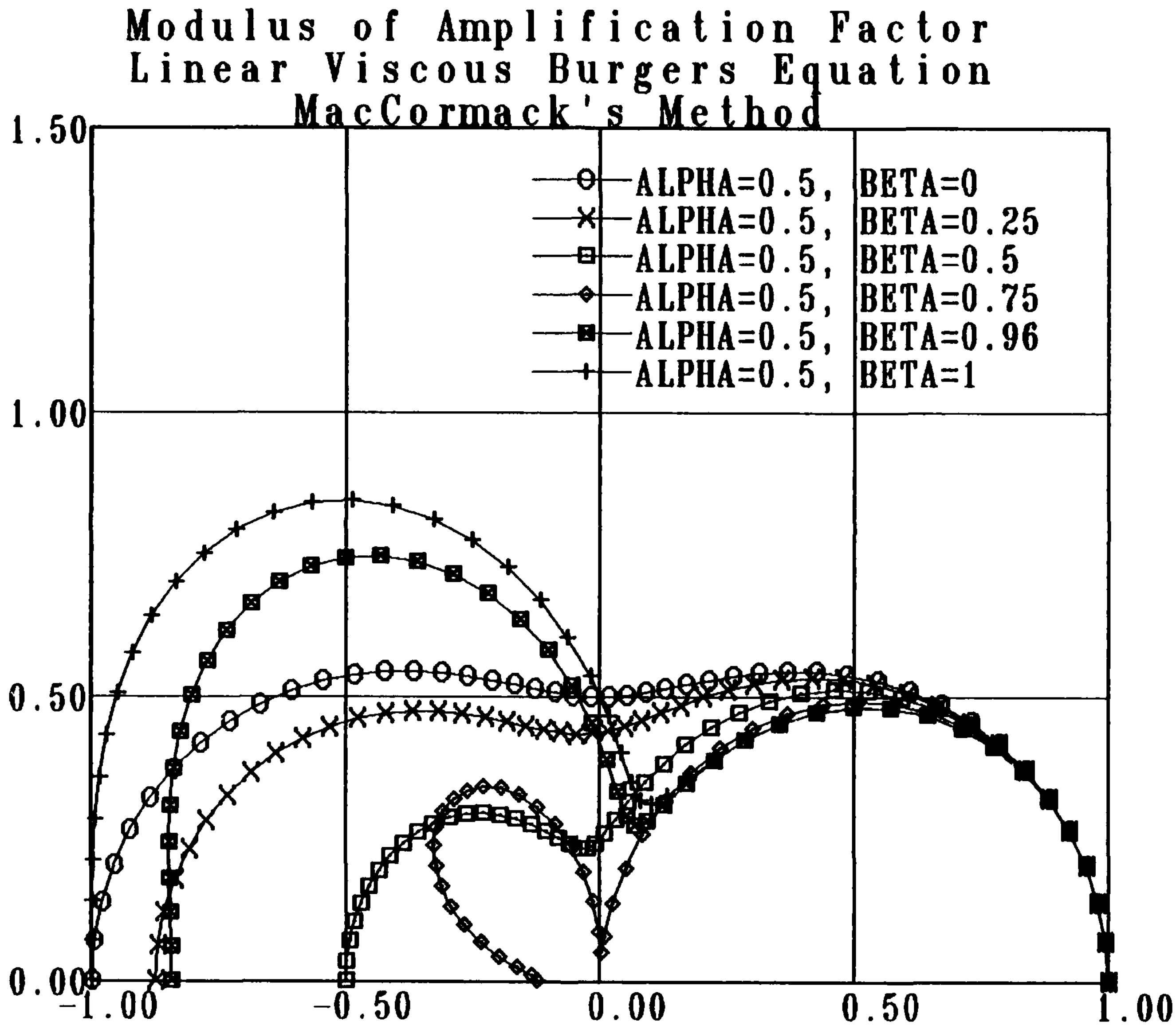

Figure 24. Modulus of amplification factor for $\alpha = .5$ and $\beta = .25, .5, .75, .96,$ and 1.

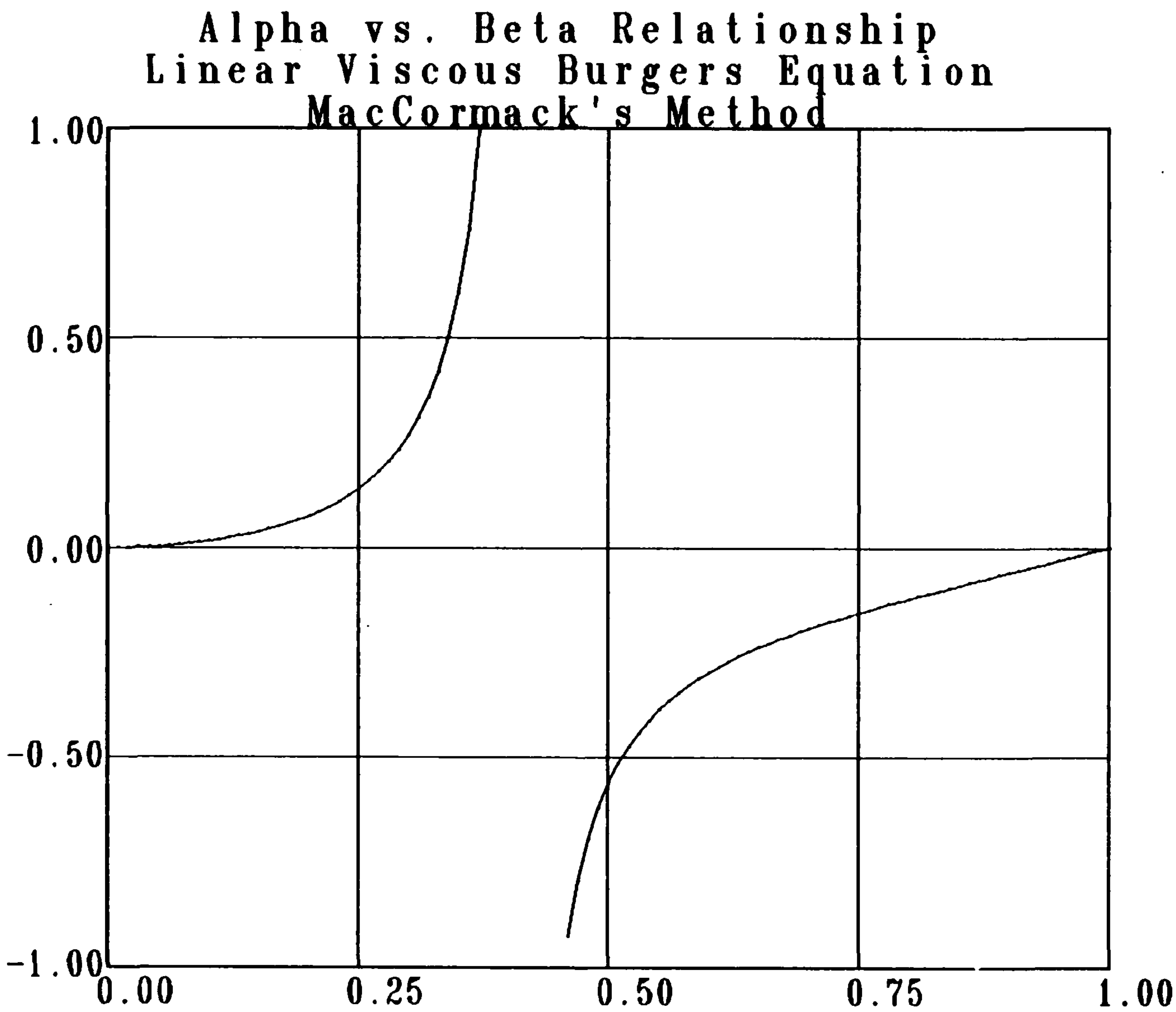

Figure 25. Relationship to eliminate 4th order dissipation. Only $0 \leq \alpha \leq .5$ is stable.

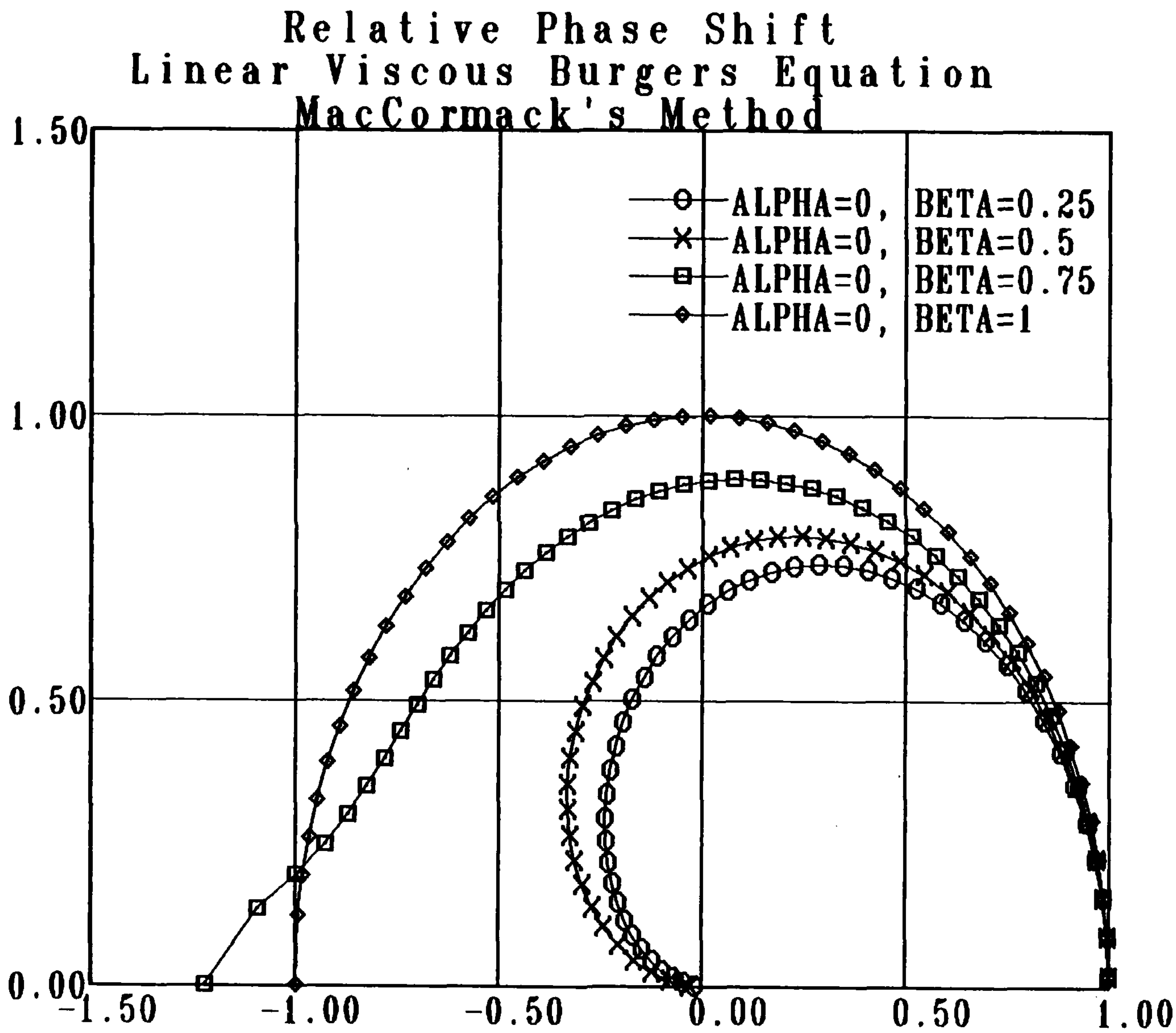

Figure 26. Phase error for $\alpha = 0$ at $\beta = .25, .5, .75,$ and 1.

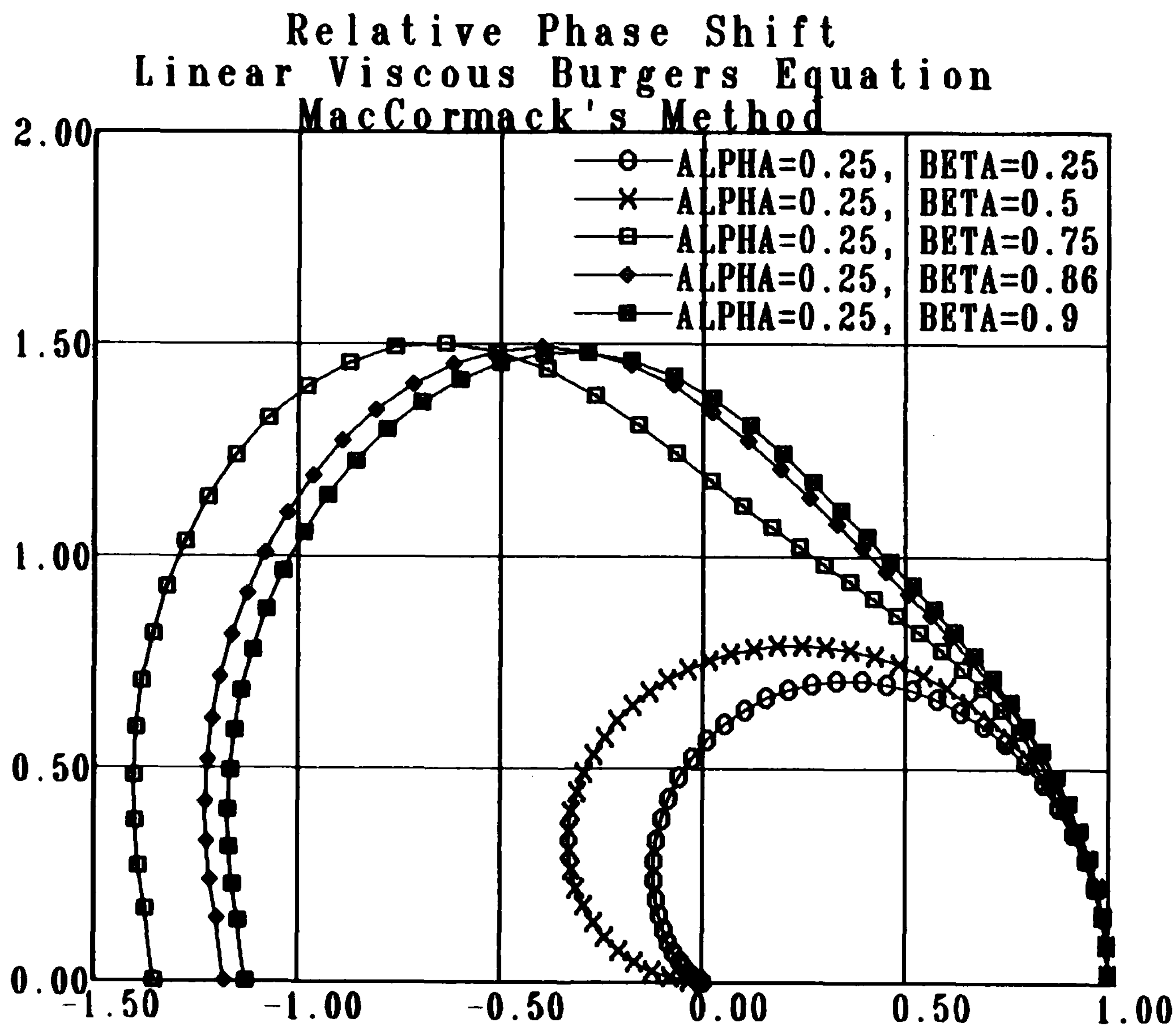

Figure 27. Relative phase shift error for $\alpha = .25$ at $\beta = .25, .5, .75, .86$, and $.9$.

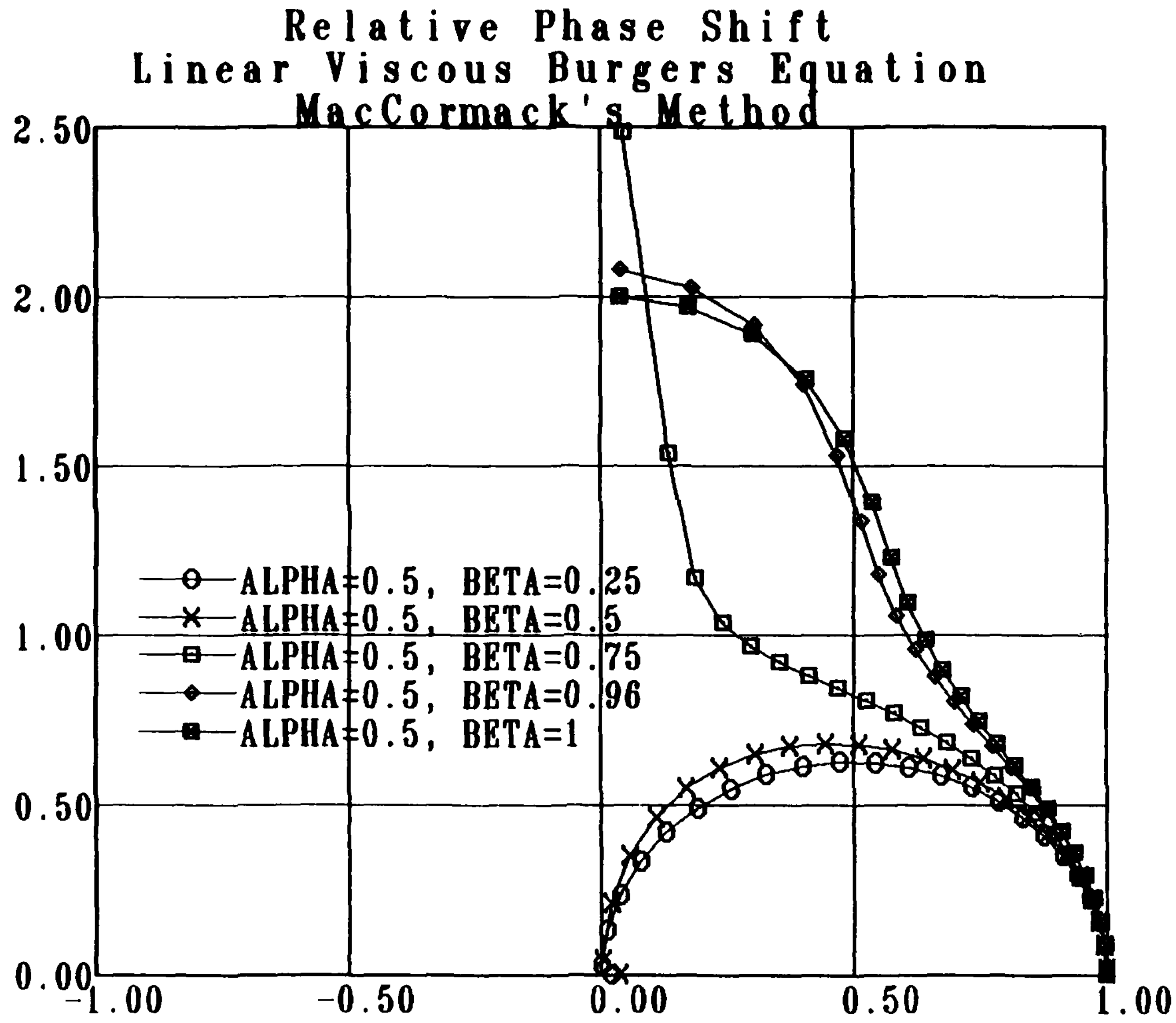

Figure 28. Relative phase shift error for $\alpha = .5$ at $\beta = .25, .5, .75, .96$, and 1.

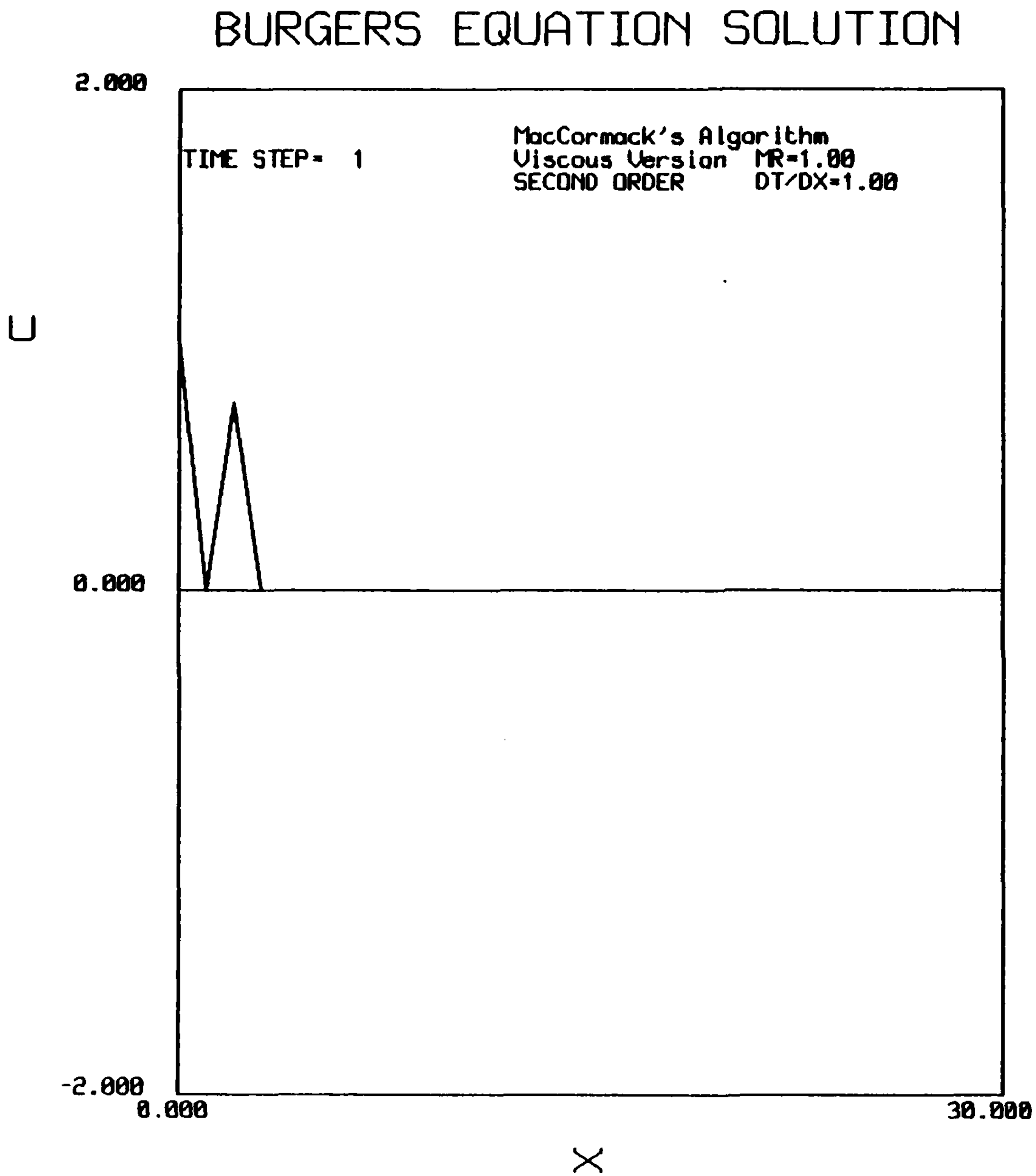

TIME STEP: 1

U(1)=	1.000000
U(2)=	0.0000000
U(3)=	0.7500000
U(4)=	0.0000000
U(5)=	0.0000000
U(6)=	0.0000000
U(7)=	0.0000000
U(8)=	0.0000000
U(9)=	0.0000000
U(10)=	0.0000000
U(11)=	0.0000000
U(12)=	0.0000000
U(13)=	0.0000000
U(14)=	0.0000000
U(15)=	0.0000000
U(16)=	0.0000000
U(17)=	0.0000000
U(18)=	0.0000000
U(19)=	0.0000000
U(20)=	0.0000000
U(21)=	0.0000000
U(22)=	0.0000000
U(23)=	0.0000000
U(24)=	0.0000000
U(25)=	0.0000000
U(26)=	0.0000000
U(27)=	0.0000000
U(28)=	0.0000000
U(29)=	0.0000000
U(30)=	0.0000000

Figure 29. Instability at $\beta = 1$.

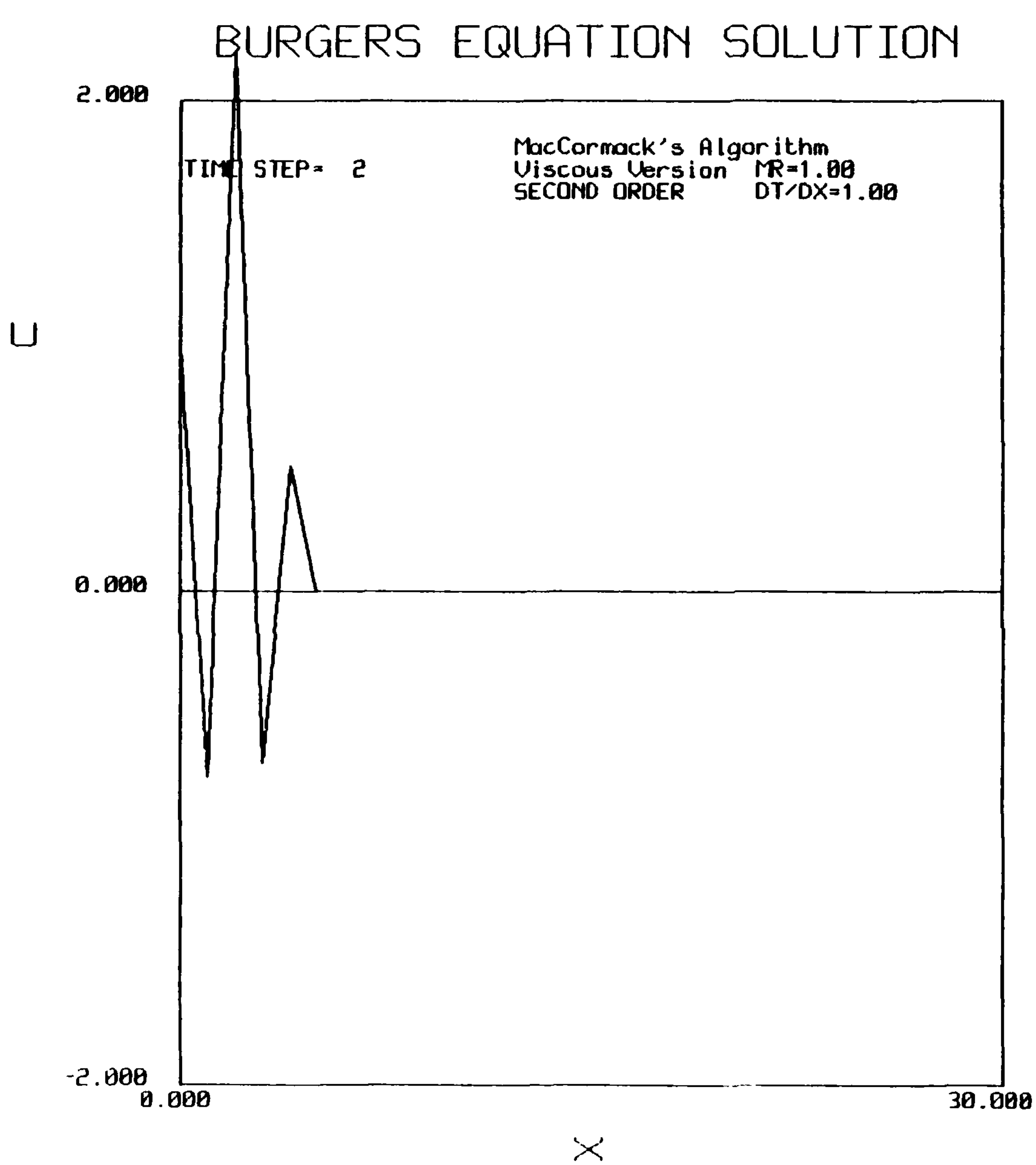

TIME STEP: 2

U(1)=	1.000000
U(2)=	-0.7580566
U(3)=	2.203125
U(4)=	-0.6950684
U(5)=	0.5156250
U(6)=	0.0000000
U(7)=	0.0000000
U(8)=	0.0000000
U(9)=	0.0000000
U(10)=	0.0000000
U(11)=	0.0000000
U(12)=	0.0000000
U(13)=	0.0000000
U(14)=	0.0000000
U(15)=	0.0000000
U(16)=	0.0000000
U(17)=	0.0000000
U(18)=	0.0000000
U(19)=	0.0000000
U(20)=	0.0000000
U(21)=	0.0000000
U(22)=	0.0000000
U(23)=	0.0000000
U(24)=	0.0000000
U(25)=	0.0000000
U(26)=	0.0000000
U(27)=	0.0000000
U(28)=	0.0000000
U(29)=	0.0000000
U(30)=	0.0000000

Figure 30. Instability at $\beta = 1$.

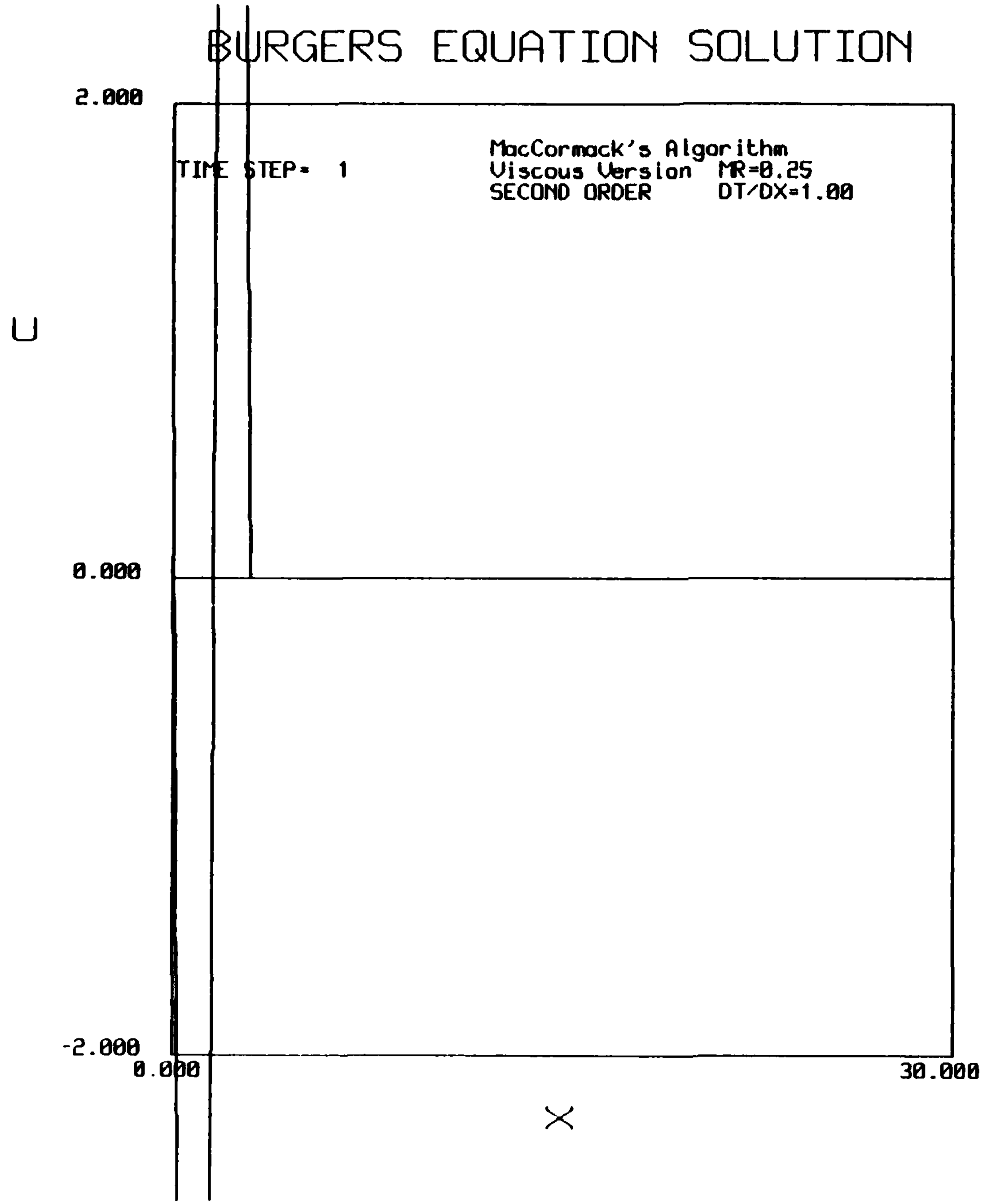

TIME STEP: 1

U(1)= 1.000000
U(2)= -15.75000
U(3)= 12.00000
U(4)= 0.0000000
U(5)= 0.0000000
U(6)= 0.0000000
U(7)= 0.0000000
U(8)= 0.0000000
U(9)= 0.0000000
U(10)= 0.0000000
U(11)= 0.0000000
U(12)= 0.0000000
U(13)= 0.0000000
U(14)= 0.0000000
U(15)= 0.0000000
U(16)= 0.0000000
U(17)= 0.0000000
U(18)= 0.0000000
U(19)= 0.0000000
U(20)= 0.0000000
U(21)= 0.0000000
U(22)= 0.0000000
U(23)= 0.0000000
U(24)= 0.0000000
U(25)= 0.0000000
U(26)= 0.0000000
U(27)= 0.0000000
U(28)= 0.0000000
U(29)= 0.0000000
U(30)= 0.0000000

Figure 31. Instability at μ = .4 and β = .4.

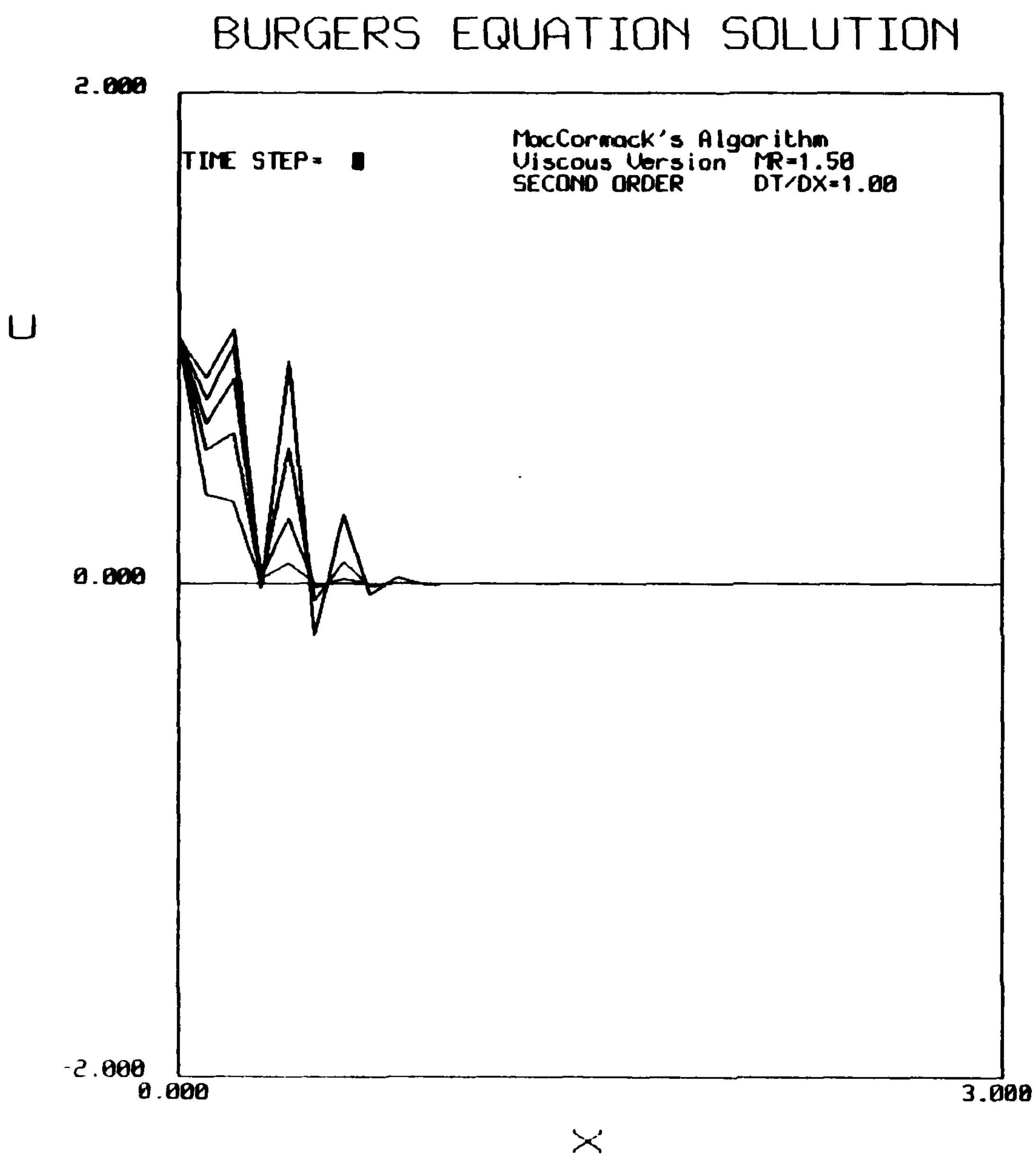

TIME STEP: 5

U(1)=	1.000000
U(2)=	0.8390695
U(3)=	1.036980
U(4)=	-0.1999497E-01
U(5)=	0.9075769
U(6)=	-0.2083742
U(7)=	0.2810604
U(8)=	-0.4239054E-01
U(9)=	0.2776599E-01
U(10)=	-0.2654756E-02
U(11)=	0.1001501E-02
U(12)=	0.0000000
U(13)=	0.0000000
U(14)=	0.0000000
U(15)=	0.0000000
U(16)=	0.0000000
U(17)=	0.0000000
U(18)=	0.0000000
U(19)=	0.0000000
U(20)=	0.0000000
U(21)=	0.0000000
U(22)=	0.0000000
U(23)=	0.0000000
U(24)=	0.0000000
U(25)=	0.0000000
U(26)=	0.0000000
U(27)=	0.0000000
U(28)=	0.0000000
U(29)=	0.0000000
U(30)=	0.0000000

Figure 32. Instability at μ = .067 and β = .67.

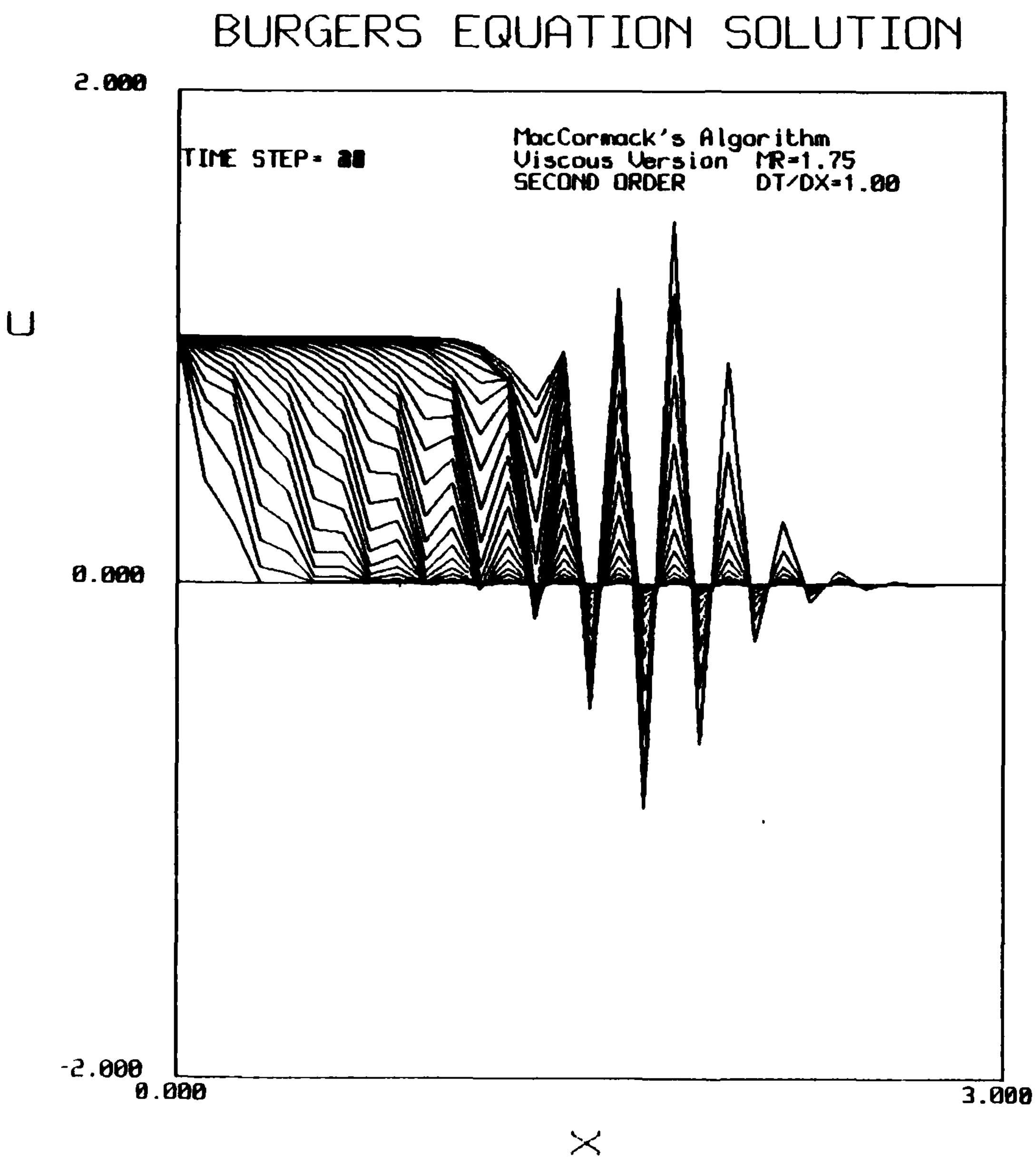

TIME STEP: 30

U(1)=	1.000000
U(2)=	1.000004
U(3)=	0.9999985
U(4)=	0.9999900
U(5)=	1.000079
U(6)=	1.000217
U(7)=	1.000229
U(8)=	1.000339
U(9)=	1.000531
U(10)=	0.9997486
U(11)=	0.9926791
U(12)=	0.9624890
U(13)=	0.8790974
U(14)=	0.7454203
U(15)=	0.9439732
U(16)=	-0.4071007
U(17)=	1.189951
U(18)=	-0.9105993
U(19)=	1.469756
U(20)=	-0.6446199
U(21)=	0.9004699
U(22)=	-0.2288693
U(23)=	0.2540987
U(24)=	-0.6925581E-01
U(25)=	0.5247844E-01
U(26)=	-0.1844207E-01
U(27)=	0.1057916E-01
U(28)=	-0.4097964E-02
U(29)=	0.1710687E-02
U(30)=	0.0000000

Figure 33. Instability at β = 0.57.

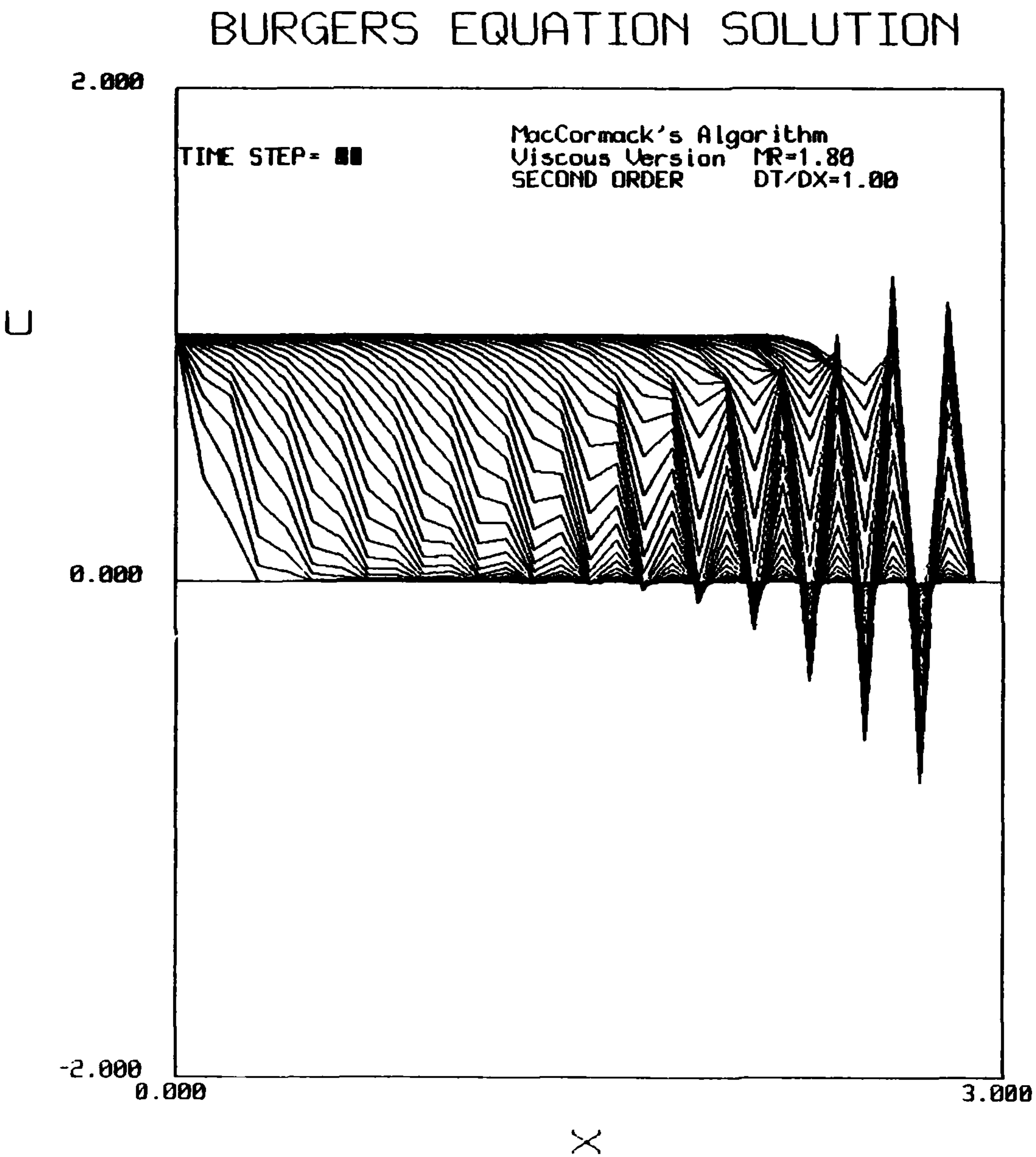

TIME STEP: 60

U(1)=	1.000000
U(2)=	1.000000
U(3)=	0.9999995
U(4)=	1.000000
U(5)=	1.000001
U(6)=	0.9999980
U(7)=	1.000003
U(8)=	0.9999959
U(9)=	1.000004
U(10)=	0.9999973
U(11)=	1.000000
U(12)=	1.000004
U(13)=	0.9999918
U(14)=	1.000013
U(15)=	0.9999726
U(16)=	0.9999846
U(17)=	1.000021
U(18)=	1.000023
U(19)=	1.000130
U(20)=	1.000422
U(21)=	1.001549
U(22)=	1.002991
U(23)=	0.9982836
U(24)=	0.9692197
U(25)=	0.8900815
U(26)=	0.7977203
U(27)=	0.9539717
U(28)=	-0.2119805
U(29)=	0.7977337
U(30)=	0.0000000

Figure 34. Instability at β = 0.556.

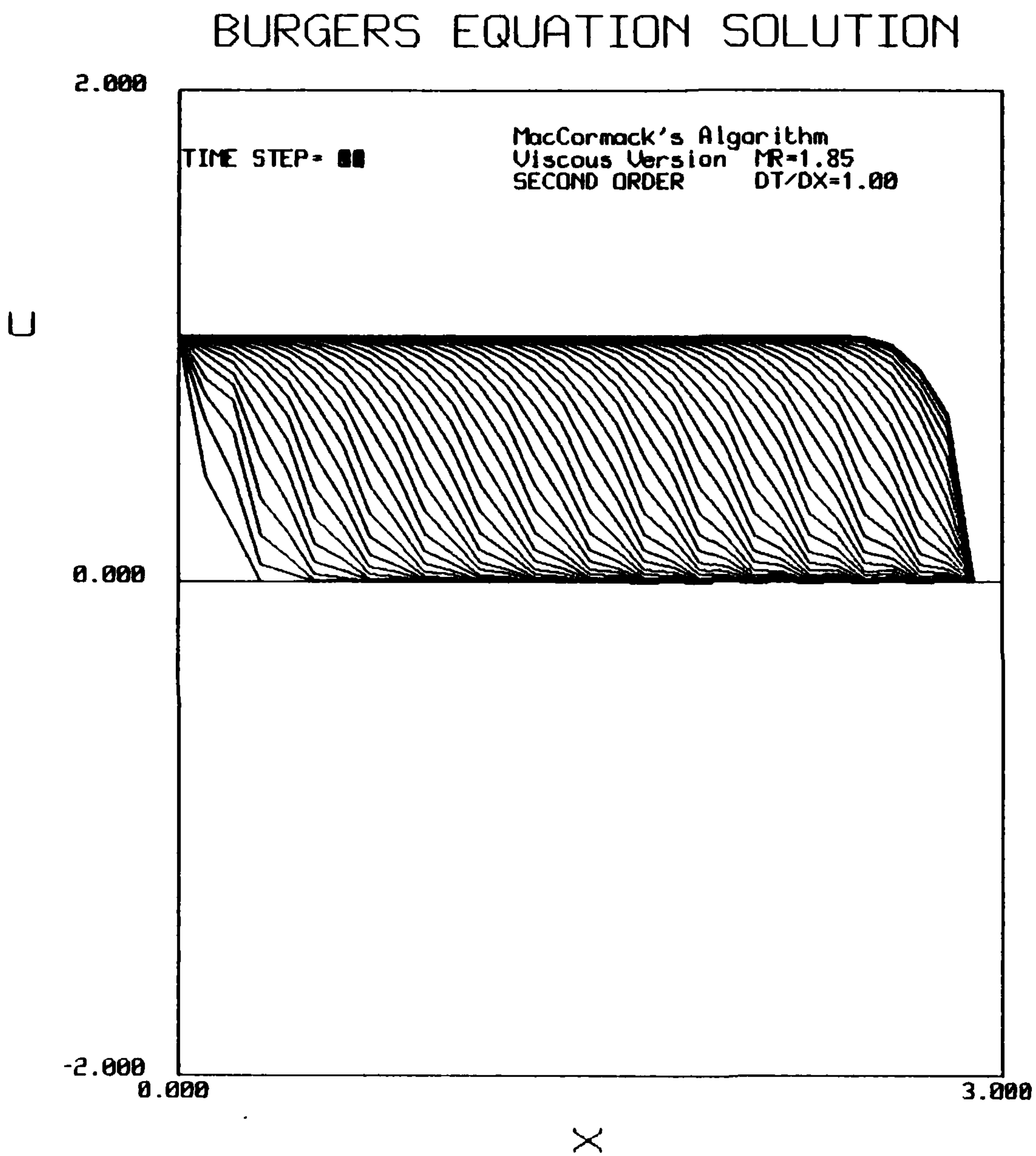

TIME STEP:	60
U(1)=	1.000000
U(2)=	0.9999998
U(3)=	1.000000
U(4)=	1.000000
U(5)=	0.9999995
U(6)=	1.000001
U(7)=	0.9999997
U(8)=	0.9999996
U(9)=	1.000001
U(10)=	0.9999993
U(11)=	0.9999998
U(12)=	1.000001
U(13)=	0.9999996
U(14)=	0.9999992
U(15)=	0.9999993
U(16)=	0.9999993
U(17)=	0.9999962
U(18)=	0.9999959
U(19)=	1.000011
U(20)=	1.000034
U(21)=	1.000092
U(22)=	1.000245
U(23)=	1.000588
U(24)=	1.001335
U(25)=	1.001711
U(26)=	0.9956194
U(27)=	0.9625447
U(28)=	0.8593771
U(29)=	0.6837888
U(30)=	0.0000000

Figure 35. Stability at β = 0.54.

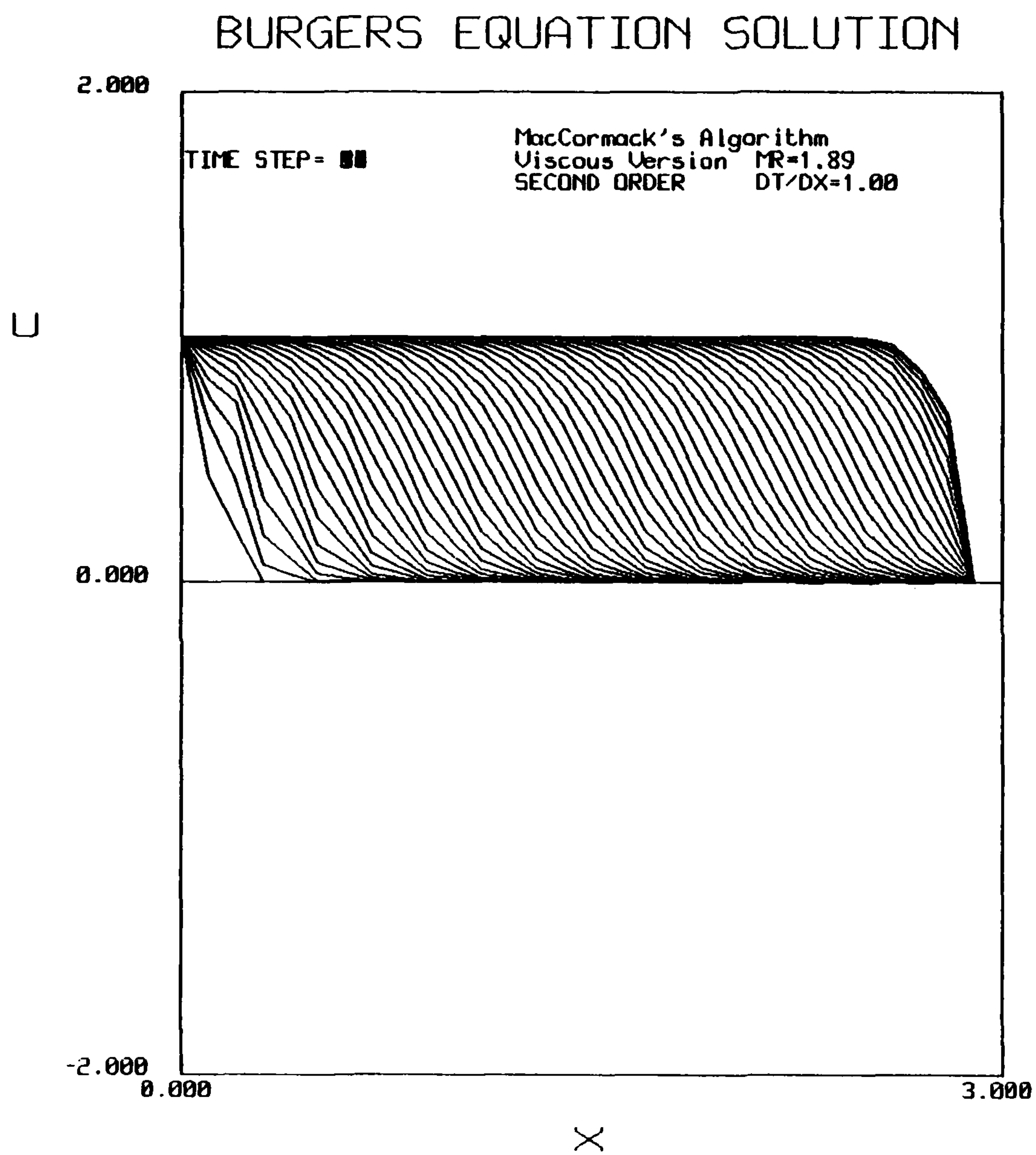

TIME STEP: 60

U(1)=	1.000000
U(2)=	0.9999998
U(3)=	1.000001
U(4)=	0.9999994
U(5)=	1.000000
U(6)=	1.000000
U(7)=	0.9999992
U(8)=	1.000001
U(9)=	0.9999998
U(10)=	0.9999997
U(11)=	1.000001
U(12)=	0.9999996
U(13)=	1.000000
U(14)=	0.9999993
U(15)=	0.9999989
U(16)=	0.9999999
U(17)=	0.9999951
U(18)=	0.9999956
U(19)=	1.000008
U(20)=	1.000027
U(21)=	1.000086
U(22)=	1.000238
U(23)=	1.000592
U(24)=	1.001394
U(25)=	1.001975
U(26)=	0.9965497
U(27)=	0.9650776
U(28)=	0.8647922
U(29)=	0.6883527
U(30)=	0.0000000

Figure 36. Stability at $\beta = 0.53$.

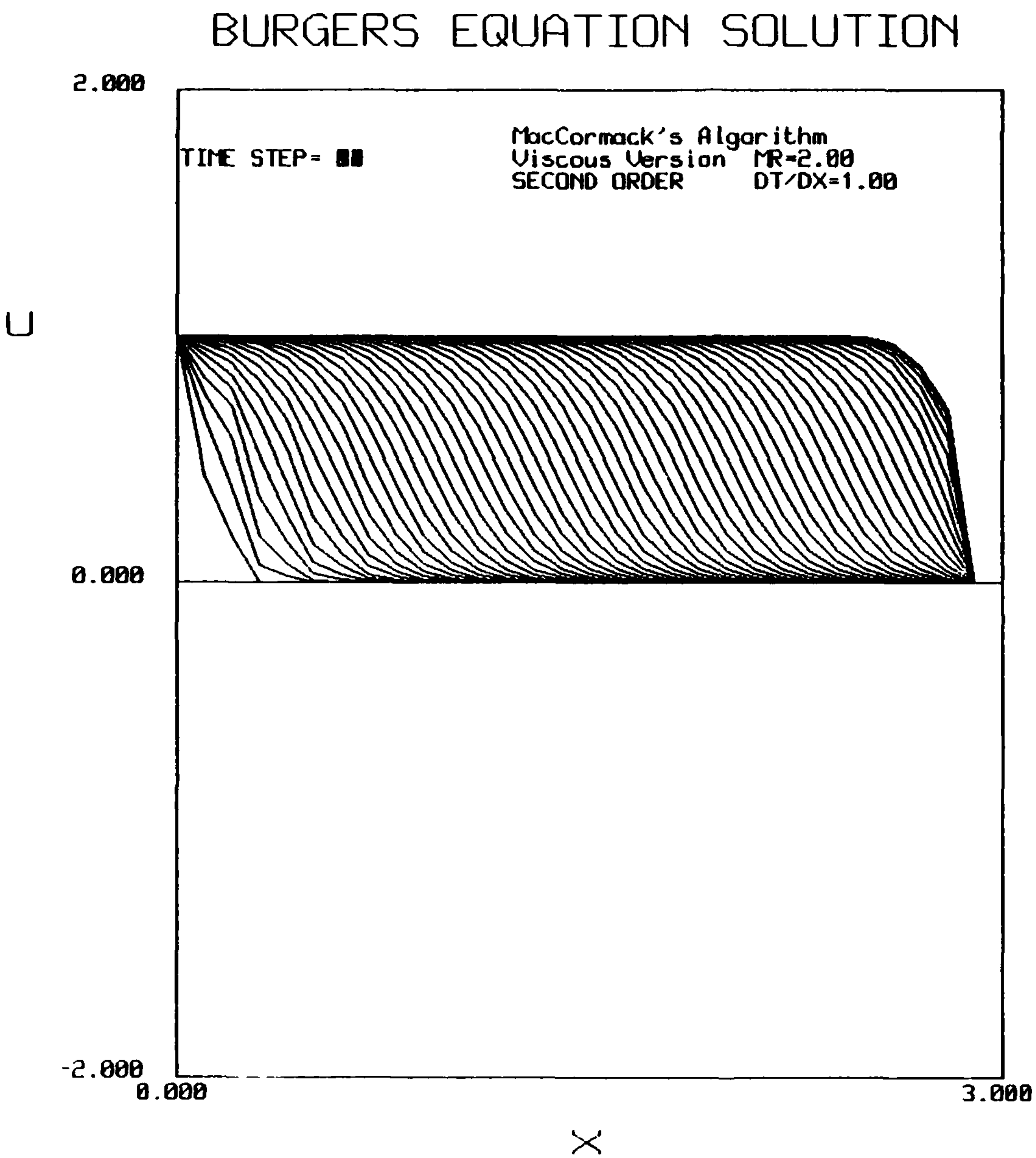

TIME STEP: 60
U(1)= 1.000000
U(2)= 0.9999999
U(3)= 1.000001
U(4)= 0.9999977
U(5)= 1.000003
U(6)= 0.9999983
U(7)= 0.9999987
U(8)= 1.000003
U(9)= 0.9999964
U(10)= 1.000002
U(11)= 1.000001
U(12)= 0.9999976
U(13)= 1.000003
U(14)= 0.9999985
U(15)= 0.9999989
U(16)= 1.000001
U(17)= 0.9999930
U(18)= 0.9999948
U(19)= 1.000000
U(20)= 1.000009
U(21)= 1.000064
U(22)= 1.000207
U(23)= 1.000575
U(24)= 1.001493
U(25)= 1.002587
U(26)= 0.9990057
U(27)= 0.9722090
U(28)= 0.8803100
U(29)= 0.7023658
U(30)= 0.0000000

Figure 37. Stability at β = 0.5.

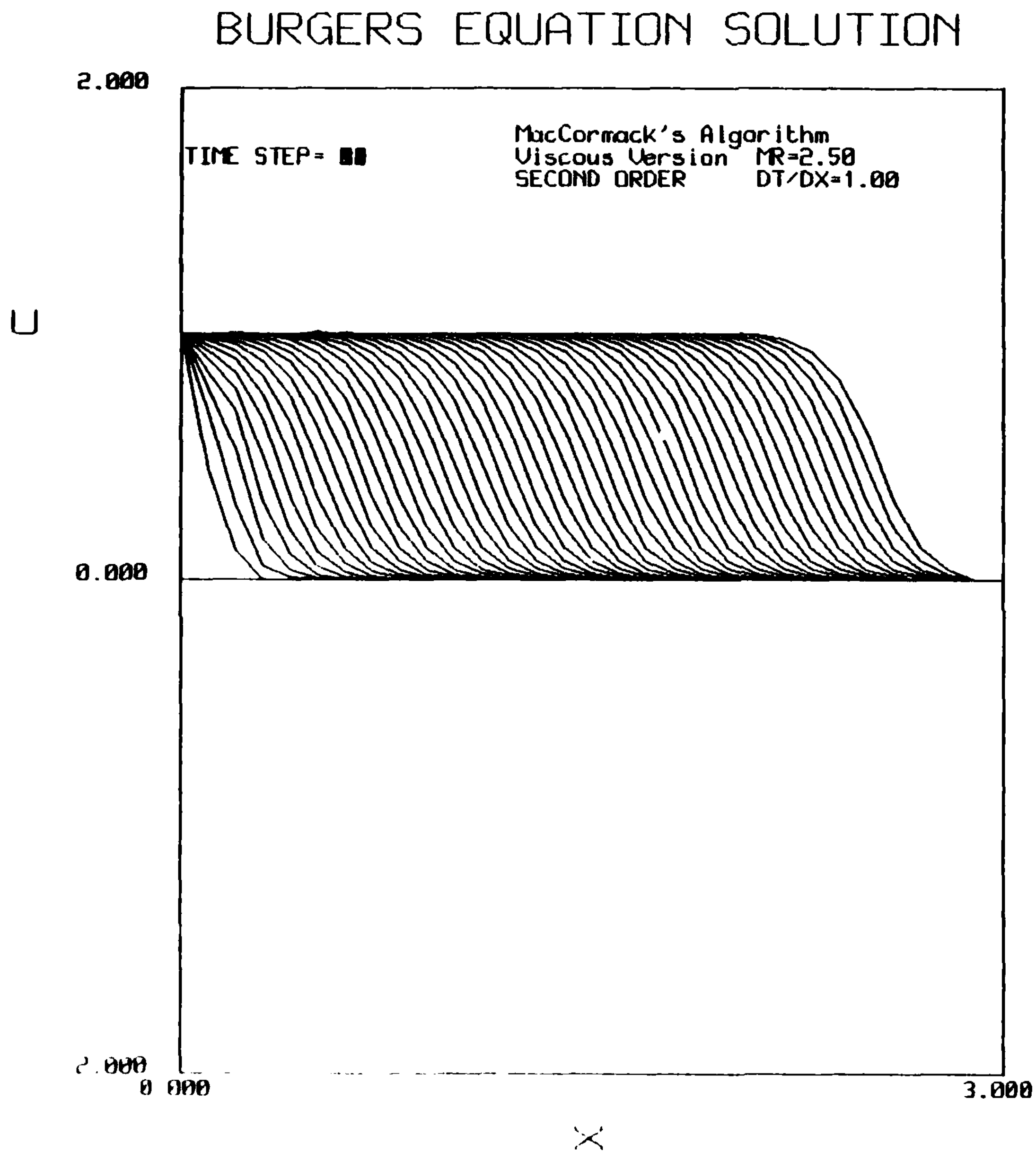

TIME STEP: 50

U(1)=	1.000000
U(2)=	0.9979122
U(3)=	1.003345
U(4)=	1.000204
U(5)=	0.9934642
U(6)=	1.010329
U(7)=	0.9909611
U(8)=	1.004027
U(9)=	1.001255
U(10)=	0.9959309
U(11)=	1.004074
U(12)=	0.9976946
U(13)=	1.000329
U(14)=	1.000912
U(15)=	0.9988065
U(16)=	1.000741
U(17)=	0.9999003
U(18)=	1.000157
U(19)=	1.001205
U(20)=	1.001830
U(21)=	1.002111
U(22)=	0.9972862
U(23)=	0.9784992
U(24)=	0.9272656
U(25)=	0.8141310
U(26)=	0.6138828
U(27)=	0.3257413
U(28)=	0.1287992
U(29)=	0.4012206E-01
U(30)=	0.0000000

Figure 38. Instabilities growing at $\beta = 0.4$ [Note the u(j) values].

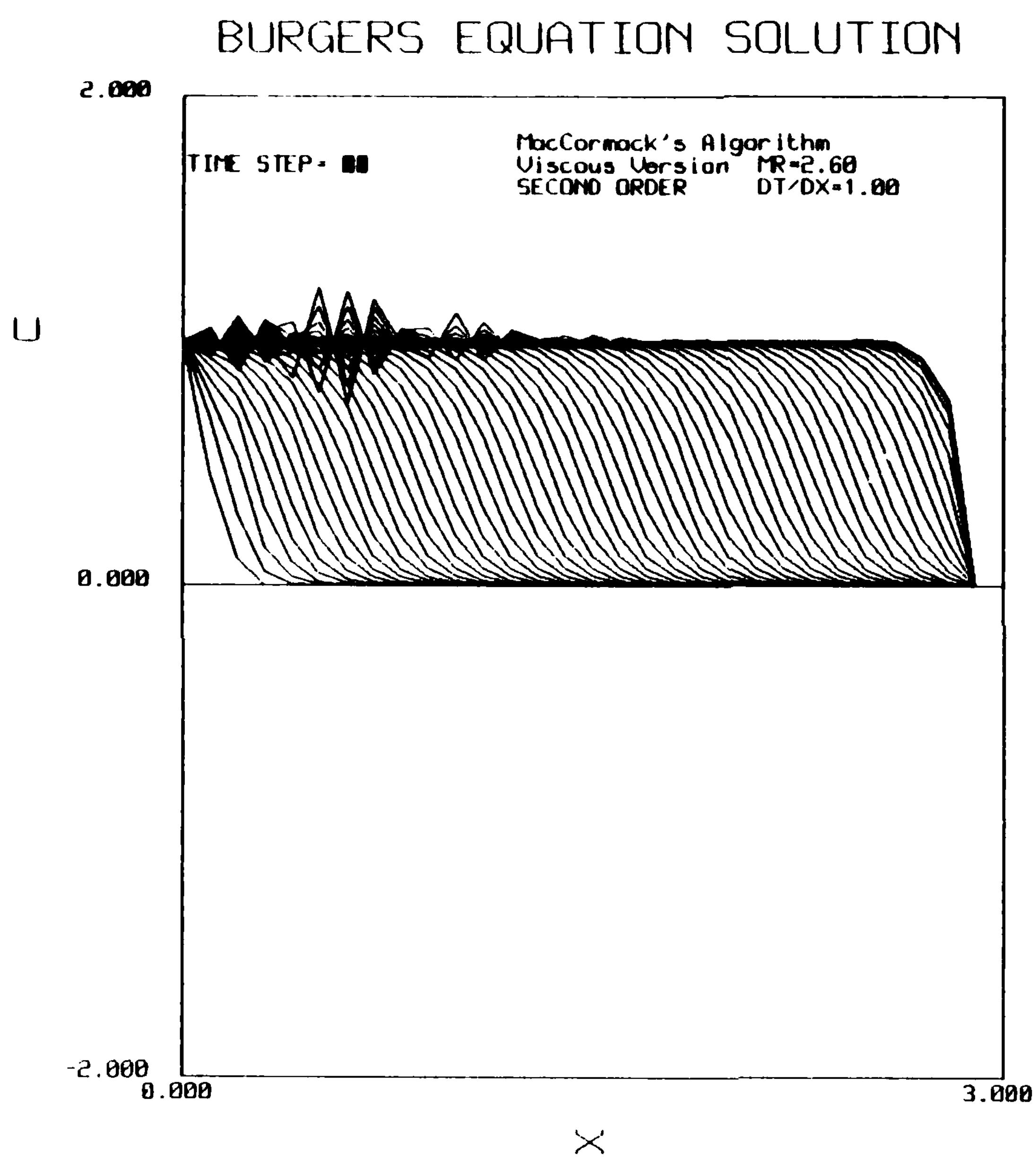

TIME STEP: 60
U(1)= 1.000000
U(2)= 0.9480979
U(3)= 1.072892
U(4)= 0.9885626
U(5)= 0.8482948
U(6)= 1.216616
U(7)= 0.7471953
U(8)= 1.170967
U(9)= 0.9859199
U(10)= 0.9327146
U(11)= 1.113820
U(12)= 0.9212963
U(13)= 1.044794
U(14)= 1.007863
U(15)= 0.9780701
U(16)= 1.028063
U(17)= 0.9863523
U(18)= 1.004267
U(19)= 1.005236
U(20)= 0.9944680
U(21)= 1.004230
U(22)= 0.9993252
U(23)= 0.9996281
U(24)= 1.002320
U(25)= 1.002501
U(26)= 1.004875
U(27)= 0.9946589
U(28)= 0.9339993
U(29)= 0.7627154
U(30)= 0.0000000

Figure 39. Instabilities at $\beta = 0.38$.

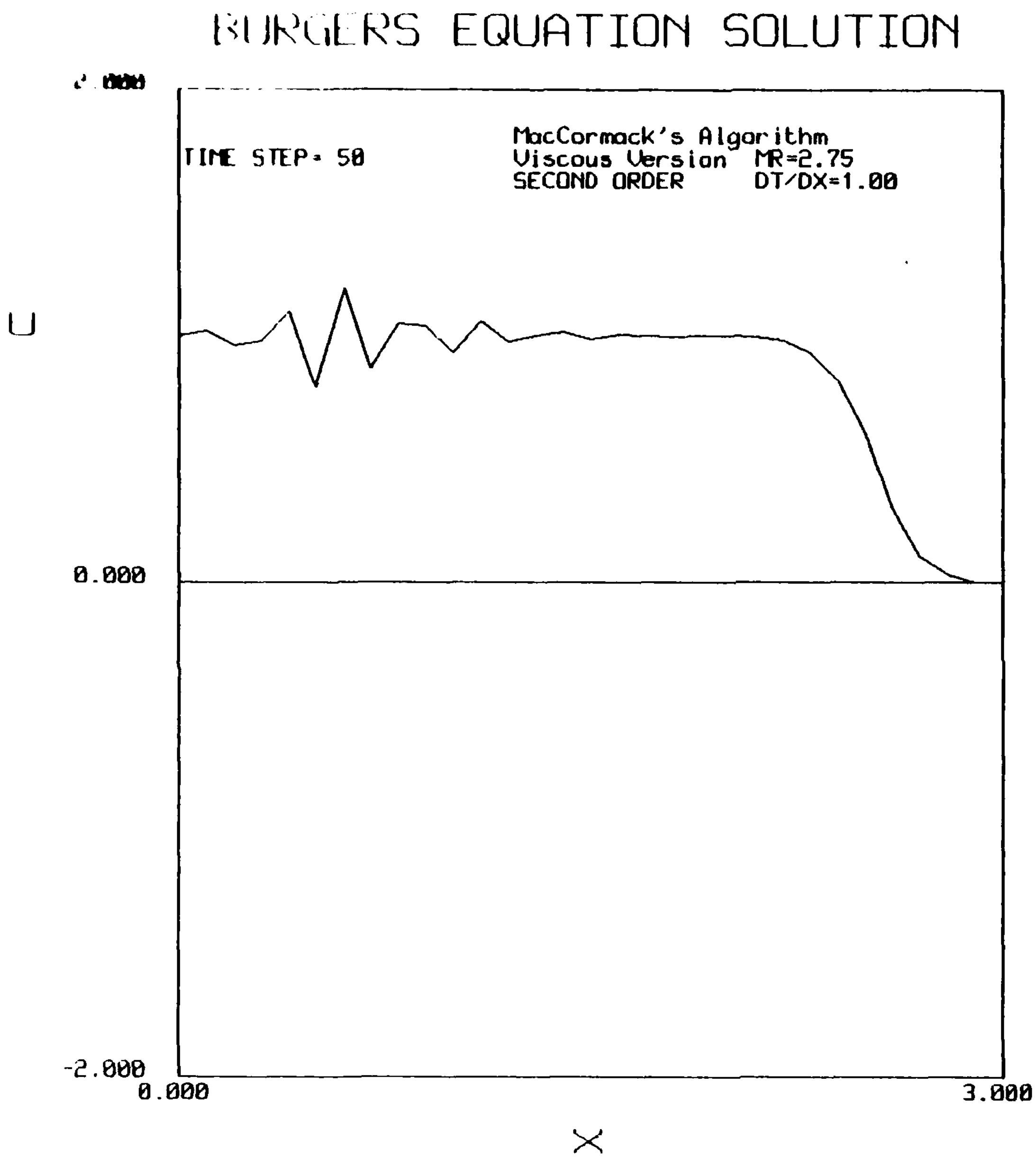

TIME STEP: 50

U(1)=	1.000000
U(2)=	1.021240
U(3)=	0.9608867
U(4)=	0.9841822
U(5)=	1.099514
U(6)=	0.7936603
U(7)=	1.196105
U(8)=	0.8676417
U(9)=	1.052261
U(10)=	1.042478
U(11)=	0.9330591
U(12)=	1.061981
U(13)=	0.9768282
U(14)=	1.001419
U(15)=	1.014687
U(16)=	0.9886312
U(17)=	1.006943
U(18)=	1.000196
U(19)=	0.9993115
U(20)=	1.004019
U(21)=	1.002291
U(22)=	0.9999137
U(23)=	0.9841938
U(24)=	0.9353526
U(25)=	0.8205203
U(26)=	0.6076787
U(27)=	0.2959394
U(28)=	0.1047831
U(29)=	0.2960709E-01
U(30)=	0.0000000

Figure 40. Instabilities at $\beta = 0.36$.

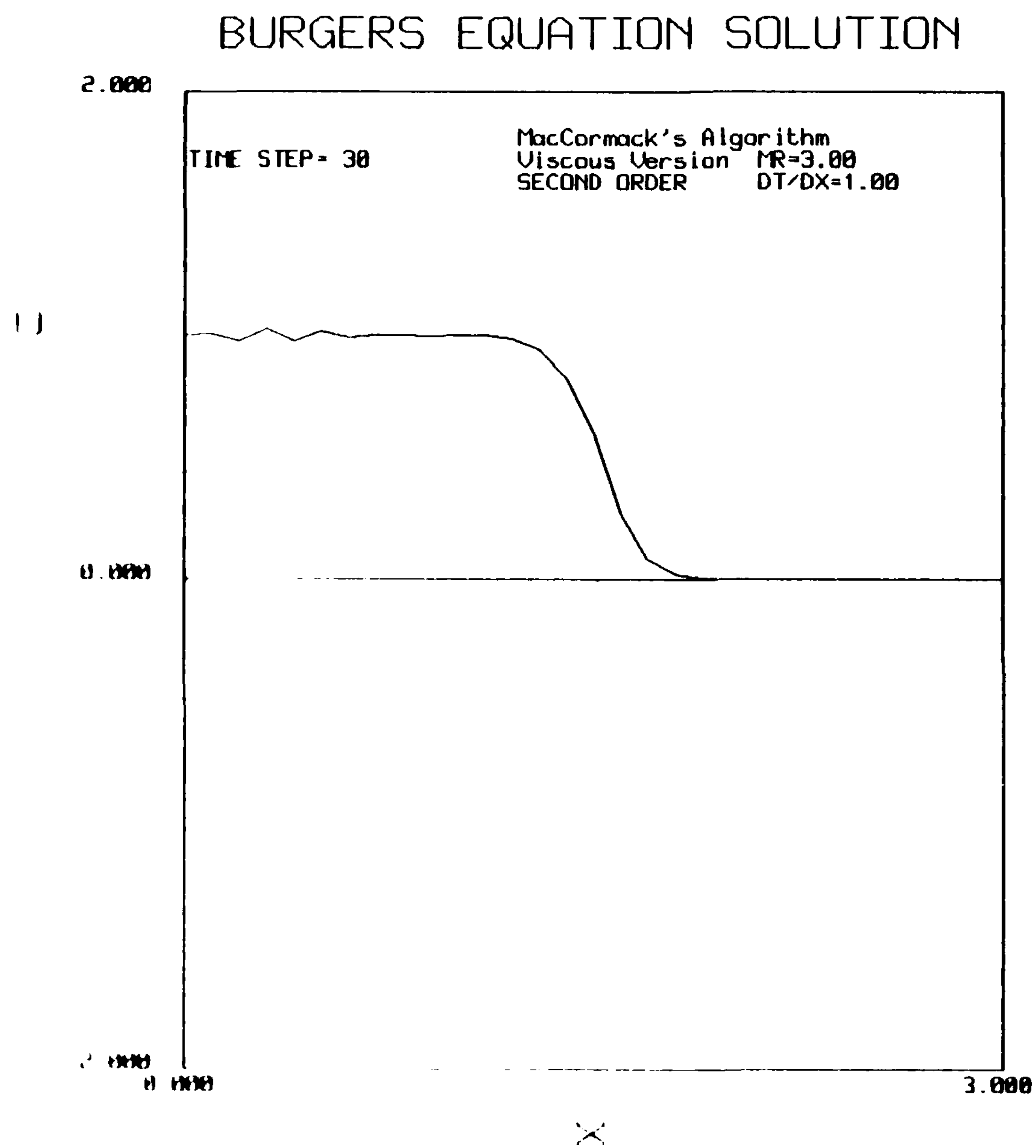

TIME STEP: 30

U(1)=	1.000000
U(2)=	1.008359
U(3)=	0.9787888
U(4)=	1.026248
U(5)=	0.9767950
U(6)=	1.015150
U(7)=	0.9936638
U(8)=	1.000760
U(9)=	1.002697
U(10)=	0.9998280
U(11)=	1.004500
U(12)=	1.001089
U(13)=	0.9878728
U(14)=	0.9421510
U(15)=	0.8256887
U(16)=	0.6008967
U(17)=	0.2686165
U(18)=	0.8589291E-01
U(19)=	0.2358983E-01
U(20)=	0.6187026E-02
U(21)=	0.1600881E-02
U(22)=	0.4122577E-03
U(23)=	0.1059189E-03
U(24)=	0.2712501E-04
U(25)=	0.6912969E-05
U(26)=	0.1749878E-05
U(27)=	0.4388352E-06
U(28)=	0.1084612E-06
U(29)=	0.2508496E-07
U(30)=	0.0000000

Figure 41. Instabilities at β = .33, time step 30.

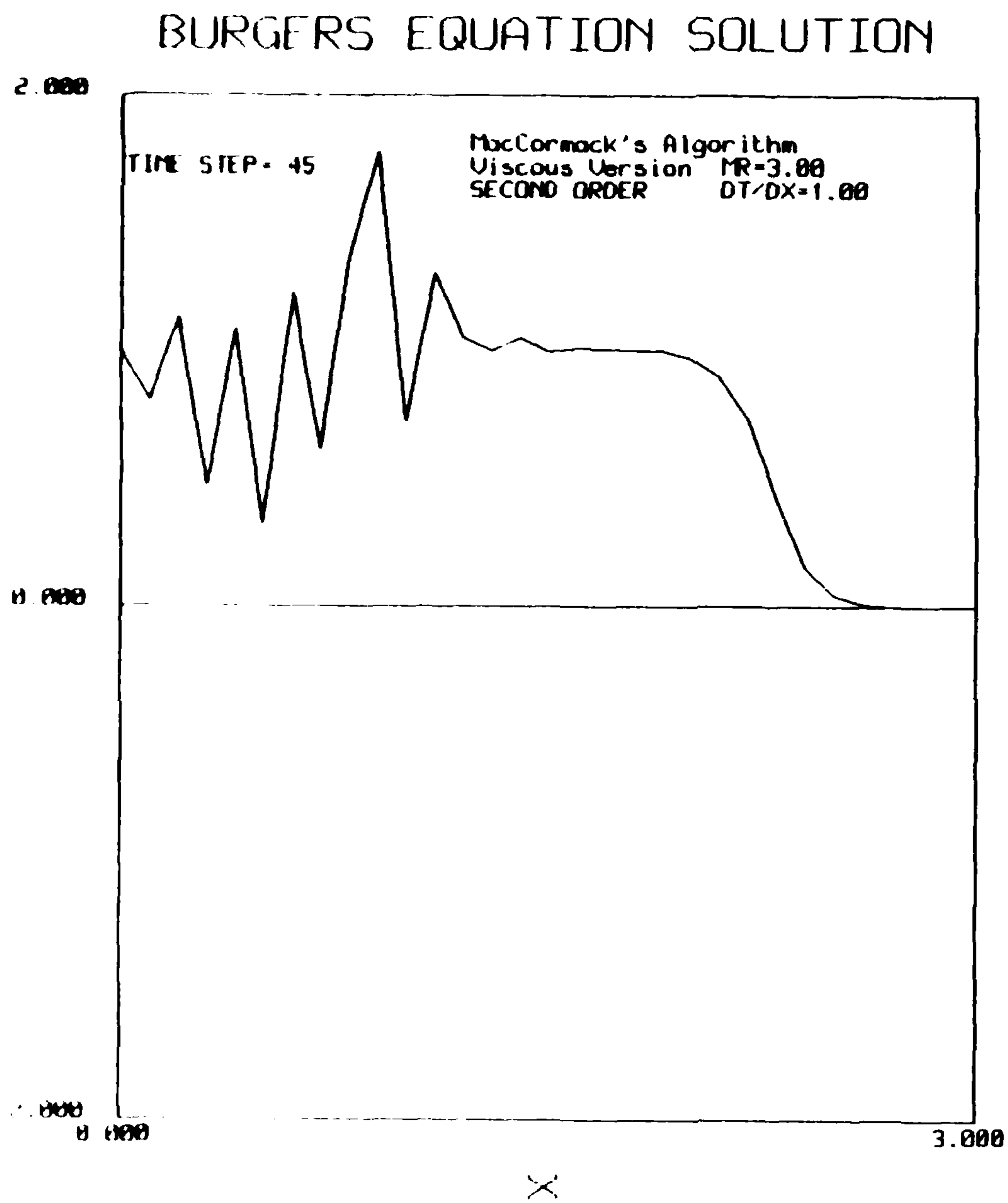

TIME STEP: 45

U(1)=	1.000000
U(2)=	0.8057060
U(3)=	1.131218
U(4)=	0.4754337
U(5)=	1.085343
U(6)=	0.3245857
U(7)=	1.226256
U(8)=	0.6157994
U(9)=	1.363583
U(10)=	1.779669
U(11)=	0.7276303
U(12)=	1.306576
U(13)=	1.050956
U(14)=	1.003330
U(15)=	1.051792
U(16)=	0.9952337
U(17)=	1.013448
U(18)=	1.007514
U(19)=	1.003656
U(20)=	1.000555
U(21)=	0.9706367
U(22)=	0.8956666
U(23)=	0.7359191
U(24)=	0.4275424
U(25)=	0.1555811
U(26)=	0.4512896E-01
U(27)=	0.1200461E-01
U(28)=	0.3095747E-02
U(29)=	0.7474796E-03
U(30)=	0.0000000

Figure 42. Instabilities for $\beta = 0.33$ at time step 45.

SECTION V

PROGRAM LISTINGS

```
      PROGRAM AMPFAC
      DIMENSION X(360),Y(360)
      OPEN (UNIT=91,FILE='[HUGHSON.TR]AMPFAC.DAT',STATUS='NEW')
      PI=4.0*ATAN(1.0)
      PIRAD=PI/180.0
      PRINT *,'INPUT VALUE FOR ALPHA!'
      READ *,AL
      PRINT *,'INPUT VALUE FOR BETA!'
      READ *,BE
      DO 2001 I=1,360,4
      GAMMA=PIRAD*I
      A=COS(GAMMA)-1.0
      X(I)=(2*AL+BE**2)*A+1+2*AL**2*A**2
      Y(I)=-BE*SIN(GAMMA)*(2*AL*A+1)
      WRITE(91,*)X(I),Y(I)
 2001 CONTINUE
      END
[EOB]
```

Program 1. **Amplification factor data generator for plotting in the imaginary plane.**

```
      PROGRAM EXP
      DIMENSION X(181),Y(181)
      OPEN (UNIT=91,FILE='[HUGHSON.TR]EXP.DAT',STATUS='NEW')
      PI=4.0*ATAN(1.0)
      PIRAD=PI/180.0
      PRINT *,'INPUT VALUE FOR ALPHA!'
      READ *,AL
      DO 2001 I=1,181
      J=I-1
      GAMMA=PIRAD*J
      G=1/EXP(AL*GAMMA**2)
      X(I)=G*COS(GAMMA)
      Y(I)=G*SIN(GAMMA)
      WRITE(91,*)X(I),Y(I)
 2001 CONTINUE
      END
[EOB]
```

Program 2. $|G|_{PDE} = e^{-\gamma^2 \alpha}$ - modulus of PDE data generator

```
      PROGRAM MOD
      DIMENSION X(181),Y(181)
      OPEN (UNIT=91,FILE='[HUGHSON.TR]MOD.DAT',STATUS='NEW')
      PI=4.0*ATAN(1.0)
      PIRAD=PI/180.0
      PRINT *,'INPUT VALUE FOR ALPHA!'
      READ *,AL
      PRINT *,'INPUT VALUE FOR BETA!'
      READ *,BE
      DO 2001 I=1,184,4
      J=I-1
      GAMMA=PIRAD*J
      A=COS(GAMMA)-1.0
      X(I)=(2*AL+BE**2)*A+1+2*AL**2*A**2
      Y(I)=-BE*SIN(GAMMA)*(2*AL*A+1)
      G=SQRT(X(I)**2+Y(I)**2)
      X(I)=G*COS(GAMMA)
      Y(I)=G*SIN(GAMMA)
      WRITE(91,*)X(I),Y(I)
 2001 CONTINUE
      END
[EOB]
```

Program 3. Modulus of amplification factor data generator.

```
      PROGRAM REL
      DIMENSION X(180),Y(180)
      OPEN (UNIT=91,FILE='[HUGHSON.TR]REL.DAT',STATUS='NEW')
      PI=4.0*ATAN(1.0)
      PIRAD=PI/180.0
      PRINT *,'INPUT VALUE FOR ALPHA!'
      READ *,AL
      PRINT *,'INPUT VALUE FOR BETA!'
      READ *,BE
      DO 2001 I=1,180,4
      GAMMA=PIRAD*I
      A=COS(GAMMA)-1.0
      X(I)=(2*AL+BE**2)*A+1+2*AL**2*A**2
      Y(I)=-BE*SIN(GAMMA)*(2*AL*A+1)
      TNUM=ATAN2(Y(I),X(I))
      REL=-TNUM/(BE*GAMMA)
      X(I)=REL*COS(GAMMA)
      Y(I)=REL*SIN(GAMMA)
      WRITE(91,*)X(I),Y(I)
 2001 CONTINUE
      END
[EOB]
```

Program 4. Relative phase shift error data generator.

REFERENCES

1. Burgers, J.M., "A Mathematical Model Illustrating the Theory of Turbulence," Advanced Applied Mechanics, Vol. 1, pp. 171-199, 1948.

2. MacCormack, R.W., "The Effect of Viscosity in Hypervelocity Impact Cratering," AIAA Paper 69-354, Cincinnati, Ohio, 1969.

3. Anderson, D.A., Tannehill, J.C., and Pletcher, R.H., Computational Fluid Mechanics and Heat Transfer, McGraw-Hill Book Co., New York, 1984.

4. Lax, P.D. and Wendroff, B., "Systems of Conservation Laws," Communications on Pure and Applied Mathematics, Vol. 13, pp. 217-237, 1960.

5. O'Brien, G.G., Hyman, M.A., and Kaplan, S., "A Study of the Numerical Solution of Partial Differential Equations, Journal of Mathematics and and Physics, Vol. 29, pp. 223-251, 1950.

6. Richtmyer, R.O. and Morton, K.W., Difference Methods for Initial-Value Problems, 2d ed., Interscience Publishers, Wiley, New York, 1967.

END
8-87
DTIC